Predicting the breaching production of a slope during a wet mining process

Althuis, Kaj

Delft University of Technology

28/09/2016

M.Sc Thesis

Predicting the breaching production of a slope during a wet mining process

Master of Science

In

European Geotechnical and Environmental Course

Part of the EMMEP

Faculty of Applied Earth Sciences

Delft University of Technology

By

Kaj Althuis

September 28th, 2016

Graduation committee:

Prof.dr.ir. C. van Rhee	TU Delft
Dr.ir. L.A. van Paassen	TU Delft
Ir. R.L.J. Helmons	TU Delft/Royal IHC
Ir. A. Hogeweg	Royal IHC

Abstract

An underwater slope can collapse by liquefaction, wedge failure or breaching. Breaching is the most unknown process and has a low predictability. Dredge mining is strongly influenced by the breaching process. If breaching can be accurately predicted, the efficiency of the dredging production can be maximised. It is the objective to know what field- and lab tests must be conducted to be able to predict the breaching behaviour of a slope.

In this report, a model is developed to predict the breaching behaviour of a slope after a single cut at the toe of the slope is made. The model is used to research the influence of several soil parameters and geometrical parameters on the breaching behaviour. The most important criterion is the difference between stable and unstable breaching. An empirical relation is created which can be used to estimate the critical cut height. This is the height at which a smaller cut height creates a stable breach and a larger cut creates an unstable breach. The critical cut height is dependent on the particle size distribution represented by the D_{50} and the D_{10}, the particle density and the slope angle. By using these parameters, the breaching process can be predicted. The critical cut height can be used to predict what the best cut depth for a certain slope and dredger is.

After the first cut, usually several more cuts are made in order to keep the production at a high level. This process is not extensively researched in the past, so a second simplified model is created which predicts the breaching production in 3D and can incorporate multiple cuts. The model incorporates a swinging motion by the cutter, which is essential for a dredging operation. The model can demonstrate different phenomena which might occur during a dredging operation. It will illustrate examples of consequences of a slow or fast swinging motion, large or small delay times between swings and differences in swing widths.

The input parameters necessary for the model can be obtained from field- and lab tests. Several field- and lab tests are advised after analysis of the model. The tendency of the soil to either breach or liquefy can be estimated by a state parameter analysis using CPT data. It might however be more suitable to use an SPT, in this case the SPT data gives a direct indication of the relative density which can also be used to estimate the ability to breach. A sieving is necessary to obtain the particle size distribution in order to obtain the D_{50} and the D_{10}. A pycnometer test is necessary in order to obtain the particle density. The angle of repose can be determined with a lab test or a correlation with SPT data. In order to get a better estimate of the permeability, it is advised to do an auger hole test to measure the permeability more accurately. The data from these tests are suitable to predict the breaching behaviour of any submerged slope around the world.

Preface

This report is written in order to graduate for the MSc degree in the European Geotechnical and Environmental Course at the Delft University of Technology. This research is conducted at IHC MTI in Delft, The Netherlands. IHC MTI is the research and development department of Royal IHC. It is a very inspiring environment to conduct a geotechnical research. This report contains the research to the breaching behaviour of a slope during dredging, a part of the investigation to smart risk quantification conducted by Royal IHC.

I am very grateful to IHC MTI for giving me the facilities and help to do the research presented in this report. Everybody at MTI and specifically Bart Hogeweg from IHC mining gave me all the help necessary. Bart Hogeweg provided the research question and gave me the opportunity to find my own path to solve the problem. He helped me choosing the right direction in the research and provided useful information from IHC.

I would like to thank the persons in the graduation committee that helped me to achieve my goals during my graduation. Firstly I would like to thank my daily supervisor Rudy Helmons. He helped me a lot with the whole process of the thesis from start to finish, including advice about programming, research, report writing and logistics. Leon van Paassen provided a very helpful insight into the problems I encountered and provided good solutions. It helped me a lot in improving my work. I would like to thank Cees van Rhee. He helped me a lot with all his knowledge and experience about breaching and dredging. His input and critical look has been essential for obtaining a reliable model describing the breaching process.

Kaj Althuis,

Delft

Table of Contents

List of figures

List of tables

List of symbols

Greek symbols

α [°]   Angle of top of outflow soil

β [°]   Slope angle

γ [N/m^3]   Volumetric weight

γ_w [N/m^3]   Volumetric weight of water

η [-]   Direction of rotated coordinate system

ξ [-]   Direction of rotated coordinate system

ρ_s [kg/m^3]   Particle density

ρ_w [kg/m^3]   Water density

σ [N/m^2]   Stress in the soil

τ [N/m^2]   Shear stress

φ [°]   Angle of repose

Latin symbols

c [N/m^2]   cohesion

C [-]   Constant

D_{10} [m]   10th percentile of particle density graph

D_{15} [m]   15th percentile of particle density graph

D_{50} [m]   50th percentile of particle density graph

F_s [-]   Safety factor

F_g [N]   Gravity force

g [m/s^2]   Gravitational acceleration

H [m]   Height

$H_{outflow}$ [m]   Height of outflow volume

h_{wall} [m]   Breaching wall height

i [-]   Gradient of inward flow perpendicular to the breaching wall

k_0 [m/s]   Initial permeability

k_1 [m/s]   Permeability of loose soil

L [m]   Length

N [N/m^2]   Normal force

M [-]   Multiplier

n_0 [-]   Initial porosity

n_1 [-]   Loose soil porosity

n_{min} [-]   Minimum porosity

n_{crit} [-]   Critical porosity

Δn [-]   Porosity change due to dilatancy

p [N/m^2]   Pore pressure

q [m/s]   Inflow of water into breaching wall

s [kg·s^{-1}·m^{-1}]   Mass flow of breaching

V [-]   Volume

V_{breach} [m^3]   Volume of soil collapsed due to breaching

v_{cut} [m/s]   Cutting velocity

v_e [m/s]   Erosion velocity

$V_{outflow}$ [m^3]   Volume of soil accumulated at the toe of a breaching slope

v_{wall} [m/s]   Wall velocity

W [m]   Width

W_F [N]   Frictional force

1 Introduction

1.1 Background

Royal IHC is specialised in dredging and wet mining equipment. Besides delivering and producing the equipment IHC also wants to give an advice about the dredging and the mining process. This way the equipment can better be adapted to the specific project. In several projects around the world sand layers with thicknesses of up to 20 meters must be mined. IHC uses different dredging techniques to undercut the slope of these layers. The cutting causes the slope to fail, after which the soil can be collected. The most important aspect for the production of these layers is to make the following sum the cheapest:

Total production = production by cutting + production by failure

In order to predict the elements in this formula, first of all the process of failure must be understood better. A failure can happen in a few different ways. Wedge failure, liquefaction and breaching are different processes in which a slope can fail. Breaching is the most unknown process and has a low predictability. These failure processes all have an influence on the production, they will be explained in chapter 2.

1.2 Problem

IHC is doing a large research to smart risk quantification. During a mining operation many unknowns are created and IHC wants to know what the minimum field investigation is to make a reliable description of the important soil layers. IHC wants to give an advice about what field tests must be executed and how many of these tests are necessary to assure the necessary level of certainty for a particular production method. The more tests are done, the lower is the risk of unexpected events during later stadia of the operation. IHC wants to quantify these risks better.

Within the research many smaller processes are important, one of these processes is breaching. At this point, using the given geotechnical and geometrical data from a field investigation, it is very difficult to predict whether a slope starts breaching or that a different failure mechanism occurs. When a slope starts breaching it is difficult to predict how fast the process is and in what extent. The actions taken by the dredger must be adapted to the behaviour of the slope and the behaviour of the slope also depends on the choices made by the dredger. When the effects of the dredging choices are not well known, the production rate and efficiency are depending on the craftsmanship of the dredging team. It would be more efficient if the production can be predicted based on the dredging movements and the geotechnical parameters of the soil.

1.3 Goal

Within the investigation of smart risk quantification, this research is focussed on the breaching behaviour of a slope. It is important to be able to predict if a slope will start breaching and in what way the breaching will continue. When the predictability of a breaching slope is high enough, an advice can be given on how to mine the sand layer in the most cost effective way. The ultimate goal is to enhance the predictability of a breaching slope on the basis of field tests, with the result that an advice can be given how to optimize the production of this slope.

The goal of this thesis is to research what soil parameters are necessary to predict the behaviour of a submerged slope of soil during dredging. The behaviour must be predicted based on the available geotechnical soil data. If extensional soil data are required, an advice will be given on the in-situ- and lab tests to be executed during a field investigation for a dredging project.

1.4 Approach

First of all, an extensive literature study will be presented. The whole spectrum of slope failure both in dry and wet conditions will be covered, but the focus will be on breaching failure. A full description will be given about the state of the art knowledge of breaching.

Important questions that will be answered during the literature study concerning breaching are:

- What happens exactly in a slope when it starts breaching?
- What are the important soil parameters that govern the process of breaching and how are they coherent?
- What are the different types of breaching (stable breaching, unstable breaching) dependent on and can they be predicted?

Besides breaching, other failure mechanisms such as liquefaction and wedge failure are very important and cannot be seen as different and unrelated processes. The different failure mechanisms have a significant influence on each other and the eventual behaviour of the slope. These failure processes can take place instead of breaching or during breaching and they can influence the production procedure significantly. It is important to find the correlation between the different failure mechanisms. The first step is to describe the mechanisms separately and the next step is to understand when a certain failure process occurs and what parameters are important to predict this. It should be clear that when a set of geometrical data and soil data is given which failure mechanism can be expected. It is also important to describe what parameters are necessary to define what failure process can be expected. In this report the focus will be on breaching slope failure described by the following questions:

- What tests need to be done in the field to predict the breaching behaviour?
- What is the influence of the important soil parameters on the process of breaching?
- What is the influence of the dredging choices on the process of breaching?

The next step is to make a model which describes the failure process that occurs. The model should be useable to predict the amount of sand produced from a slope depending on the way it is cut. In this report two models are presented which can be used for breaching slopes. A breaching model which described the process of breaching in two dimensions and a production model which can illustrate some phenomena during dredging in three dimensions. The models will be explained and results will be given and described. The limits and uncertainties of the models will be discussed at the end of the report. It is important to estimate what reliability can be reached when the production of a breaching slope is predicted. In the end, it is the goal to be able to give a reliable prediction of the breaching behaviour of a slope based on available field and lab tests.

1.5 Report outline

- *Chapter 2:* Gives a full explanation about the failure of a slope in both dry and wet conditions. The failure of a slope will be explained on the basis of a flow chart containing the main failure

paths, types and possible calculation methods. The main failure processes are described, but the focus will be on breaching failure.

- *Chapter 3:* Explains the breaching model in detail. First a full explanation of the method is given, after which the model is compared with lab tests. Model results are presented and discussed at the end of the chapter.
- *Chapter 4:* Gives a full explanation of the method of the production model. Some examples of results are given to illustrate the possible problems occurring in dredge mining. All the results are discussed.
- *Chapter 5:* The soil parameters necessary to create the breaching model must be obtained from lab- and field tests. This chapter explains possible tests which can be executed in the field and in the lab and which might be best to obtain the necessary field information.
- *Chapter 6:* This chapter consists of the conclusions and recommendations covering everything explained in the previous chapters.
- *Appendices:* Additional information and results are merged in the appendices on the end of the report.

2 Slope failure processes

In this chapter the different processes of slope faiure will be explained. In order to give a schematic overview, the flowchart given in Figure 2-1 is created. The flowchart is subdivided into three parts. The starting situation is a slope of a given height and slope angle. The different failure types corresponding with a certain starting situation are given. A possible calculation method is given for the failure types. In this chapter, every step will be explained.
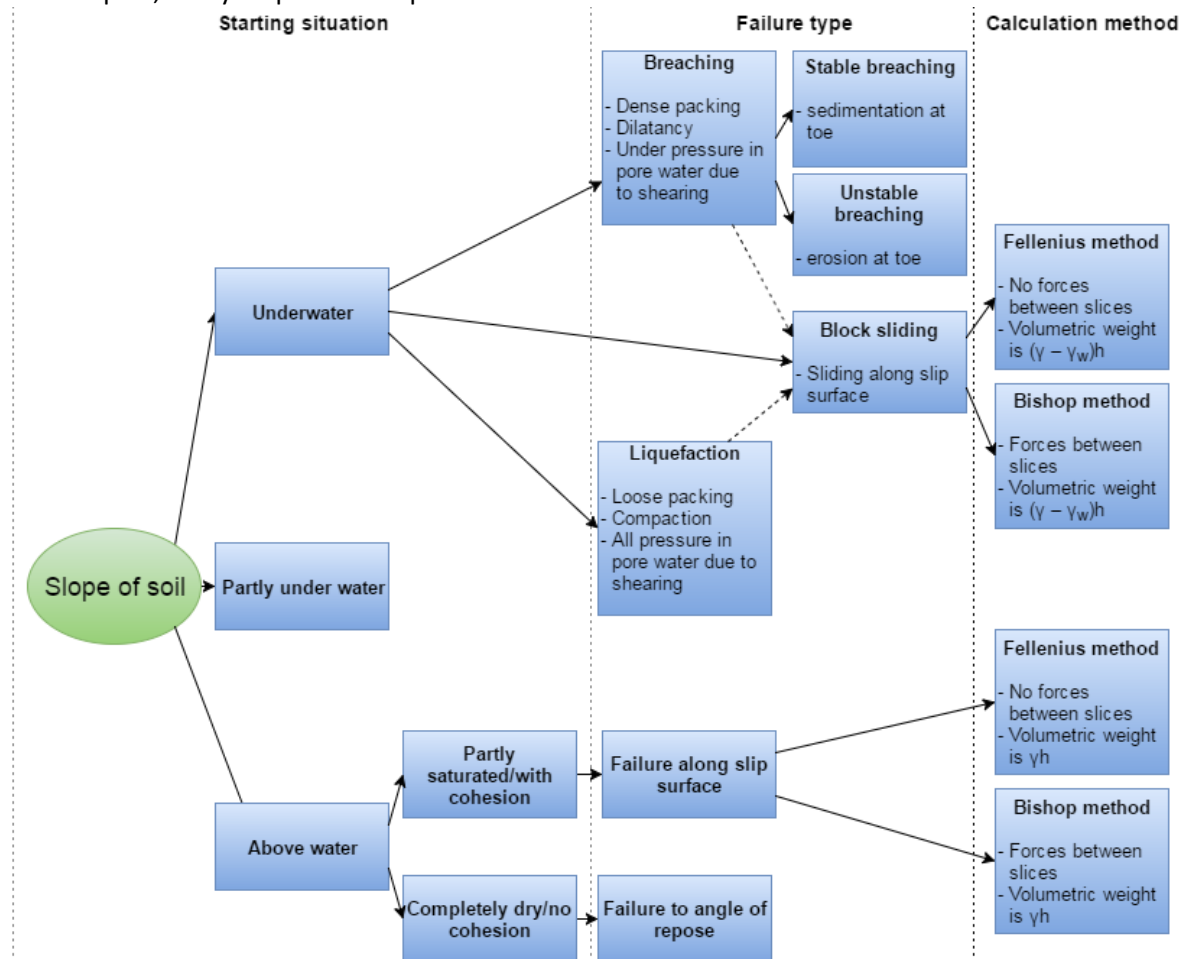
Figure 2-1: Slope failure flowchart

2.1 Starting situation

The starting situation is a homogeneous slope which is stable with a slope angle equal to or lower than the angle of repose. This slope is stable under all static conditions. The slope will be divided into three different possibilities. This is a part of the full flowchart given in Figure 2-1. A slope can be completely under the water surface, in this case the slope must be dredged. A slope can also be completely above the water surface, in this case there can still be water present in the pores of the soil, but there is no water table through the slope. A slope can also be partly submerged in the water. In this case a combination of the processes happening in the wet and dry slope will govern the failure process. A slope is stable under the angle of repose both above and under water, although under water processes like wave forces and flow forces often cause a lower slope angle. The stability of slopes above and under water is explained in the next two paragraphs.

2.1.1 Stability of an infinite slope of dry sand
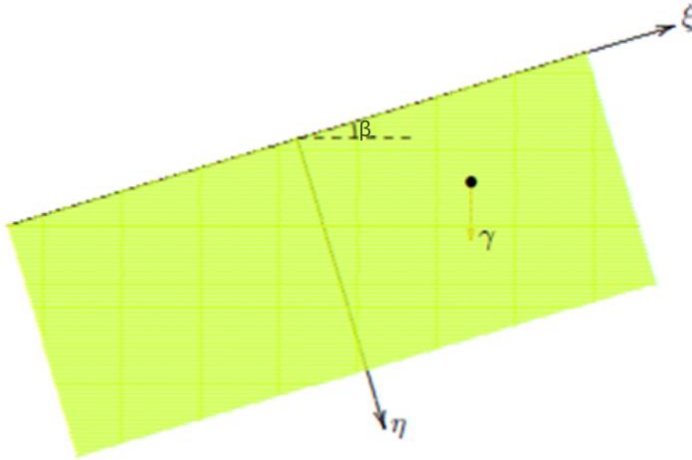
Figure 2-2: Section of an infinite slope of dry sand, Verruijt, 2007

In this case we look at an infinite slope of homogeneous frictional material, without cohesion (c=0, φ>0). The slope is infinitely long at an angle of β as illustrated in Figure 2-2. The cohesion is zero, so it can be considered the slope exists of dry sand. In this case the coordinate system is rotated according to the slope angle β. ξ is the coordinate parallel to the slope and η is perpendicular to the slope. For an infinite slope in dry sand, the equilibrium of forces can be described as (2.1) and (2.2), (Verruijt, 2007):

$$\frac{\partial \sigma_{\xi\xi}}{\partial \xi} + \frac{\partial \sigma_{\eta\xi}}{\partial \eta} + \gamma \sin\beta = 0 \tag{2.1}$$

$$\frac{\partial \sigma_{\xi\eta}}{\partial \xi} + \frac{\partial \sigma_{\eta\eta}}{\partial \eta} - \gamma \cos\beta = 0 \tag{2.2}$$

There is no water in the pores of the dry sand so all the stresses in the above equation are effective stresses. It can be assumed that the state of stress is independent of the distance in ξ, because it is an infinite slope. In that case it follows (Verruijt, 2007):

$$\sigma'_{\eta\xi} = -\gamma\eta \sin\beta \tag{2.3}$$

$$\sigma'_{\eta\eta} = \gamma\eta \cos\beta \tag{2.4}$$

Combining these equation gives:

$$\frac{|\sigma'_{\eta\xi}|}{|\sigma'_{\eta\eta}|} = \tan\beta \tag{2.5}$$

According to the Mohr-Coulomb failure criterion, for a cohesionless material the ratio in (2.5) cannot be larger than tan φ. This means that β cannot be larger than φ. The safety factor (F_s), which is independent of γ, can be calculated as given in (2.6):

$$F_s = \frac{\tan\varphi}{\tan\beta} \tag{2.6}$$

If F_s>1, the slope is stable and if F_s<1, the slope is unstable and will fail until the angle of the slope is decreased to at least φ. The safety factor F_s is independent of the volumetric weight γ of the material. This theory proves that the maximum angle of a stable slope equals the angle of internal friction for a cohesionless material. This property only holds if the soil is completely dry, only a small amount of water can increase the stable slope angle dramatically.

2.1.2 Stability of an infinite slope under water
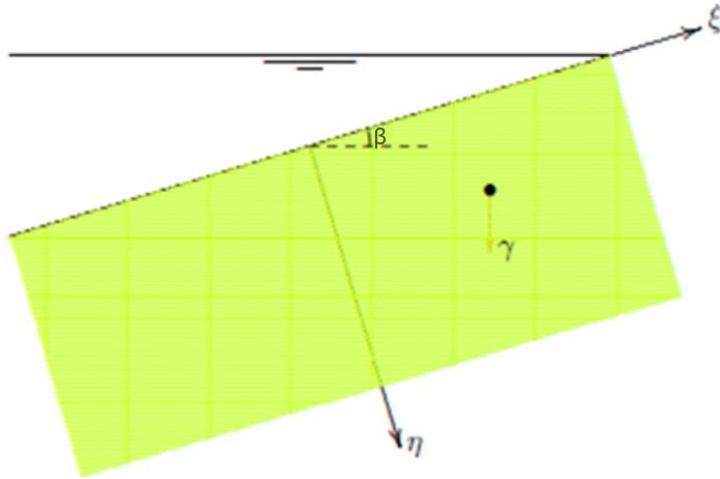
Figure 2-3: Section of an infinite slope of wet sand Verruijt, 2007

For an infinite slope under water there is an extra element for the pore pressure added to the stability equations. Also the stresses are not effective: $\sigma_{\xi\xi} = \sigma'_{\xi\xi} + p$ and $\sigma_{\eta\eta} = \sigma'_{\eta\eta} + p$. The equilibrium stress equations in this case are as given in (2.7) and (2.8), (Verruijt, 2007):

$$\frac{\partial \sigma'_{\xi\xi}}{\partial \xi} + \frac{\partial \sigma'_{\eta\xi}}{\partial \eta} + \frac{\partial p}{\partial \xi} + \gamma \sin \alpha = 0 \tag{2.7}$$

$$\frac{\partial \sigma'_{\xi\eta}}{\partial \xi} + \frac{\partial \sigma'_{\eta\eta}}{\partial \eta} + \frac{\partial p}{\partial \eta} - \gamma \sin \alpha = 0 \tag{2.8}$$

If the groundwater is at rest, the pressure distribution is hydrostatic. In that case the pressure in the groundwater can be written as in (2.9), (Verruijt, 2007):

$$p = p_0 - \gamma_w z = p_0 + \gamma_w \eta \cos \alpha - \gamma_w \xi \sin \alpha \tag{2.9}$$

In this equation p_0 is the reference pressure at the level z=0. Substitution of (2.9) in respectively (2.7) and (2.8) gives:

$$\frac{\partial \sigma'_{\xi\xi}}{\partial \xi} + \frac{\partial \sigma'_{\eta\xi}}{\partial \eta} + (\gamma - \gamma_w) \sin \alpha = 0 \tag{2.10}$$

$$\frac{\partial \sigma'_{\xi\eta}}{\partial \xi} + \frac{\partial \sigma'_{\eta\eta}}{\partial \eta} - (\gamma - \gamma_w) \sin \alpha = 0 \tag{2.11}$$

These equations are almost the same equations as the one for a dry slope given in (2.1) and (2.2). The only difference is the volumetric water density in this equation. The safety factor is independent of γ, so it follows that the same safety factor as in (2.6) is valid for a slope under water:

$$F_s = \frac{\tan \varphi}{\tan \alpha} \tag{2.12}$$

So a slope under water can also maintain an angle of φ according to theory, the same angle as the angle of repose in dry sand. However, in practice this angle is usually smaller, because the water disturbs the slope by erosion, waves or flowing groundwater.

2.2 Slope above water

If a slope is situated completely above the water surface, there are two options. It can consist of a completely dry soil which has no cohesion. In this case when the slope is disturbed, the grains will flow down the slope until the angle of repose is reinstalled. This is only the case when there is no water present in the pores. If the soil is partly saturated, the water can give the soil a cohesion. In this case the slope can be stable at much higher slope angles. It depends on the cohesion whether the slope will fail. The failure will happen along a slip surface. The question if the slope will fail and in what way it will fail can be answered by using a limit

Figure 2-4: Dry or wet sand

equilibrium method. There are several limit equillibrium methods that use a safety factor to indictate if a slope will fail along a certain slip surface. These methods can be used to calculate the behaviour of a slope with cohesion.
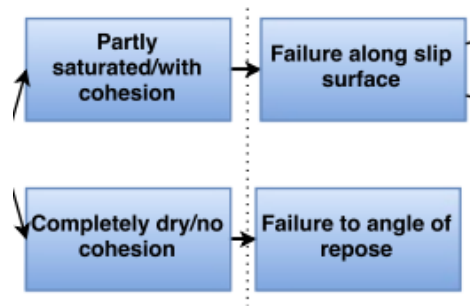
2.2.1 Limit equilibrium methods

Various approximate methods have been developed for the analysis of slopes of arbitrary shape and composition above the water level as illustrated in Figure 2-6 (Verruijt, 2007). These methods define a safety factor F_s for a certain circular slip surface. The safety factor of many slip surfaces is calculated and the slip surface with the lowest safety factor is the critical slip surface. The safety factor can be calculated using different methods that make different assumptions. The two most used methods will be explained in this paragraph.
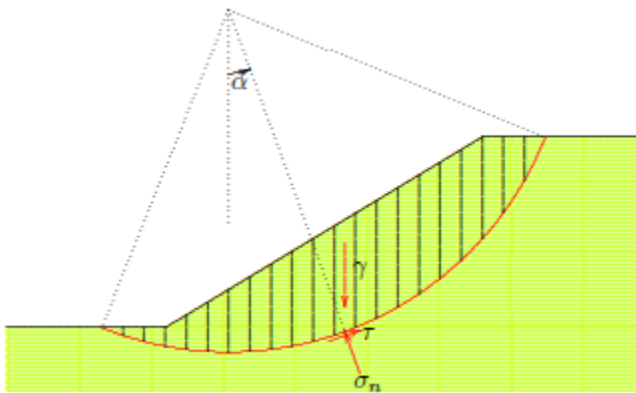
Figure 2-6: Section of a circular slip surface, Verruijt, 2007

Figure 2-5: Limit equilibrium methods

It is assumed that the soil fails along a circular slip surface. The soil above the slip surface is subdivided into a number of slices bounded by vertical interfaces. At the slip surface the shear stress is τ, which is linked to the safety factor as follows:

$$\tau = \frac{1}{F_s}(c + \sigma'_n \tan \varphi)$$

(2.13)

The safety factor F is assumed to be the same for all slices. The equilibrium equation for every slice is the equation of equilibrium moments with respect to the slip surface as given in (2.14):

$$\sum \gamma hbR \sin \alpha = \sum \frac{\tau bR}{\cos \alpha}$$

(2.14)

h = height of a slice
b = width of a slice
γ = volumetric weight of a slice
R = radius of circle

If all slices have the same width, equations (2.13) and (2.14) can be combined and it follows:

$$F_s = \frac{\sum[(c + \sigma'_n \tan\varphi)/\cos\alpha]}{\sum \gamma h \sin\alpha} \tag{2.15}$$

This is the basic equation for the calculation of the safety factor of a certain slip surface. There are a few limit equilibrium methods that approach this equation in a different way. The procedure needs to be repeated for many slip surfaces, until the slip surface with the lowest safety factor is found.

2.2.1.1 Fellenius

The first limit equilibrium method is the Fellenius method, which is the oldest method. It is often called the ordinary method. This method assumes that there are no forces between the slices, so only the weight of a slice, the shear stress τ and the normal stress σ_n play a role. By expressing the normal stress into the known weight with respect to the direction of the normal stress (perpendicular to the slip surface), the basic Fellenius equation becomes:

$$F_s = \frac{\sum[(c + (\gamma h \cos^2\alpha - p)\tan\varphi)/\cos\alpha]}{\sum \gamma h \sin\alpha} \tag{2.16}$$

This is the Fellenius equation for calculating the slope stability of an arbitrary slope. This method could in theory also be used for slopes completely under the water surface. In that case the factor for the volumetric weight under water, $(\gamma - \gamma_w)h$ instead of γh must be used in (2.16). Also the excess water pressure with respect to the hydrostatic water pressure should be used for p. However, this is a somewhat artificial method which is rarely used.

2.2.1.2 Bishop

The second method is the Bishop method. In this method the forces between the slices are taken into account. It is assumed that the resultant force between the slices is horizontal. The safety factor is calculated as follows:

$$F_s = \frac{\sum \dfrac{c + (\gamma h - p)\tan\varphi}{\cos\alpha\,(1 + \tan\alpha \tan\varphi\,/F_s)}}{\sum \gamma h \sin\alpha} \tag{2.17}$$

The disadvantage of this method is that the safety factor also appears on the right side of the equation. This means the safety factor must be derived iteratively. This will take computers longer to derive a result. If φ = 0 Fellenius and Bishop give the same answer, but if this is not the case, the Bishop method usually gives a slightly lower value for F_s than the Fellenius method.

2.3   Slope under water

Three fundamentally different types of large bank failures can be distinguished, liquefaction slope failures and breach failures are the main failure processes. Breaching will be divided into the sub processes of stable and unstable breaching.

There are different methods a submerged slope failure can be initiated. A slope failure can start naturally caused by a little earthquake or other vibrations. It is also possible that a failure is initiated by wave or groundwater flow action. This paper will be focused on the initiation of a failure by subaqueous mining or dredging. One method of subaqueous soil mining is dredging from a sandpit with a suction dredger. The suction pipe is lowered several meters below the bed and a cylindrical crater with a very steep slope is formed around the suction mouth, breaching follows. Turbulent density flow follows down slope. At the base of the slope, a gradual transition into a gentler slope occurs. Another way of causing slope failure by dredging is by undercutting an existing slope. Depending on the dimensions of the cut, several failure mechanisms can be initiated.

2.3.1 Liquefaction

Liquefaction is the process where a mass of soil suddenly starts behaving like a viscous fluid, so that it is able to flow out over very gentle slopes (Silvis & de Groot, 1995). A liquefaction flow slide can be initiated by cyclic stresses, earthquakes or by tidal or river flow (Van den Berg et al., 2002). The main process which initiates liquefaction is increased pore pressure. When pore pressure increases, effective stresses decrease. This decreases the strength of the soil. When the point is reached that the effective stresses in

Figure 2-7: Underwater slope failure methods

the soil have decreased enough, the soil starts behaving like a fluid and starts sliding down.

In contrast to breaching, liquefaction often occurs in loosely packed sands. If the pores are filled with water, loose soils will tend to compact during shearing, but they cannot withstand quick compaction easily. The grains will not decrease in volume, so all the volume decrease is in the pores, which causes an increasing pore pressure. This is why loosely packed soils are very liquefiable. A big amount of soil will slide down in one action. This type of failure happens over a time interval in the range of seconds.

2.3.2 Breaching

Breaching failure refers to a thin surficial layer of sediment and is restricted to steep slopes underwater, composed of medium to densely packed sand. The initiation of the steep slope causes shearing of the outer layer of the slope, due to gravity. This shearing causes the pore volume in the outer layer to expand. The water cannot fill up the extra pore space immediately which causes a temporary under pressure in the soil. The effect of expanding pore space due to shearing is called dilatancy. The under pressure in the sand caused by the dilatant behaviour can maintain a steep (up to vertical) subaqueous slope. The slope will gradually fail due to inflow of water into the pores. This is followed by individual particles raining down the slope (Van den Berg et al., 2002). De Groot et al. (2009) described this as thin layers of sand that become unstable and flow down the slope. In contrast to liquefaction failure, breaching can take several hours until the failure is finally ended. Both types of failure appear to produce a similar morphology of the outflow (Van den Berg et al., 2002). However, the processes of sand transport after the initial failure are quite different.
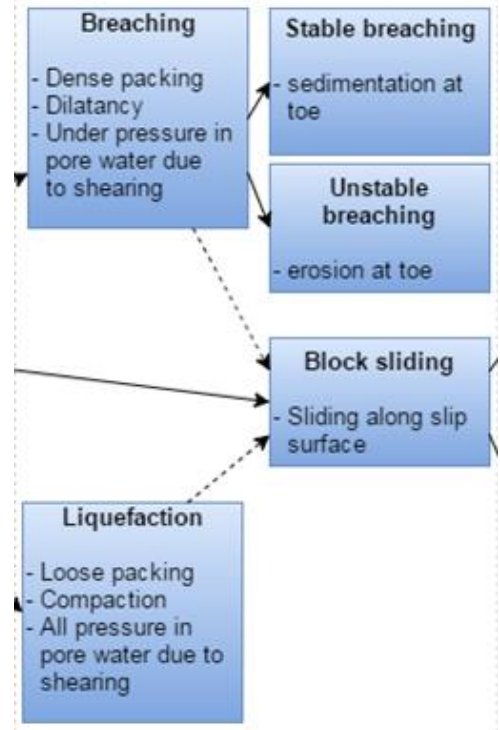
Breaching as a failure method for dredging is the most important failure mechanism analysed in this report, so it will be explained in detail in the following paragraphs. On the surface of a vertical breaching wall there is a thin layer of soil where particles slowly rain down the wall. The soil mass just behind the raining curtain is just in equilibrium with the vertical forces. The breaching wall retrogrades with a horizontal velocity described as the wall velocity v_{wall}. A square unit block of soil surfacing at the active breaching wall will be analysed. The block has a volume of ΔL^3 and it is just in equilibrium before it will undergo breaching. Figure 2-8 illustrates all the forces on this volume of soil. The forces acting on this volume are in equilibrium and will be described in this paragraph.
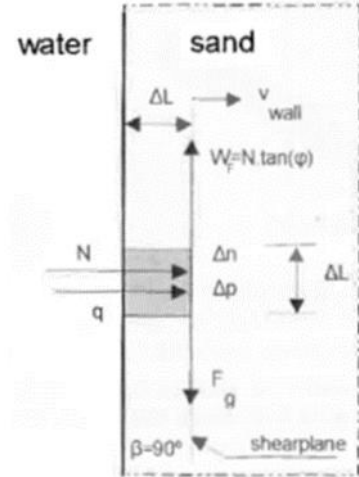
Figure 2-8: Breaching process (Van der Schrieck, 2012)

2.3.2.1   *Gravity force*
The volume ΔL^3 is pulled down by a gravity force F_g. In case of a vertical breaching wall, the gravity force acts parallel to the wall.

2.3.2.2   *Normal force due to under pressure*
The unit volume of soil is held against the wall by a normal force $N = \Delta p \cdot \Delta L^2$ caused by an under pressure in the pore water of Δp. The under pressure is caused by the water which has to flow into the soil to the shear plane. The inflow is necessary due to the dilatancy effect caused by the shearing of the outer soil layer.

2.3.2.3   *Dilatancy*
The grains can only shear when the pore volume increases to a level equal to or larger than the critical porosity n_{crit}. A certain amount of dilatancy (Δn) must occur to loosen the soil from the in-situ position n_0 to n_{crit} before shearing of the soil is possible. Figure 2-9 shows the permeability of several types of Dutch sand as a function of porosity given in percentage. It is visible that the relation between the maximum porosity and the critical porosity is variable. The relation is approximated as $n_{crit} = n_{max} - 0.01$ (Van der Schrieck, 2012). In this relation, n_{crit} and n_{max} are given in ratios.
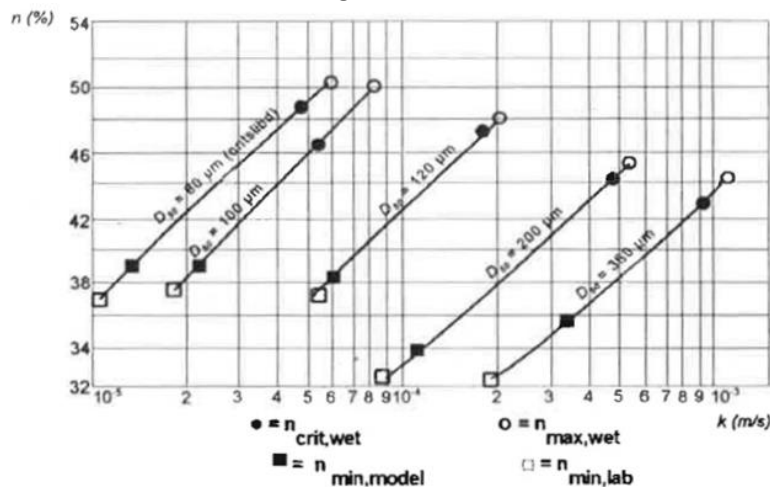
Figure 2-9: Porosty vs permeability per D_{50} (Van der Schrieck, 2012)

2.3.2.4   *Friction force*
The normal force caused by the pressure difference causes friction of the soil unit. This friction force is $W_F = N \cdot \tan \varphi$ and it is in equilibrium with the gravity force acting down on the block.

2.3.2.5 Wall velocity

Due to the raining down of particles, the wall retrogrades with a constant velocity v_{wall}. There is a continuous inflow of water $q = v_{wall} \cdot \Delta n$ that fills the enlarged pore space. This inflow q causes the under pressure Δp, which is described by Darcy's law: $q = k_0 \cdot i$. In this equation k is the permeability of the outer layer of soil and i is the gradient $\Delta H/\Delta L = \Delta p/(\rho \cdot g \cdot \Delta L)$.

The wall velocity is described as the horizontal velocity of the wall. It is the most important parameter concerning the breaching process. The wall velocity is only dependent on the soil and will be further elaborated in the following paragraph.

2.3.2.6 Analysis of the wall velocity
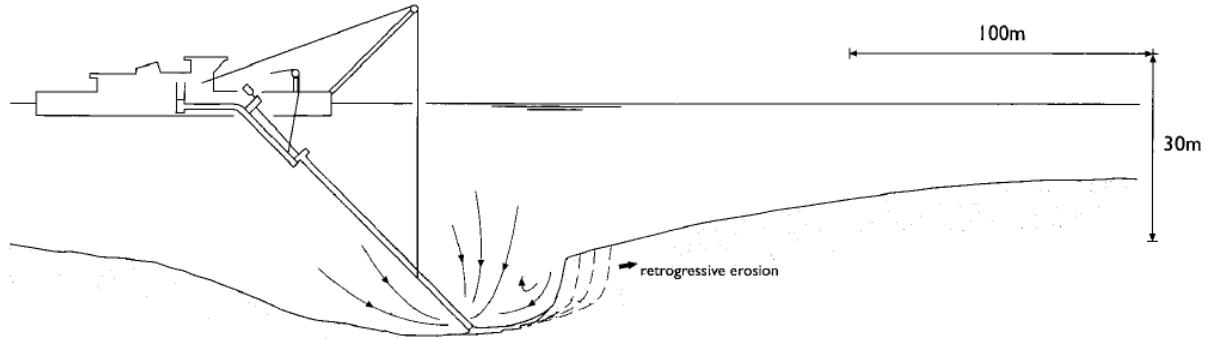
Figure 2-10: Retrogressive erosion during dredging, Van den Berg, 2002

The permeability of the slope is important in this process as it has a big influence on the amount of particles released from the slope. Water needs to infiltrate into the wall to release particles. As more and more particles flow down, the wall moves backwards while the angle stays approximately the same. The wall retrogrades at a constant velocity, the horizontal value of this speed is called the wall velocity v_{wall}. The wall velocity is mainly a function of permeability k_0 (m/s) and, to a lesser extent, the internal friction angle, relative particle density, initial porosity and porosity increase during dilatancy. A rough approximation of the wall velocity is: $v_{wall} = 25 \cdot k_0$

2.3.2.7 Derivation of the wall velocity

There are several ways to obtain an equation for the wall velocity, but the final result is always similar. The amount of water which flows into the wall per unit of time is approximately:

$$q = \Delta n \cdot v_{wall} = \frac{(n_1 - n_0)}{(1 - n_1)} \cdot v_{wall} \tag{2.18}$$

This flow inhibits a force on the wall with the magnitude of $\rho_w \cdot g \cdot \Delta L \cdot i$. In this equation, i is the gradient of the inward flow perpendicular to the wall and can be described as $i = q/k_1$. k_1 is the permeability of the outer layer of the wall, this is the layer where shearing takes place. This value is usually higher than the original permeability of the soil k_0. The thin surficial layer is in balance when the force of the inward flow is neutralised, this is given in (2.19):

$$\rho_w \cdot g \cdot \Delta L \cdot i = (1 - n_0) \cdot (\rho_s - \rho_w) \cdot g \cdot \Delta L / \tan \varphi \tag{2.19}$$

A combination of (2.18) and (2.19) gives for v_{wall}:

$$v_{wall} = k_1 \cdot \frac{1 - n_0}{\Delta n} \cdot \frac{\rho_s - \rho_w}{\rho_w} \cdot \cot \varphi \tag{2.20}$$

In this equation $\Delta n = (n_1 - n_0)/(1 - n_1)$ and it is assumed that the breaching wall has an angle of $\beta = 90°$ with the horizontal. It is not always the case that the breaching wall is perfectly vertical. The angle β can be smaller than 90° and must be larger than the internal angle of friction φ. This angle can be incorporated into (2.20) as given in (2.21):

$$v_{wall} = k_1 \cdot \frac{1 - n_0}{\Delta n} \cdot \frac{\rho_s - \rho_w}{\rho_w} \cdot \frac{\sin(\beta - \varphi)}{\sin \varphi} \tag{2.21}$$

2.3.2.8 Elimination of k_1

The value k_1 is the permeability of the outer layer of the breaching wall, which is higher than the initial permeability k_0. The initial permeability can be measured in the field, but k_1 cannot be measured, so it cannot directly be used in prediction models. The value k_1 is still present in equation (2.20) for the wall velocity. A method is developed (Van Rhee, 2015) to eliminate k_1 from equation (2.20). It is assumed that:

$$(1 - n_0) \cdot \frac{k_1}{\Delta n} = F \cdot k_0 \tag{2.22}$$

It is assumed that F is a constant. The factor in (2.20) containing k_1 and the porosity can be replaced by $F \cdot k_0$. The factor F can be derived as given in (2.23):

$$F = \frac{(1 - n_0)}{\Delta n} \cdot \frac{k_1}{k_0} = \frac{n_l{}^3}{n_0{}^3} \cdot \frac{(1 - n_0)^3}{(n_1 - n_0) \cdot (1 - n_1)} \tag{2.23}$$

The theory (Van Rhee, 2015) makes sure that the wall velocity can be derived from ordinary field tests if it is assumed that $n_1 = n_{max}$.

2.3.2.9 Stable and unstable breaching

Two different types of breaching can be distinguished, which are illustrated in Figure 2-11. An active breaching wall moves up a slope in both processes, only the result is very different. The breaching process is called unstable when the height of the breaching wall increases. This can be caused by erosion at the toe of the wall. The erosion causes the breaching wall to increase, which causes a higher mass flow and more erosion. Unstable breaching can act as a self-reinforcing process. It is also possible that unstable breaching is caused by the phenomena that the soil has a low outflow angle, which is usually caused by a high mass flow. If the slope above the breaching wall is steeper than the outflow angle at the bottom, the wall height will increase. This will in turn cause the self-reinforcing unstable breaching process. The increase of the wall height can continue until the wall reaches the top of the slope or the bottom of the active wall reaches the sea bottom (van Rhee & Bezuijen, 1998). The active wall can cover a very large horizontal distance. This process has led to multiply shore failures around dredging sites.

During stable breaching, sedimentation is the main process at the toe of the breaching wall. The height of the active wall decreases due to the accumulation of soil at the toe of the wall. This soil blocks breaching at the toe of the wall, which decreases the wall height. If the breached soil has a higher outflow angle than the angle of the top of the slope, stable breaching will happen. Due to the decrease of the wall height, the mass flow decreases, which will cause more sedimentation. Stable breaching can act as a self-weakening process. It is possible that a stable breaching wall stops retrograding very soon after the initiation.

The outflow angle of the breached soil can be obtained by using the following empirical relation (Mastbergen et al., 1988):

$$\tan \alpha = 0.0049 \cdot D_{50}{}^{0.92} \cdot s^{-0.39} \qquad (2.24)$$

In this equation, α is the outflow angle, D_{50} is the median particle size in μm and s is the mass flow down the slope in $kg \cdot s^{-1} \cdot m^{-1}$. The outflow angle is very important for the difference between stable and unstable breaching, it is illustrated in Figure 2-11. When unstable breaching happens after cutting the toe of a slope, the production increases and only a small amount of sand needs to be cut to maintain the production level. When stable breaching is the main process, the dredger has to cut the slope continuously to maintain a high enough production level, but the process is more controlled and less dangerous.
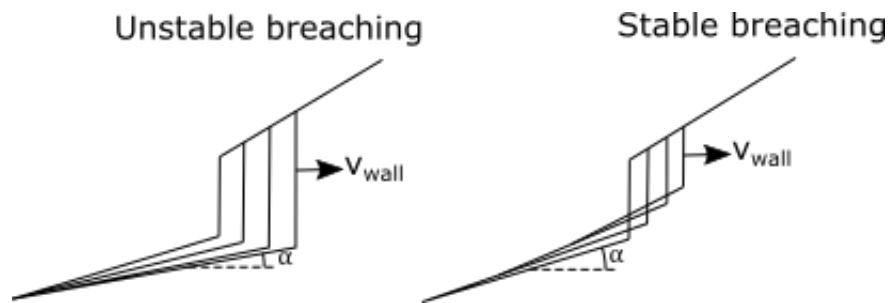
Figure 2-11: Stable vs unstable breaching

2.3.3 Block sliding

Concerning subaqueous slopes, a smaller third failure process can be identified. This third process is the failure of wedges of soil, which can happen simultaneously with breaching. The higher the active breaching wall, the higher should the under pressure be to maintain the wall. It can happen that a block of soil slides down the slope in one action, which increases the average wall velocity. The higher the active breaching wall, the higher the influence of block sliding will be on the wall velocity. For an underwater process, it is difficult to predict the exact dimensions of the sliding block and what the influence on the breaching process is. The process is often incorporated in breaching by introducing an increased wall velocity for high breaching walls.

2.4 Influence of the density flow on the slope

At a slope steeper than the natural angle-of-repose, the downslope component of gravity is larger than the shear resistance, unlimited erosion would result until a slope smaller than the angle-of-repose is retained. This is true even without any flow velocity induced shear stress. However, the erosion rate is retarded due to the under pressure created by the dilatancy which is caused by shearing of the outer layer of the slope. The wall velocity v_{wall} appears to be independent of the local flow conditions.

The sand particles released from the breaching wall form a density flow downslope. If the breaching wall is high enough, the density flow causes erosion of the breach surface. For lower breaching walls, sedimentation effects can occur on the slope. The eventual displacement of the bed slope is a combination of sedimentation and erosion. Erosion means that a smaller slope is necessary for a given horizontal slope speed, which is why in practice the slopes involved in breaching are often curved, with a steeper slope at the top than at the toe.

The influence of the density flow on the erosion of the bed is extensively explained in Van der Schrieck, 2012. In this report, the erosion velocity will not be taken into account directly. The empirical relation given in (2.24) will be used to describe the outflow of soil after breaching.

2.5   Dredging method

There are several types of dredgers which can dredge a submerged slope. All of the dredgers have a cutter and a mechanism to transport it to the surface. A schematic image of a cutter suction dredger is given in Figure 2-12. All of the dredgers have a cutter ladder with a cutter head at the end. The cutter head cuts the soil and a pump system pumps the soil up to the vessel. The spud poles on the back make sure the ship stays in position and only rotational motion around the spud pole is possible. The working spud pole is lowered in the subsurface to keep the vessel in place. The vessel can rotate around the working spud pole. The side anchors stabilise the cutter head. A lateral swing can be made by tightening one of the side anchors and loosening the other one. A top view of the lateral swinging motion is given in Figure 2-13. A forward motion of the cutter head is regulated by the spud poles. Once the cutter head reaches the end of a lateral swinging stage, a forward step has to be made. The entire vessel is stepped forward a certain distance by pushing back on the spud pole by moving it relative to the vessel. A step is made by moving the spud carriage backwards.

After a number of steps the spud carriage cannot move backwards anymore. It has to be repositioned by lifting the working spud pole up, moving the spud carriage forward and reinstalling the working spud pole in the subsurface. During this process the auxiliary spud pole is lowered in the subsurface to maintain the stable position of the vessel.

The dredger can make two different types of swings. A cut swing is a swing executed just after a forward step. The cutter moves through the initial slope and has to actively cut the soil. During this swing a new breaching wall is created. The second type of swing is a clean-up swing. During this type of swing there has not been a forward step and the cutter moves through the breached soil which is flowing down the slope. There is no active cutting needed, the cutter only collects the loose material flowing towards it. If the mass flow is high enough many clean-up swings can be executed while keeping a constant production level.
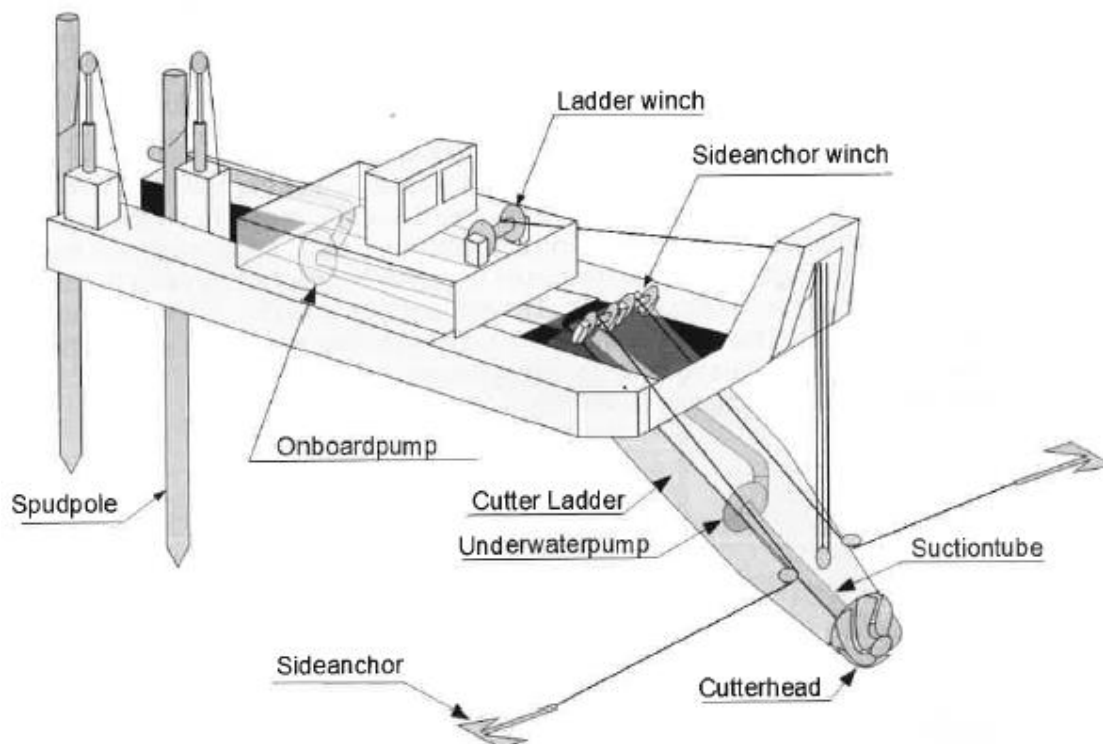
Figure 2-12: Cutter suction dredger (Van der Schrieck, 2012)
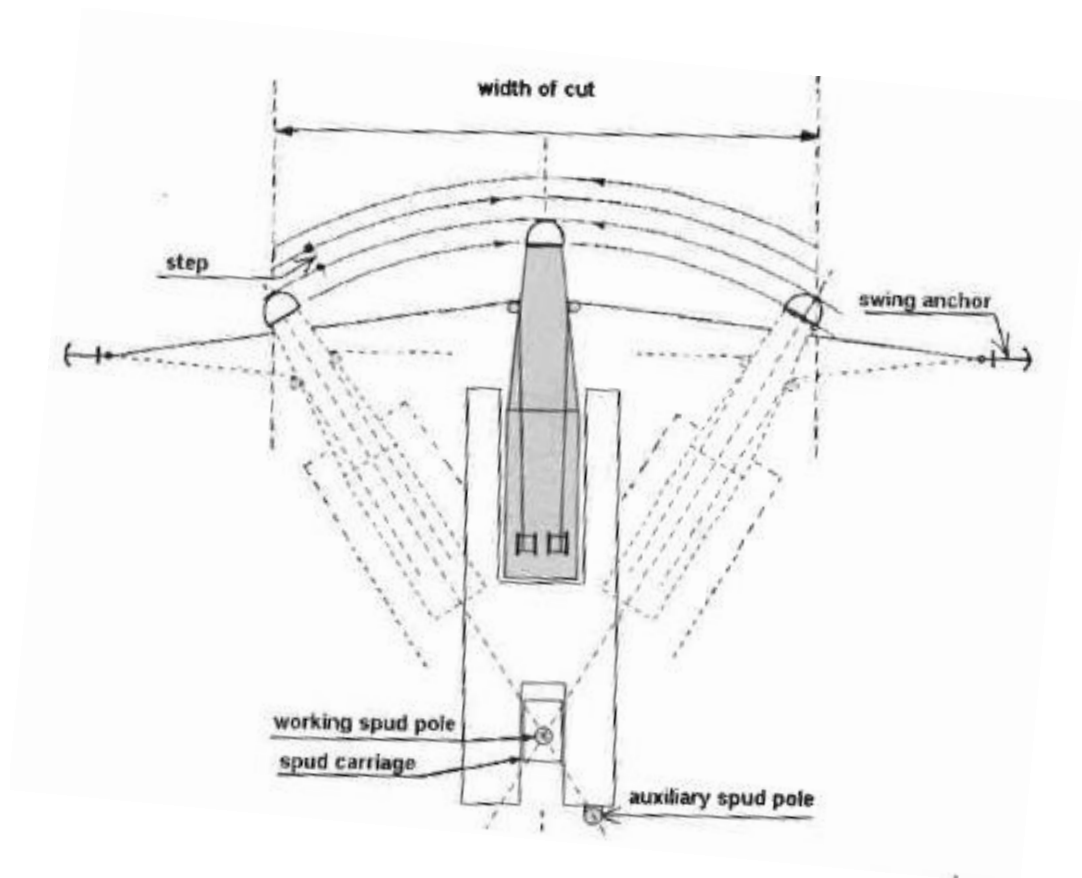
Figure 2-13: Swinging motion (Van der Schriek, 2014)

3 Breaching model

In order to investigate a breaching slope, a model is developed for this research. In this chapter the method of the breaching model will be explained and results will be presented. It is a two dimensional model which can predict the behaviour of a slope in the case when breaching is initiated. All volumes will be calculated in two dimensions or assuming a length in the third dimension of 1 meter.

3.1 Scenario

The initial situation is a completely submerged stable slope of soil. The slope can in theory be of arbitrary shape as long as the slope is never steeper than the angle of repose (φ). The slope can in theory be of arbitrary height, but in reality it has a maximum height. It is assumed the soil in the slope is packed dense enough that it will cause dilatancy when it is sheared. After the initial situation the toe of the slope is cut, which makes the slope unstable. A vertical wall of a known height is created at the toe of the slope. The material cut is removed from the model. This is the situation after which breaching will start, from this point on no volume will be removed from the model.

3.2 Method and physics

In this paragraph the method and the physics on which the breaching model is based will be explained in detail. Schematic figures will be given to clarify the method and the parameters.

3.2.1 Basic process

The breaching behaviour of the slope is modelled in a stepwise manner, every step is identical. Figure 3-1 gives a schematic illustration of the first two steps of the process. The initial wall height $h_{wall,1}$ is created by the initial cut and is given as an input parameter. The step size (Δx) defines the accuracy of the model. Every step starts with the volume $V_{breach,n}$ still in the initial position. the subscript n is the number of the step (n=1,2,3,…). The wall velocity (v_{wall}) is a soil parameter and is independent of the geometry of the slope. As explained before, the wall velocity can be determined with equation (3.1):

$$v_{wall} = k_1 \cdot \frac{1 - n_0}{\Delta n} \cdot \frac{\rho_s - \rho_w}{\rho_w} \cdot \cot \varphi \tag{3.1}$$

Based on the wall height, the mass flow of soil down the slope can be calculated as given in (3.2). The initial wall height ($h_{wall,1}$) caused by the cutter is referred to as h_{cut} later in the report.

$$s_n = h_{wall,n} \cdot v_{wall} \cdot (1 - n_0) \cdot \rho_s \tag{3.2}$$

The outflow angle (α_n) can be calculated by using the relation as given in (3.3) based on tests carried out by Mastbergen et al. (1988). These test were done with mass flows of s < 10 kg·s^{-1}·m^{-1}. For mass flows higher than 10 kg·s^{-1}·m^{-1}, the model extrapolates the equation. For mass flows of s < 1 kg·s^{-1}·m^{-1}, the outflow of soil will be under a constant angle of repose. The angle can never be larger than the angle of repose (φ) of the soil. In the case that (3.3) gives an angle α_n larger than φ, α_n is taken equal to φ.

$$\tan \alpha_n = 0.0049 \cdot D_{50}{}^{0.92} \cdot s_n{}^{-0.39} \tag{3.3}$$

The angle α_n is the angle at which the volume will flow out during this step. Erosion of the bed at the toe of the wall is not taken into account in this model. The volume $V_{breach,n}$ is the volume which will fall down the wall during this step. The volume is estimated by equation (3.4):

$$V_{breach,n} = \Delta x \cdot h_{wall} \tag{3.4}$$
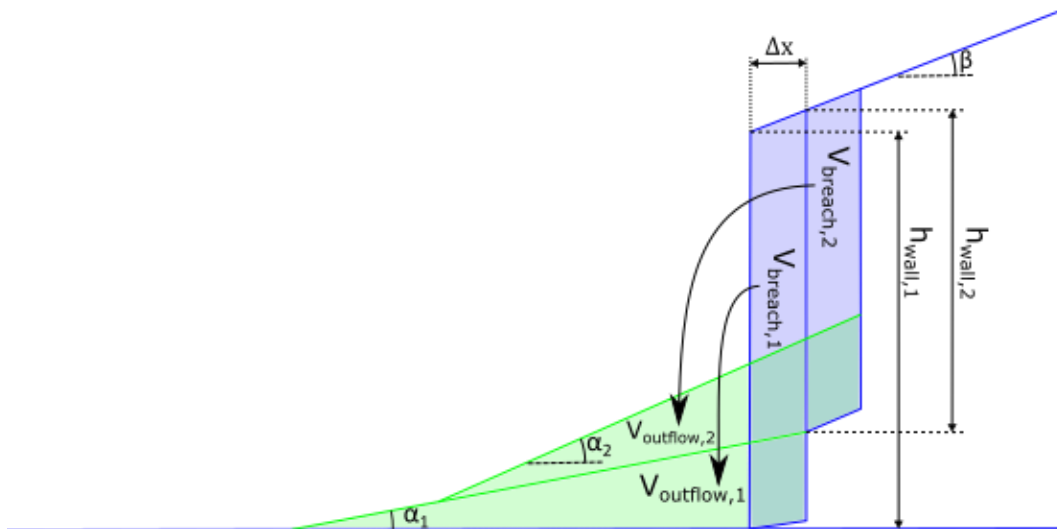
Figure 3-1: Breaching model process

The volume $V_{breach,n}$ is released from the wall by shearing. Due to dilatancy the porosity increases from n_0 to n_1 when it flows down the slope. n_1 is the porosity of the outflow material. The volume of $V_{breach,n}$ increases to $V_{outflow,n}$ as given in (3.5):

$$V_{outflow,n} = V_{breach,n} \cdot \left(\frac{1 - n_0}{1 - n_1}\right)$$

(3.5)

The volume $V_{outflow,n}$ is positioned under an angle α_n as illustrated in Figure 3-1 with the right side of $V_{outflow,n}$ aligned with the right side of $V_{breach,n}$. All the actions of the step are now finished and a new step can start. The wall is moved up the slope with the step size Δx. The top of the wall is elevated due to the angle of the slope. The bottom of the wall is elevated due to the build-up of breached material. The new wall height can be calculated as given in Figure 3-1, this is the start of a new step. As many steps are executed until the wall height is reduced to zero. The placement of a volume at the toe of the breach is a complicated process in the model. It is extensively explained in Appendix A. An example of how the build-up of soil volume after each step looks in the model is given in Figure 3-2.
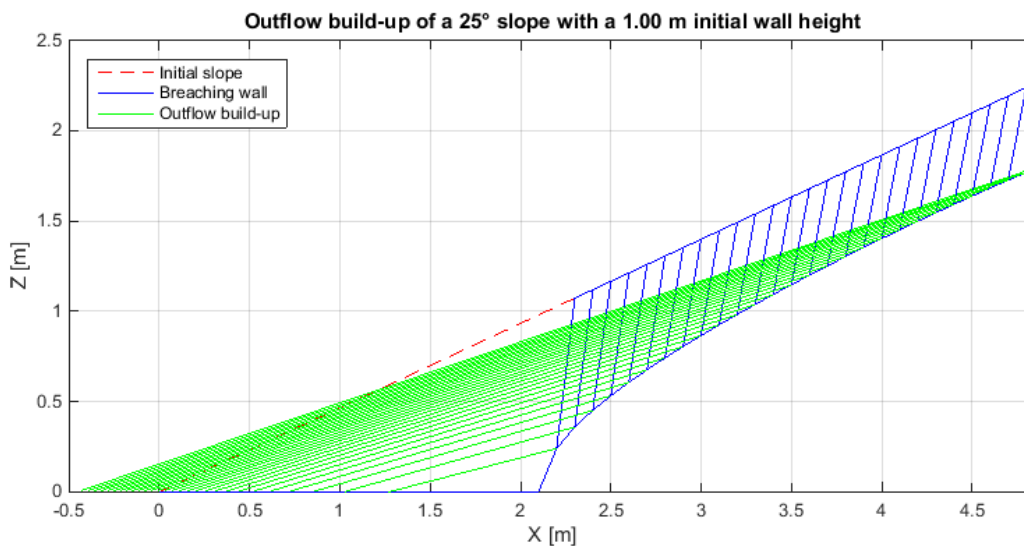
Figure 3-2: Outflow build-up modelling

3.2.2 Conservation of mass

The correctness of the model can be proven by ensuring conservation of mass. The removed mass by breaching should be equal to the outflow mass. The volume of the outflow soil is larger due to the dilatancy, but the mass of the particles must stay the same. In Figure 3-3 the cumulative mass is plotted versus the time for the soil before and after breaching.
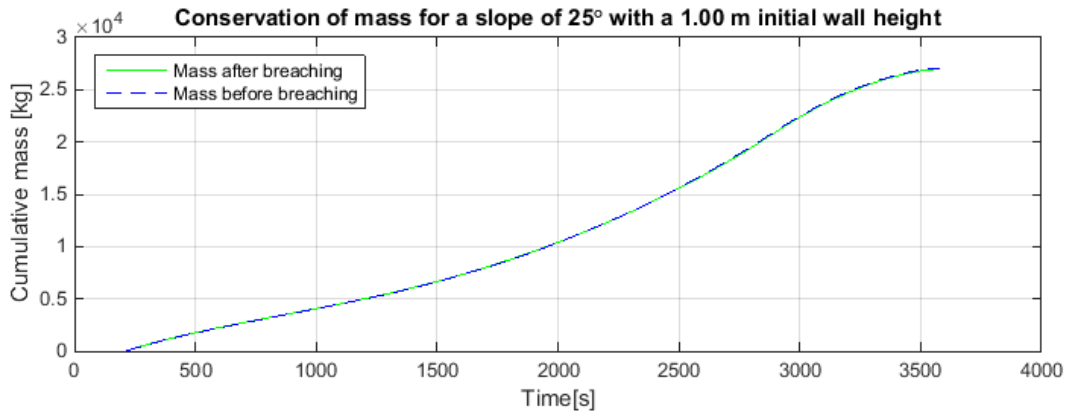
Figure 3-3: Conservation of mass

V_{breach} is the removed volume and $V_{outflow}$ is the outflow volume. This graph can be generated for every simulation and proves the correctness of the maths behind the model.

3.3 Model validation experiment

The breaching model is compared with lab tests executed by IHC Mining. These tests are conducted in a basin filled with water, the initial situation in given in Figure 3-4a. The right side of the basin is filled with soil and compacted in order to create a dilative soil. The soil is kept in place by a dividing wall in the middle of the basin. The soil height in the initial situation is 8 cm. The dividing wall is removed and the soil starts breaching with an initial breaching wall height similar to the height of the layer.

The difference between the lab test and the dredging situation where the model is based on is the scale. The model has a limit in the height of the soil layer. If the initial situation has a layer height smaller than 50 cm, the model becomes unreliable, so the lab test is compared with the model taking a scale factor 10 into account. This will give some insight in the phenomena of scale enlargement. In the lab test the production is very small due to the small layer of soil of only 8 cm. This causes a high outflow angle almost equal to the angle of repose. This high outflow angle stays constant throughout the whole test. If the scale would be enlarged, the production would be larger and the outflow angle would be smaller.
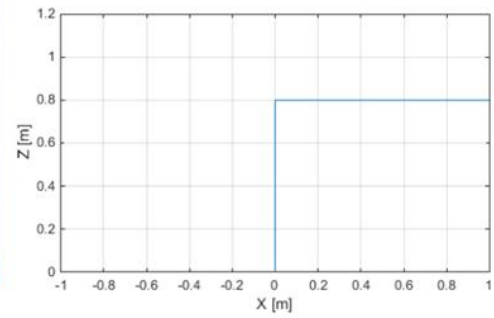
a)   Initial situation
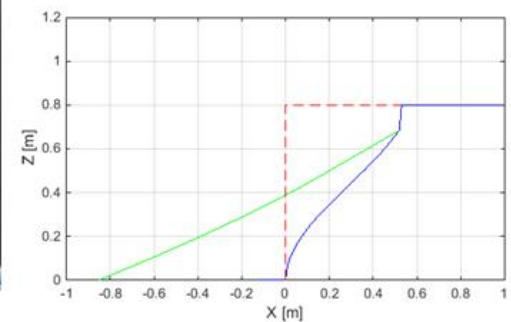
b)   Lab test result

Figure 3-4: Breaching lab test

Figure 3-4b shows the end result of the lab test. The soil has reached an outflow distance of 5.5 cm. The model predicts an outflow distance of 8.2 cm. This difference is caused due to the effect of scale enlargement. The shape of the dense soil is very similar in the model and the lab test, this gives confidence that the model predicts the breaching behaviour in a right way. The lab test shows that the top of the layer settles a little bit, which is not visible in the lab test, this phenomena is small in this lab test and does not have a large influence on the process. However it is unknown how much this phenomena will increase if the scale is enlarged.

The model shows a similar shape to the lab test and proves that the process is correctly implemented in the model. The differences which are still present are caused by scale differences. To make a better validation of the model and to understand the influence of scale enlargement, more tests at different scales must be conducted in the future.

3.4   Results and discussion
The breaching model can predict the breaching behaviour of a slope of soil of arbitrary shape. Different parameters can have an effect on the behaviour. In this paragraph some of the effects on the behaviour will be explained. The eventual influence on the dredging plan can be large, it will be explained with graphs and figures. The results are based on a reference soil with the parameters given in Table 3-1.

Table 3-1: Reference soil parameters

Parameter	Value
k_0	$1.0 \cdot 10^{-4}$ m/s
φ	30°
D_{50}	150 µm
n_0	0.40
n_1	0.45
ρ_s	2650 kg/m^3
ρ_w	1000 kg/m^3

3.4.1 Stable versus unstable breaching

An important aspect of a field investigation is whether a slope will develop as a stable or an unstable breaching wall. An unstable breaching wall will result in a much higher and longer mass flow than a stable breach. The difference between stable and unstable breaching depends on the angle and geometry of the initial slope, the initial wall height and the soil characteristics. The model can predict if the slope in combination with the cut will develop a stable or an unstable breach. An example of the influence of the slope angle on the breaching process is given in Figure 3-5. These figures give the result of an initial cut of 1.0 meter for three different slope angles. The initial cut is the vertical wall created by the cutter. After the initial cut, the vertical wall starts breaching, which means the height of this wall can increase or decrease. The model calculates the top of the undisturbed soil and the top of the breached soil. In all the breaching sections, the area under the top is filled with the corresponding colour in order to clarify the figures. The initial angle of the slopes is constant with a maximum height of 5.0 meter.

Figure 3-5a gives the result of a slope of 20°. The cut has a small influence on the slope, because only a small part of the slope is disturbed due to breaching. This is a stable breach. Figure 3-5b gives the result of a slope of 25°. In this case the breach continues until the top of the slope is reached. The outflow of soil is much larger and the mass flow will continue much longer. This is an example of an unstable breach. If the slope is even steeper such as in Figure 3-5c, the outflow distance will be even larger and the disturbance at the top of the slope will be larger. For this type of soil and initial wall height, the transition between stable and unstable breaching is somewhere between 20° and 25°. For a dredging application it is important to be able to predict this transition point in order to estimate the production.

a) Slope angle is 20°

b) Slope angle is 25°
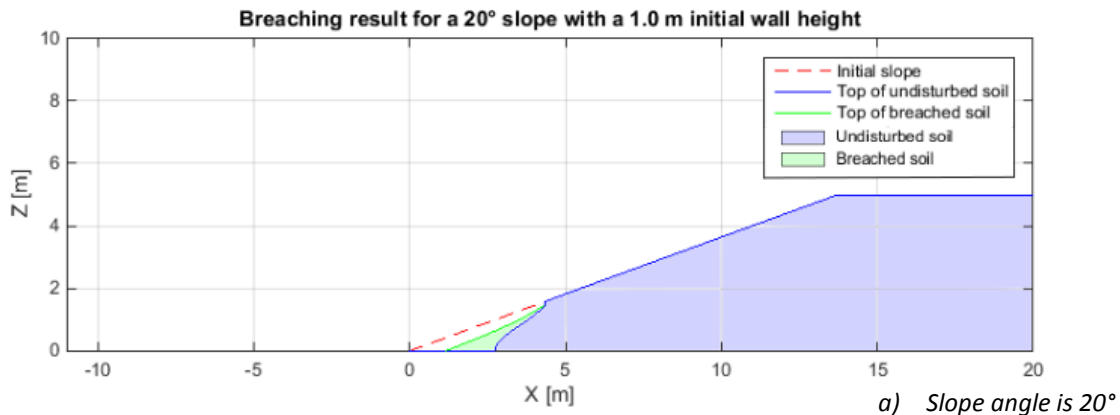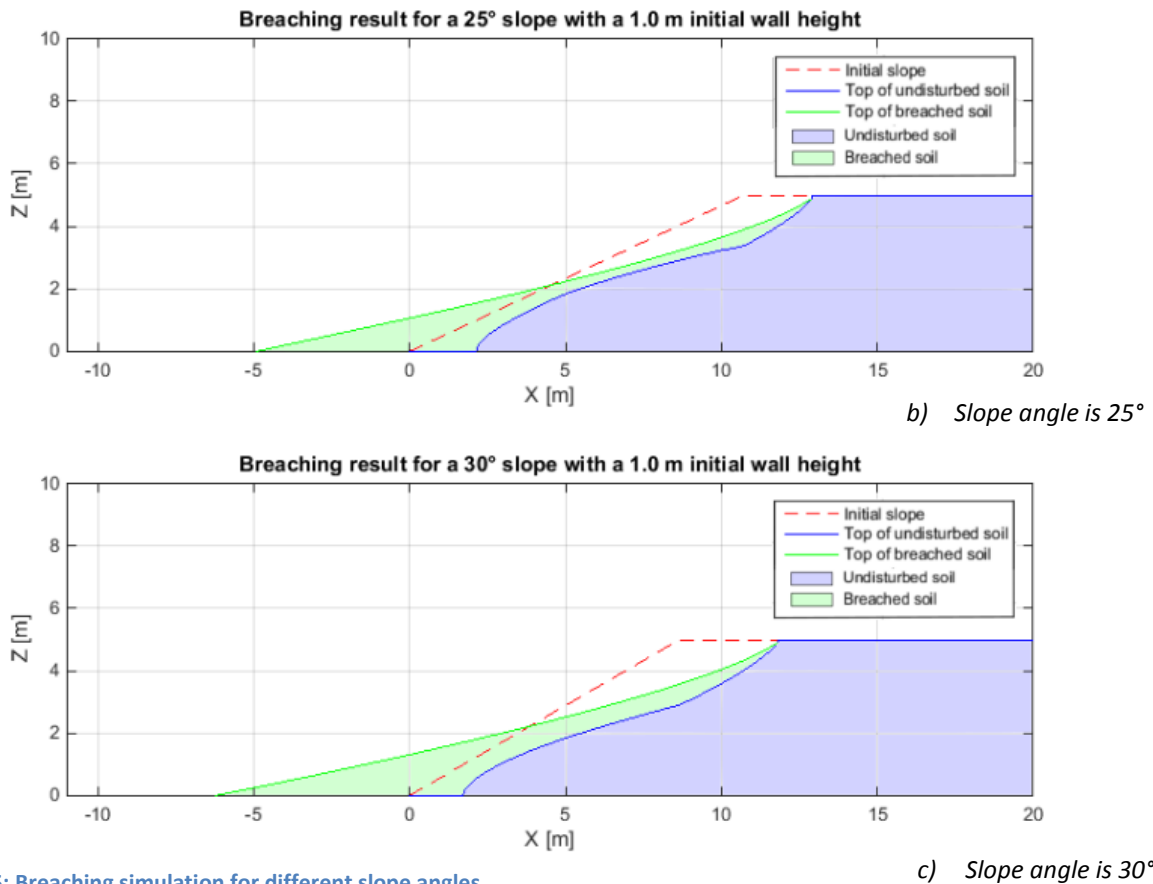
Figure 3-5: Breaching simulation for different slope angles

c) Slope angle is 30°

For the mining industry it will be important to create a breach which continues for a long time. An unstable breach is unwanted, because it is unpredictable and can cause spillage and damage to the shore. The best scenario is to initiate a breach, which is just not unstable. This way the dredger can stay at the same position for a longer time collecting the soil. For the dredging of a sea-lane or a channel, it is more important to create the demanded geometry of the slope. In this case more stable breaches are initiated in order to prevent damage the coast line at the top of the slope.

In order to determine the maximum cutting depth at which the breach is stable, several simulations of the breaching model can be executed with different cutting depths. Figure 3-6 gives the results of these simulations for the three slopes given in Figure 3-5. The wall height is plotted versus the time. Every line start with a linear increase, this is the cutting time. The cutter moves horizontally forward with a constant velocity while cutting the soil. When the chosen cutting depth is reached it stops and breaching starts. After the linear increase, every lines start to descend, so every slope combined with every initial wall height starts with stable breaching. This is because of the build-up of material on the horizontal bed just in front of the wall. This process is most extreme during the first seconds of breaching, which will decrease the wall height in the first stages.

After the wall has retrograded up the slope for a while, two things can happen. The wall height can continue decreasing until it reaches zero, in this case the whole breach is stable and will terminate before the top of the slope is reached. The second option is that the wall height reaches a point at which

21

it starts increasing. In this case the breach becomes unstable and can continue far up the slope. In Figure 3-6a the wall heights for a slope of 20° is plotted. The breach only becomes unstable when an initial wall of 2.00 meter is created. Figure 3-6b shows the results for an initial slope of 25°. In this case the breach is unstable for an initial wall height of 1.00 meter and higher. The difference between the stable and the unstable breaches is very clear. An unstable breach can stay active up to eight times longer than a stable breach. Figure 3-6c shows the results for an initial slope of 30°. It shows that the breach becomes unstable from an initial wall height of 0.75 meter. The steeper the slope, the smaller the wall height needs to be to initiate an unstable breach. More specific research into the critical wall height depending on the soil characteristics is explained in paragraph 3.5.
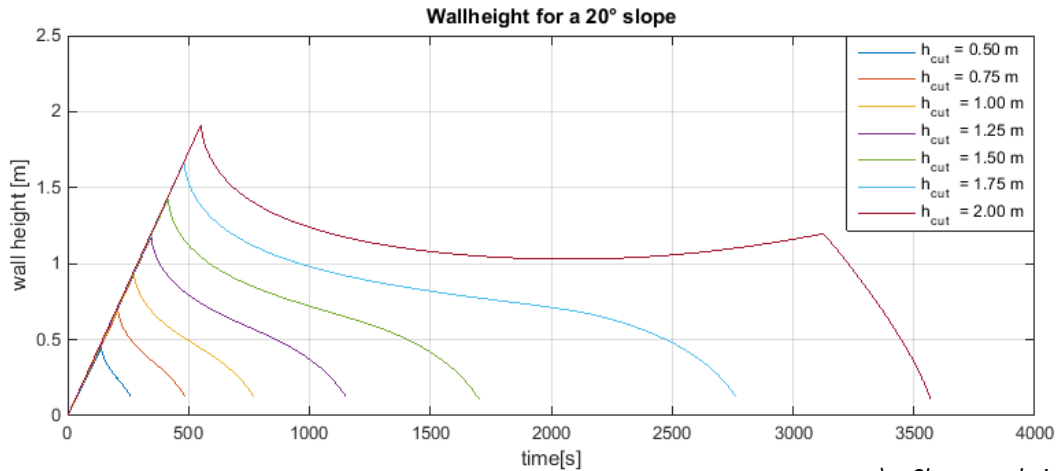
a) Slope angle is 20°
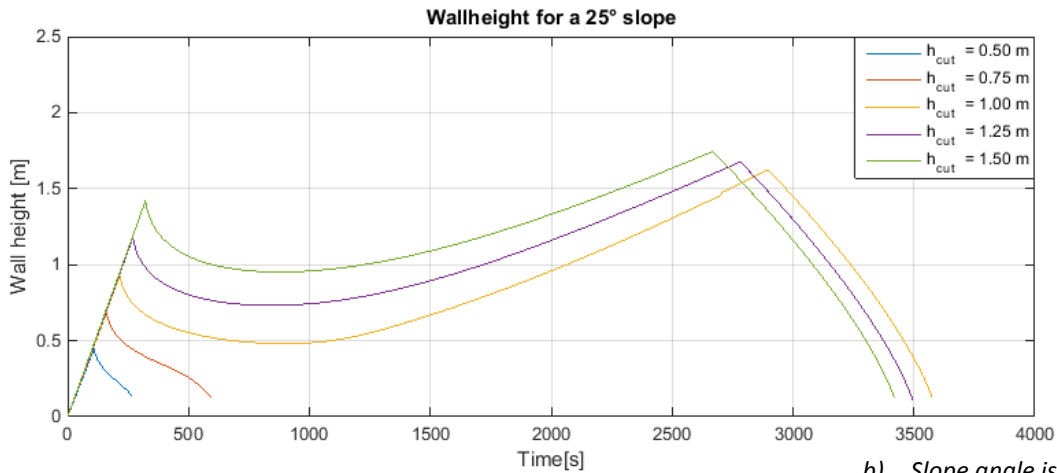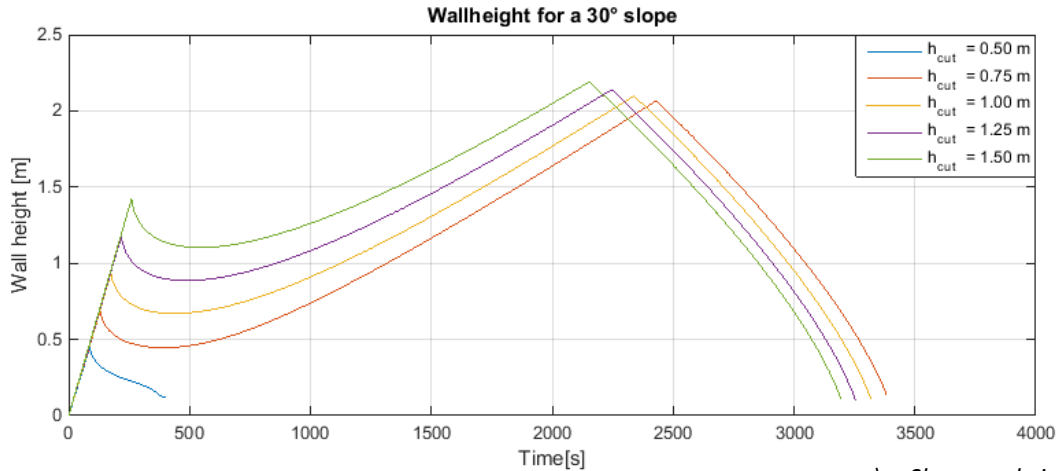
b) Slope angle is 25°

c) *Slope angle is 30°*

Figure 3-6: Dependency of height of initial wall

3.4.2 Soil type dependency

The behaviour of the breach also depends on the soil characteristics. The main parameters which are of influence on the breaching model are the permeability, the particle density and the particle size represented by the D_{50} and the D_{15}. Another parameter which is of influence is the angle of repose. This parameter however has a small influence and will not differ much from φ = 30°. The angle of repose is a parameter with a low variability, so in the breaching model φ is kept constant at 30°. A similar choice is made for the density of the water ρ_w. Although ρ_w can change according to the salinity of the water, the influence on the breaching behaviour is negligible. In the breaching model, ρ_w is kept at a normal level of 1000 kg/m³. Simulations of the model are executed to investigate the separate influence of the parameters on the breaching behaviour of the soil.

The soil with parameters given in Table 3-1 is used as a reference soil and specific parameters are varied in different simulations to investigate the influence of these parameters on the breaching behaviour. All other parameters are kept constant. In these simulations the influence of a single parameter is investigated, so only one parameter is changed in every simulation. This will give a clear result in which only one parameter is investigated. Soils with sets of parameters obtained from field investigation results are discussed in paragraph 3.4.3. The input parameters for the simulations given in the coming figures are given in the top left corner of the figures. The parameters which are adjusted are written in bold.

3.4.2.1 Particle size

The average particle size represented as D_{50} is an important parameter in the soil mechanics. In the breaching model, the D_{50} has a direct influence on the outflow angle of the soil, which has an influence on the stability of the breach. Figure 3-7 gives three simulations with a varying D_{50}. Figure 3-7a uses a soil with D_{50} = 100 μm, Figure 3-7b gives the breaching result for the soil with D_{50} = 150 μm and Figure 3-7c gives the breaching result for a soil with a D_{50} of 200 μm. It is visible that the lower the D_{50}, the more unstable is the behaviour of the breaching wall.
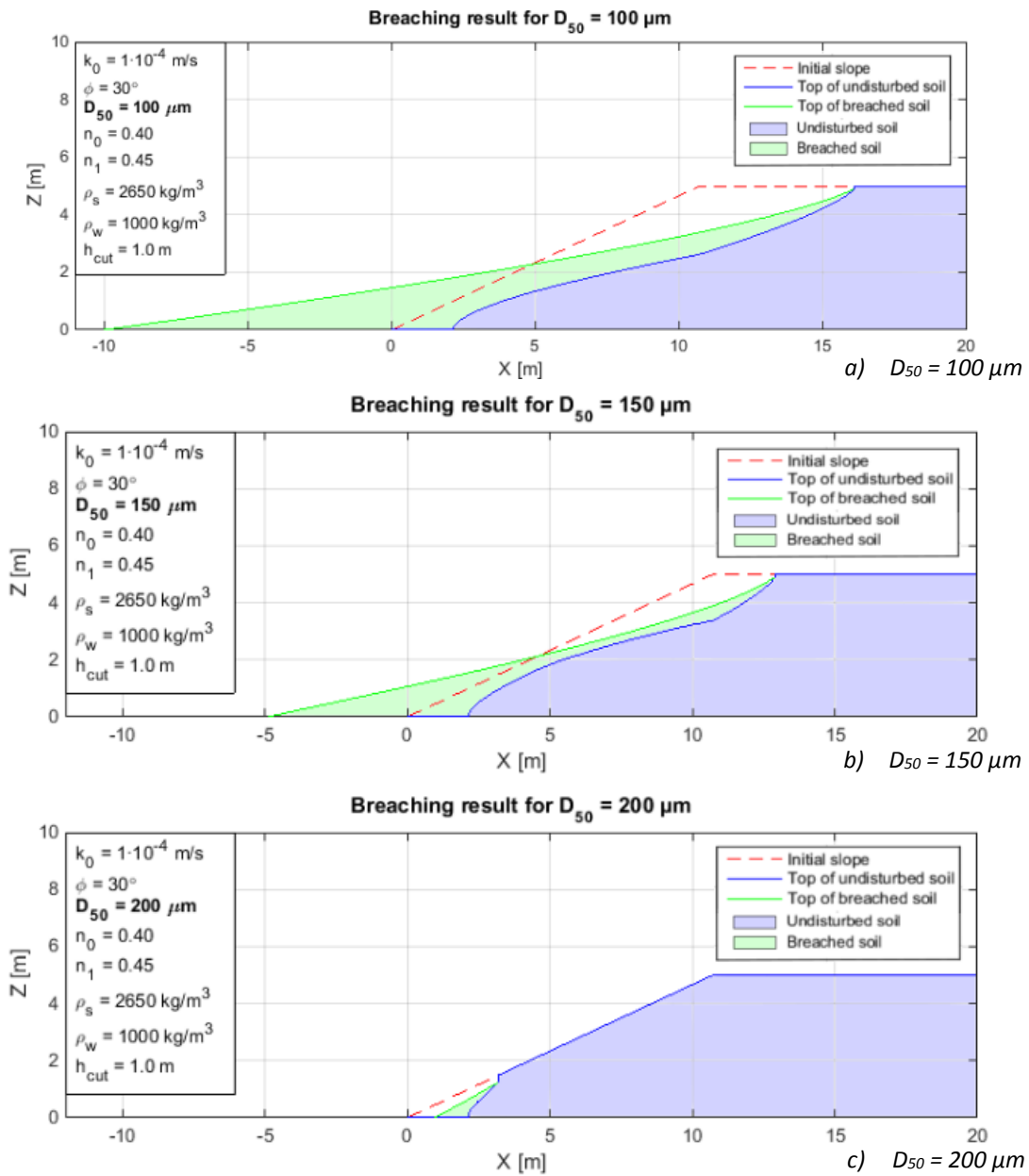
Figure 3-7: D$_{50}$ dependency

3.4.2.2   Permeability

Figure 3-8 shows three simulations of the same slope with a varying permeability. It is visible that the soil with the lowest permeability acts the most unstable. Permeability has a direct correlation with the particle size, because a lower particle size will cause a lower permeability. The results of Figure 3-7 and Figure 3-8 correspond with this relationship and cause a similar unstable tendency of the slope. The higher the permeability, the more unstable is the behaviour of the breaching wall.

Breaching result for $k_0 = 5 \cdot 10^{-5}$ m/s

$k_0 = 5 \cdot 10^{-5}$ m/s
$\phi = 30°$
$D_{50} = 150 \ \mu m$
$n_0 = 0.40$
$n_1 = 0.45$
$\rho_s = 2650 \ kg/m^3$
$\rho_w = 1000 \ kg/m^3$
$h_{cut} = 1.0 \ m$

Legend:
- Initial slope
- Top of undisturbed soil
- Top of breached soil
- Undisturbed soil
- Breached soil

a) Low permeability

Breaching result for $k_0 = 1 \cdot 10^{-4}$ m/s

$k_0 = 1 \cdot 10^{-4}$ m/s
$\phi = 30°$
$D_{50} = 150 \ \mu m$
$n_0 = 0.40$
$n_1 = 0.45$
$\rho_s = 2650 \ kg/m^3$
$\rho_w = 1000 \ kg/m^3$
$h_{cut} = 1.0 \ m$

Legend:
- Initial slope
- Top of undisturbed soil
- Top of breached soil
- Undisturbed soil
- Breached soil

b) Medium permeability

Breaching result for $k_0 = 2 \cdot 10^{-4}$ m/s

$k_0 = 2 \cdot 10^{-4}$ m/s
$\phi = 30°$
$D_{50} = 150 \ \mu m$
$n_0 = 0.40$
$n_1 = 0.45$
$\rho_s = 2650 \ kg/m^3$
$\rho_w = 1000 \ kg/m^3$
$h_{cut} = 1.0 \ m$

Legend:
- Initial slope
- Top of undisturbed soil
- Top of breached soil
- Undisturbed soil
- Breached soil

c) High permeability

Figure 3-8: Permeability dependency

3.4.2.3 Particle density

The particle density is an independent parameter. During dredging of a slope of ordinary quartz sand, the particle density will usually be around 2650 kg/m³. However during dredge mining of ore sands, it is possible that the particle density of the sand is lower or higher than that of quartz sand. The dependency of the breaching result on the particle density is illustrated in Figure 3-9. It is visible that the lower the particle density, the more stable is the result of the breach. However, this is an illogical result of the model. The particle density is present in two different aspects of the model. A higher particle density increases the wall velocity, which makes the breach more unstable. The particle density also has an influence on the outflow angle. A higher particle density causes a higher mass flow, which causes a

25

smaller outflow angle according to (3.3). This also makes the breach more unstable for a higher particle density. The second phenomena might however be an illogical result of empiricism. Particles with a higher density are heavier, so they will sediment quicker, which makes the breach more stable. This phenomena is not represented in the empirical relations used for the model. The question is if the higher wall velocity or the higher sedimentation has the largest influence on the stability of the breach. It is expected that dense particles sediment right after breaching, so it is expected that sedimentation has the highest influence. This results in a more stable breach for denser particles. More research must be done in order to support this claim. The influence of the particle density is smaller than the influence of the permeability, because for a reasonable change in the particle density, the breaching result has only little changes in the output.

a)   *Low particle density*

b)   *Medium particle density*

c)   *High particle density*
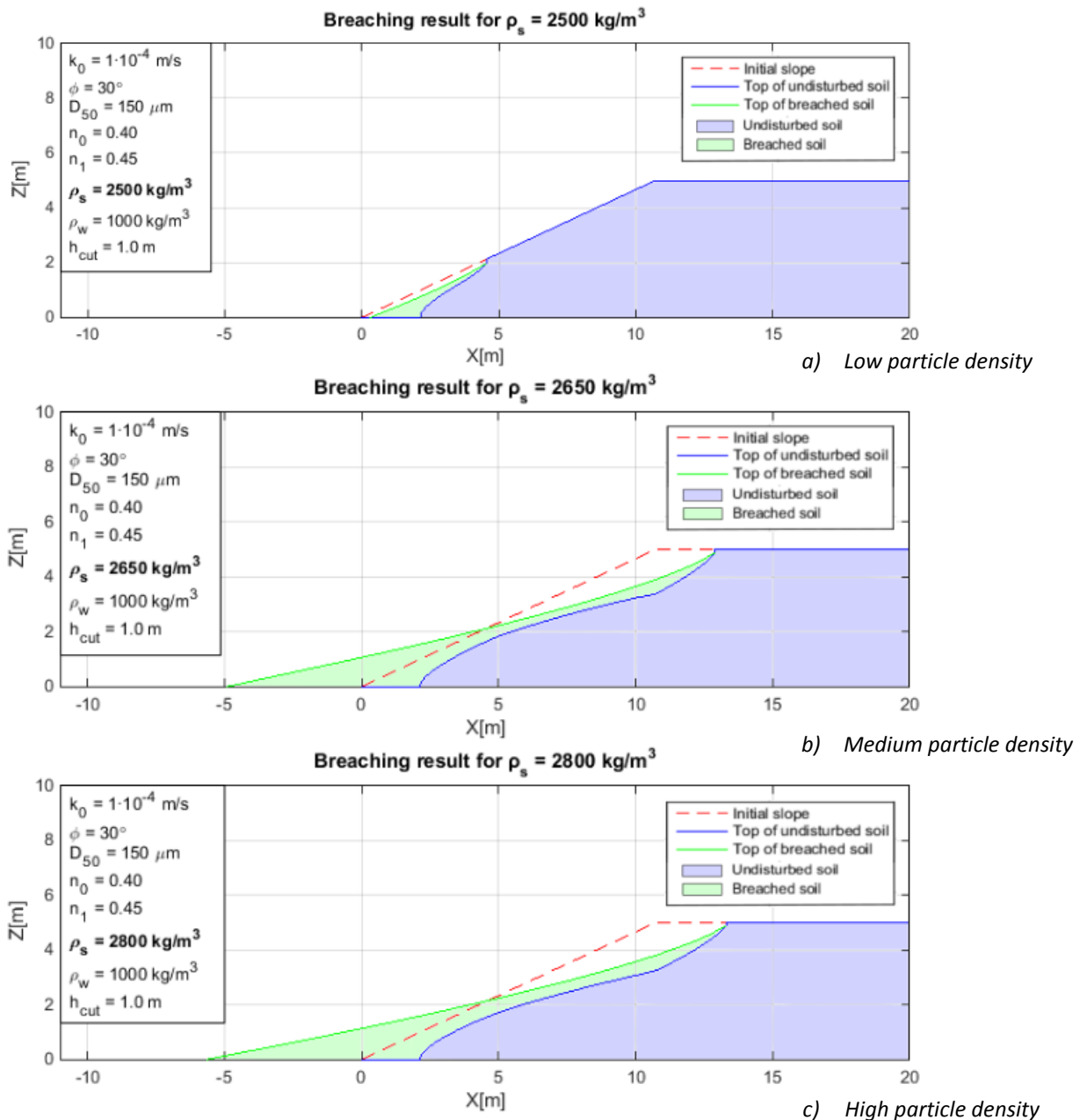
Figure 3-9 Particle density dependency

3.4.2.4 Porosity

The porosity and the porosity change of the soil are also of influence on the breaching behaviour. An assumption of the model is that there is a porosity increase due to shearing of the outer layer of soil. This causes that n_1 is always larger than n_0, which decreases the variability of the porosity. The porosity, permeability and particle size are strongly related, so the influence of the porosity is linked to a particle size distribution, this is explained in the following paragraph.

3.4.3 Particle size distribution

In the previous paragraphs the breaching behaviour is analysed by varying one parameter at a time. This is very useful for determining the influence of a single parameter on the breaching process. In reality many of the parameters discussed are dependent on each other. In this paragraph the breaching of three different soils will be analysed with the particle size distributions given in Figure 3-10. All three soils have a D_{50} of 150 µm, but the amount of fines is different. The amount of fines is usually described by the D_{10} or the D_{15} of the soil. The permeability is strongly dependent on the amount of fines. A relation between the permeability and the D_{10} by Hazen (1892) is used to obtain the initial permeability of the soil. The relation is given in (3.6):

$$k_0 = C \cdot 10^{-2} \cdot D_{10}{}^2 \tag{3.6}$$

C = constant ranging from 0.4 to 1.2, typically assumed to be 1.0.

D_{10} [mm] is the particle size corresponding to 10% of the weight passage.

This is a very old formula, but it is still used nowadays during field investigations. It is an easy and fast way to calculate the permeability. The permeability depends on the porosity and the D_{15} value by the Den Adel equation given in (3.7), which is a version of the Kozeny-Carman equation.

$$k_0 = \frac{g}{160 \cdot v} \cdot D_{15}{}^2 \cdot \frac{n_0{}^3}{(1 - n_0)^2} \tag{3.7}$$

This equation provides a way to relate the porosity to the permeability. For this analysis the initial porosity is determined from the initial permeability and the D_{15} obtained from the particle size distribution graph. The gravity (g) and the kinematic viscosity (v) are constant for the different soil examples. The soil parameters based on the D_{50} and the D_{10} of the three soils tested are given in Table 3-2.

Table 3-2: Soil parameters of tested soils

	Poorly sorted	Medium sorted	Well sorted
D_{50} [µm]	150	150	150
D_{15} [µm]	87	120	130
D_{10} [µm]	75	100	125
k_0 [m/s]	5.63E-05	1.00E-04	1.56E-04
n_0 [-]	0.366	0.360	0.385
n_1 [-]	0.45	0.45	0.45
φ [°]	30	30	30
ρ_s [kg/m³]	2650	2650	2650
ρ_w [kg/m³]	1000	1000	1000
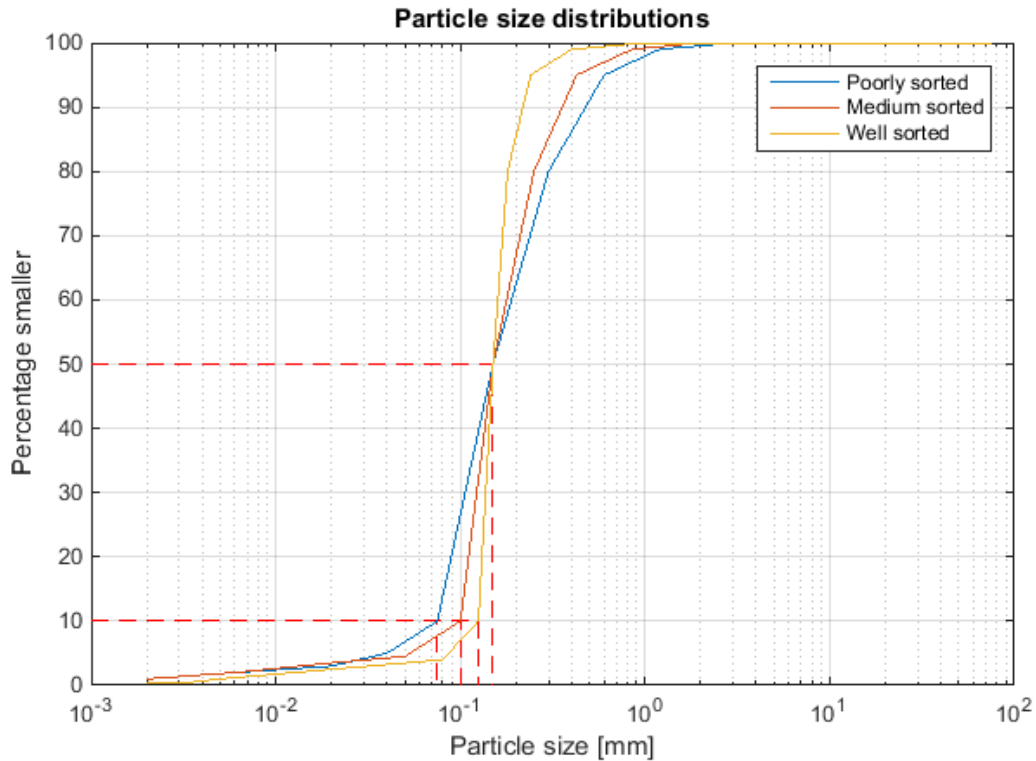
Figure 3-10: Particle size distributions

The closer the D_{10} value to D_{50}, the better sorted is the soil. An analysis of a slope with an initial angle of 25° and a height of 5 meter is executed for the three soils. The breaching result for a cut of 1 meter initial wall height is given in Figure 3-11. Figure 3-11a gives the breaching result for a poorly sorted sand. It is visible that a poorly sorted sand is much more stabilising than a well sorted sand such as given in Figure 3-11c. This is mainly the result of a lower permeability for a poorly sorted sand. A low permeability decreases the wall velocity, which makes the breach more stable.
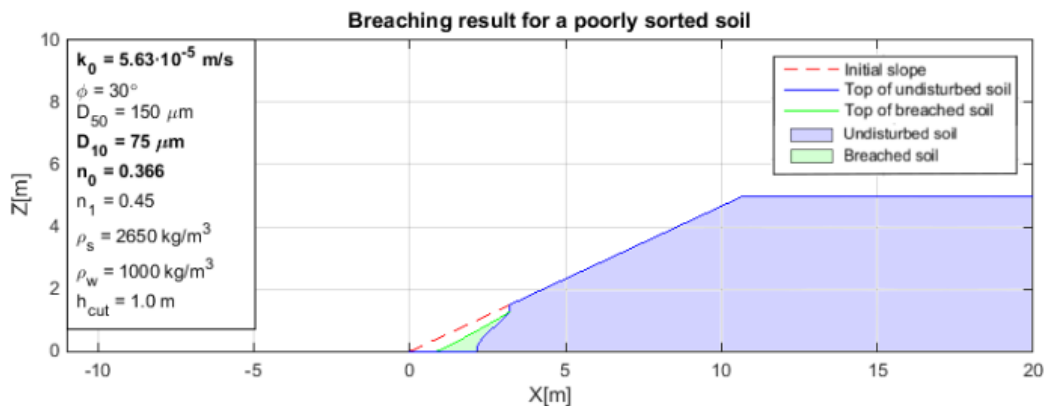
a) Poorly sorted soil
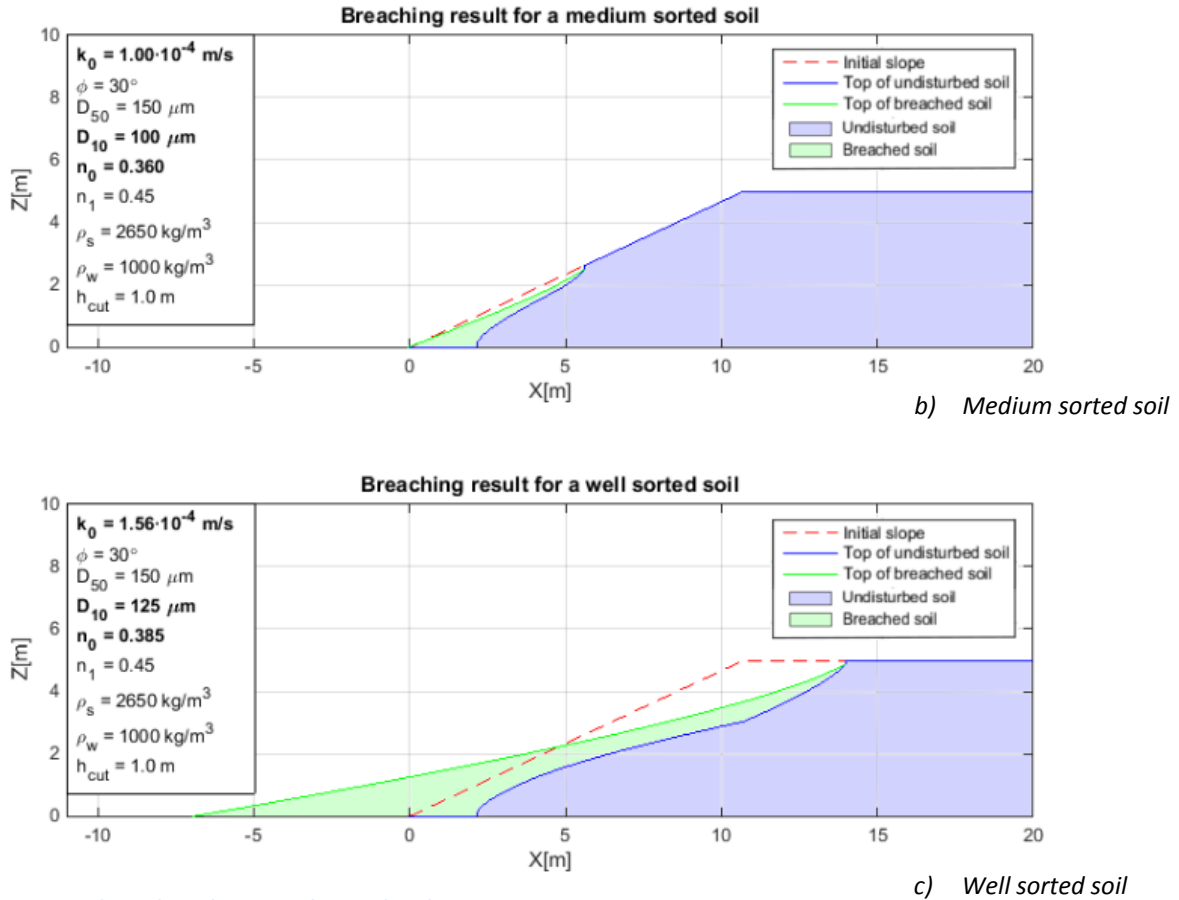
Figure 3-11: Dependency based on particle size distributions

3.4.4 Arbitrary slope

The slopes in the previous paragraphs had a constant slope angle and a maximum slope height. The transition between the slope and the top was discontinuous. Those examples are perfect for testing the influence of parameters on a slope, but in reality the geometry of the slope is continuous. The breaching model also works for slopes with an arbitrary geometry. An example of such a slope is given in Figure 3-12. In this case the slope angle is not constant and the surface of the slope is a continuous function. If the full geometry of a slope is known, every possible slope can be modelled with the previously explained breaching model.
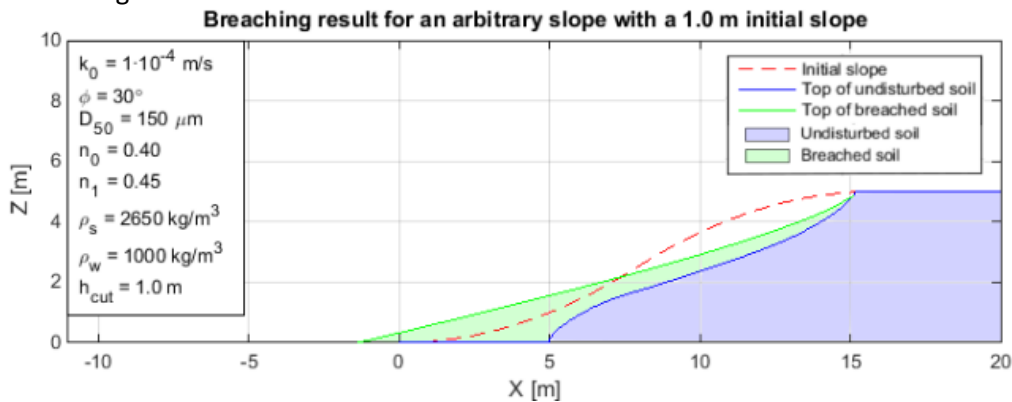
Figure 3-12: Arbitrary slope breaching result

29

3.5 Critical cut height relation

The behaviour of the breach can be stable or unstable, this difference is the most important phenomena for the dredging production. As can be concluded from the results in the previous graph, there is a critical height (H_{crit}) of the initial breaching wall for which a higher initial wall will create an unstable breach and a smaller initial wall will create a stable breach. An explanation on how the critical wall height is obtained by the model is illustrated in Appendix D.

Table 3-3: Test soil parameters

	Reference soil	Soil 1	Soil 2	Soil 3	Soil 4	Soil 5	Soil 6	Soil 7
		D_{10} dependence			D_{50} dependence		ρ_s dependence	
D_{50} [µm]	150	150	150	150	**100**	**200**	150	150
D_{15} [µm]	120	**87**	**120**	**130**	120	120	120	120
D_{10} [µm]	100	**75**	**100**	**125**	100	100	100	100
k_0 [m/s]	1.00E-04	**5.63E-05**	**1.00E-04**	**1.56E-04**	1.00E-04	1.00E-04	1.00E-04	1.00E-04
n_0 [-]	0.40	**0.3655**	**0.3595**	**0.3848**	0.40	0.40	0.40	0.40
n_1 [-]	0.45	0.45	0.45	0.45	0.45	0.45	0.45	0.45
φ [°]	30	30	30	30	30	30	30	30
ρ_s [kg/m³]	2650	2650	2650	2650	2650	2650	**2500**	**2800**
ρ_w [kg/m³]	1000	1000	1000	1000	1000	1000	1000	1000

Bold: adjusted parameters

The critical cut height depends on the type of soil and the angle of the slope. A reference soil is chosen with basic soil parameters and 7 other sets of soil parameters are chosen to investigate the influence of every parameter. The sets of parameters are given in Table 3-3, the parameters which are adjusted from the reference soil are given in bold. As explained before, the angle of repose and the density of the water are assumed to be constant. The loose porosity n_1 is kept constant at 0.45, because it has a low variability and has a negligible influence on the critical cut height. The three soil parameters which are chosen as the main parameters which determine the critical cut height are the D_{10} particle size, the D_{50} particle size and the particle density ρ_s. The initial porosity n_0 and the permeability k_0 are dependent on the D_{10} and will change when the D_{10} is changed. The permeability k_0 depends on the D_{10} by the Hazen equation as explained in paragraph 3.4.3. The D_{15} is estimated from a particle size distribution constructed based on the D_{50} and the D_{10}. The initial porosity can according to the Den Adel equation be determined from the D_{15} and the permeability. The D_{50} and the particle density are independent of the other parameters used in the model.

The critical cut height can be determined from the breaching model by iterative analysis of a slope with a chosen slope angle and one of the soil sets (see Appendix D). For the reference soil, the H_{crit} is calculated for all integer slope angles between 18 and 30 degrees. A power curve fit, illustrated in Figure 3-13, results in the following relation for the reference soil:

$$\text{Reference soil: } H_{crit} = 10211 \cdot \beta^{-2.889} \tag{3.8}$$

The critical cut height of the other 7 soils is calculated by the breaching model for the slope angles of β = 20°, β = 25° and β = 30°. The results and power curve fits are plotted in Figure 3-13, Figure 3-14 and Figure 3-15. The figures illustrate the influence of the three main parameters on the critical cut height.
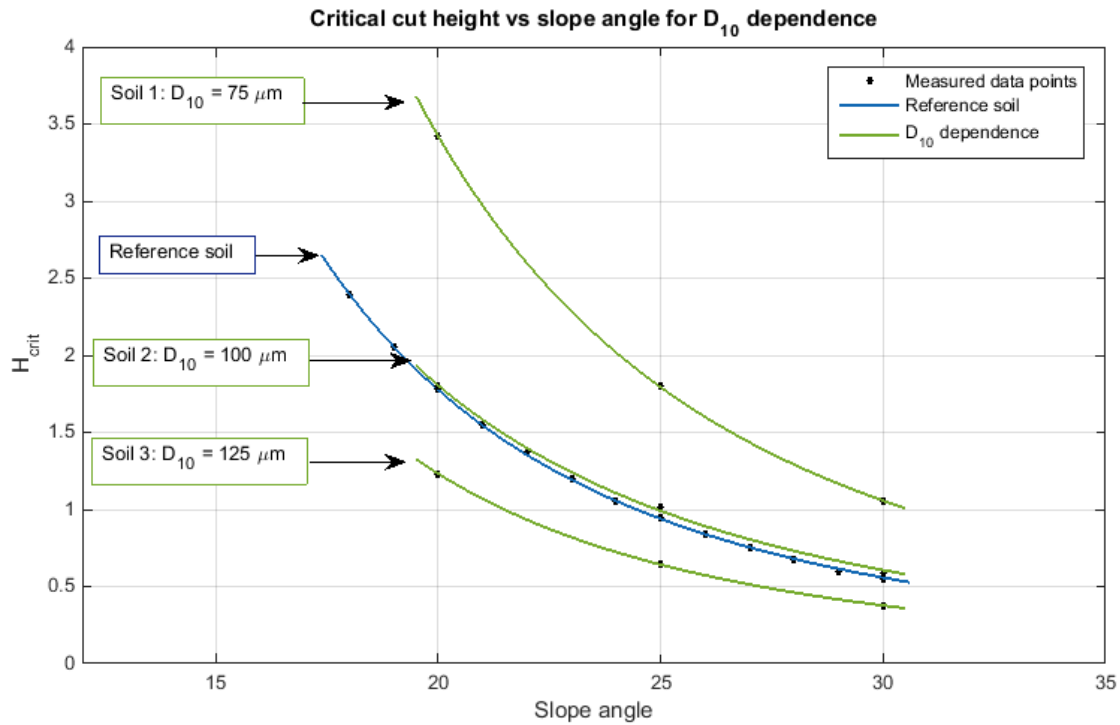
Figure 3-13: Critical cut height relation for D_{10} dependence
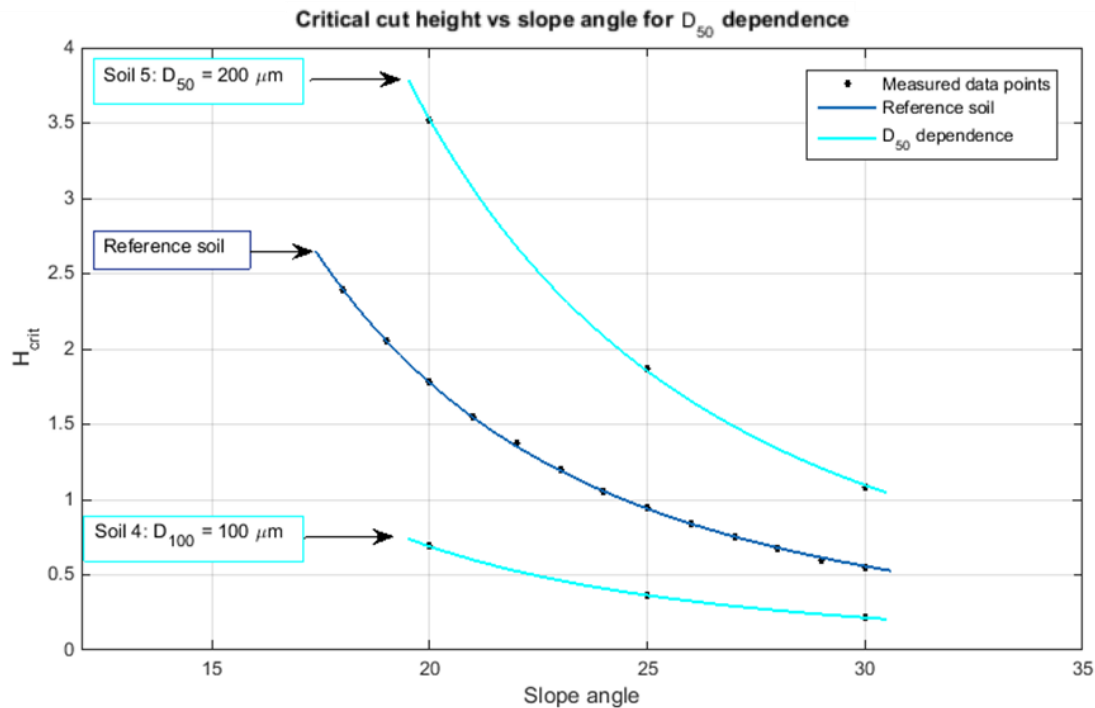
Figure 3-14: Critical cut height relation for D_{50} dependence
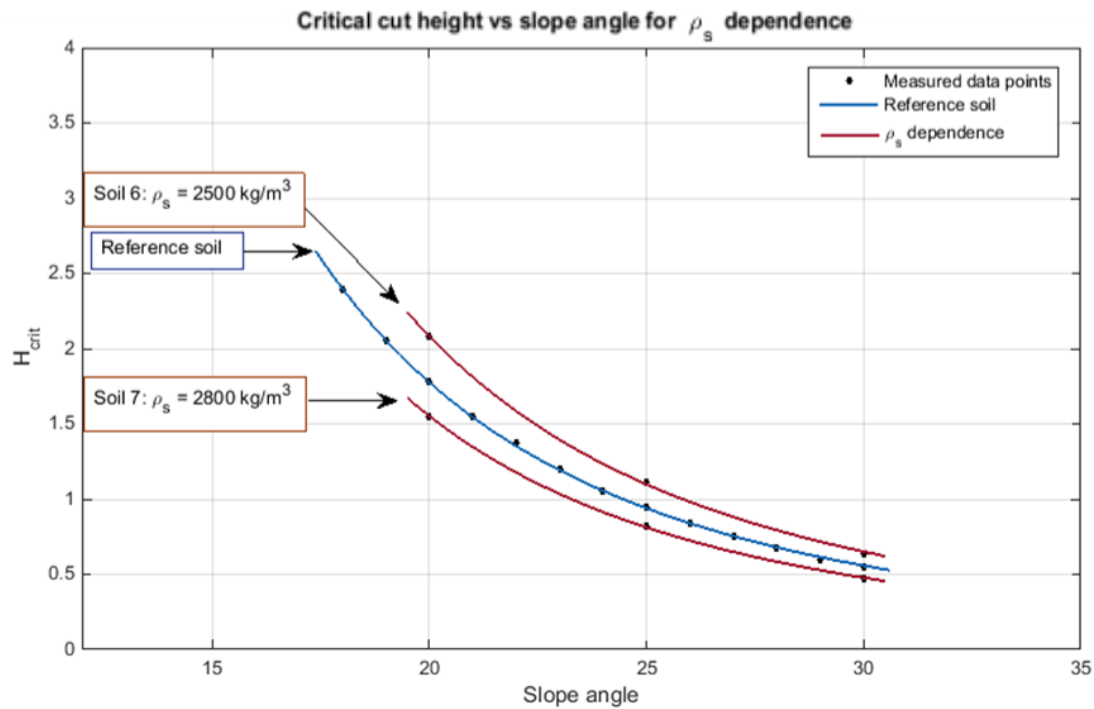
Figure 3-15: Critical cut height relation for ρ_s dependence

A power curve fit for all the soils is made in the form: $y = a \cdot x^b$. the multiplier a and the power value b determine the shape of the curve fit. The fits to the 7 soils are:

$$\text{Soil 1: } H_{crit} = 21008 \cdot x^{-2.911}$$

$$\text{Soil 2: } H_{crit} = 6781 \cdot x^{-2.745}$$

$$\text{Soil 3: } H_{crit} = 8759 \cdot x^{-2.959}$$

$$\text{Soil 4: } H_{crit} = 3225 \cdot x^{-2.823}$$

$$\text{Soil 5: } H_{crit} = 21685 \cdot x^{-2.911}$$

$$\text{Soil 6: } H_{crit} = 12540 \cdot x^{-2.904}$$

$$\text{Soil 7: } H_{crit} = 10412 \cdot x^{-2.940}$$

It can be observed that there is little variation in the power value of all the fitting functions. If this value is assumed to be a constant, it can be neglected from the final relation and the multiplier will be the decisive parameter for the shape of the curve. After a second round of fitting assuming the power value for every soil is b = -2.889, the corrected multipliers per soil are given in Table 3-4.

Table 3-4: Multipliers per soil

Soil	Multiplier
Reference	10211
Soil 1	19496
Soil 2	10746
Soil 3	7017.1
Soil 4	4080.5
Soil 5	20278
Soil 6	11984
Soil 7	8932.5

Soil 1,2 and 3 are used to determine the relation between the D_{10} particle size and the multiplier (M_1) given in Figure 3-16. A relation between the multiplier and the D_{10} in μm is given in Figure 3-16. A power trend line gives a good fit and results in the following relation for the multiplier M_1:

$$M_1 = 1.231 \cdot 10^8 \cdot D_{10}^{-2.027} \tag{3.9}$$
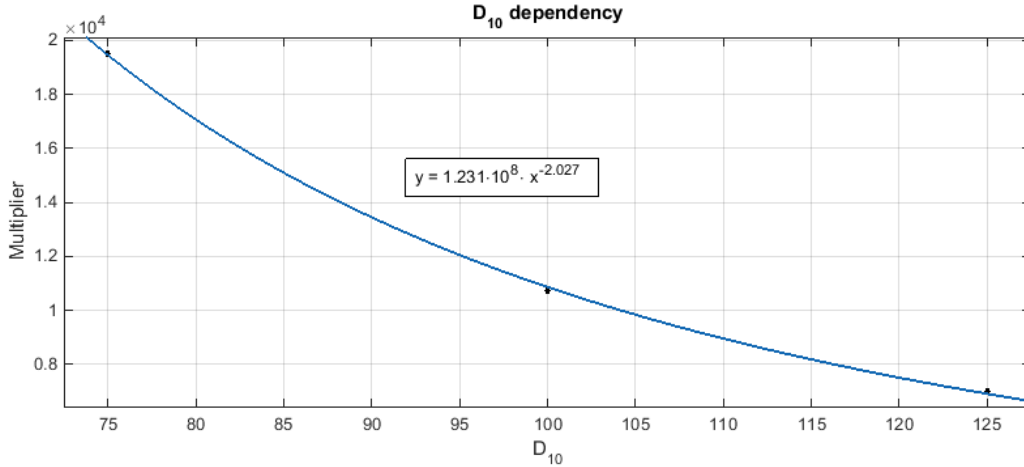
Figure 3-16: D_{10} multiplier dependency

The relation between the D_{50} and the multiplier (M_2) derived by the power trend line is given in Figure 3-17. Two extra soils with D_{50} values of 125 μm and 150 μm are analysed in order to improve the precision of the trend line. The formula for the power trend line is as follows:

$$M_2 = 0.07626 \cdot D_{50}^{2.358} \tag{3.10}$$
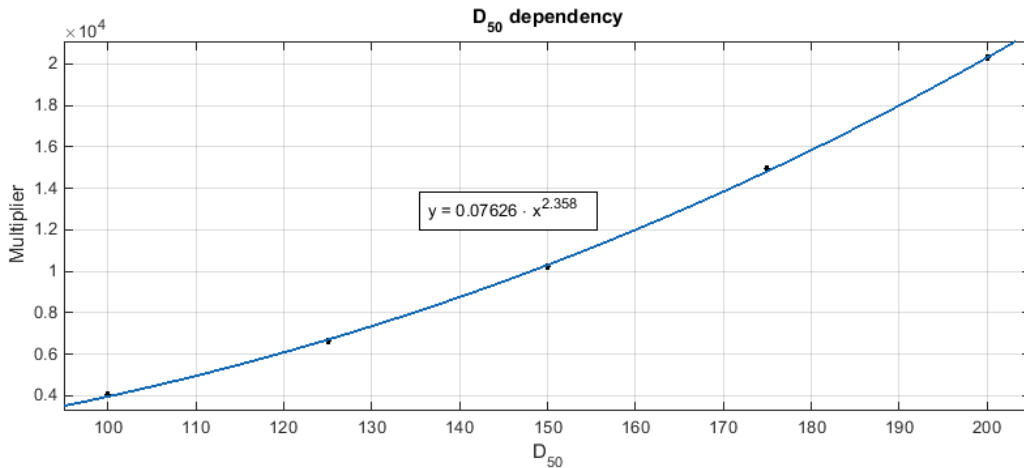
Figure 3-17: D_{50} multiplier dependency

The relation between the particle density and the multiplier (M_3) is given in Figure 3-18. Also for this parameter two extra soils are analysed in order to improve the precision of the trend line. The extra soils have a particle density of ρ_s = 2350 kg/m³ and ρ_s = 2950 kg/m³. The relation estimated by a power trend line is:

$$M_3 = 9.1 \cdot 10^{12} \cdot D_{10}^{-2.613} \tag{3.11}$$
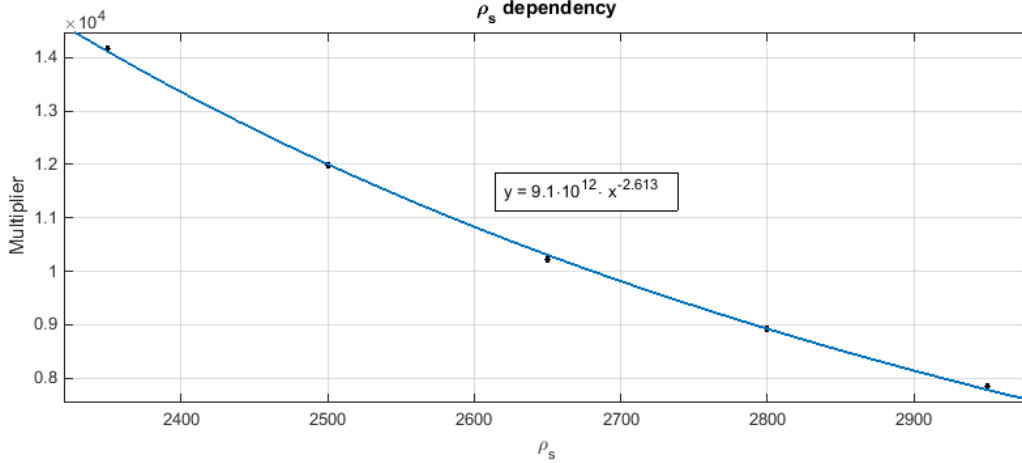
Figure 3-18: Particle density multiplier dependency

The relations between all the important parameters and the critical cut height can now be obtained by using the relations (3.9), (3.10) and (3.11) and combining them with (3.8) for the reference soil. Equation (3.12) shows the calculation method for this relation. All the multipliers are recalculated to weights which affect the multiplier for the reference soil. After recalculating the weights, the final expression for the critical cut height is given in (3.13).

$$H_{crit} = \frac{9.1 \cdot 10^{12} \cdot \rho_s{}^{-2.613}}{10211} \cdot \frac{0.07626 \cdot D_{50}{}^{2.358}}{10211} \cdot \frac{1.231 \cdot 10^8 \cdot D_{10}{}^{-2.027}}{10211} \cdot 10211 \cdot \beta^{-2.889} \quad (3.12)$$

$$H_{crit} = 8.193 \cdot 10^{11} \cdot \rho_s{}^{-2.613} \cdot D_{50}{}^{2.358} \cdot D_{10}{}^{-2.027} \cdot \beta^{-2.889} \quad (3.13)$$

When a cut is made in the toe of a slope with a wall height smaller than H_{crit}, the breaching wall will behave stable and when an active wall is created which is bigger than H_{crit}, the breach will behave unstable. The only parameters which need to be obtained are the particle density, the particle size distribution graph and the slope angle.

3.5.1 Comparison of theories

A similar relation has been obtained by Van Rhee, 2015, which is given in (3.14). The relation provides a way to calculate the critical wall height, based on the slope angle (i_{slope}), the median particle size (D_{50}), the particle density (ρ_s), the initial porosity (n_0) and the initial permeability (k_0). The equation is a result of two other empirical relations, a relation for the wall velocity given in (3.1) and a relation for the outflow angle of soil after breaching given in (3.3). Equation (3.14) and equation (3.13) are based on the same equations, but are derived differently from each other, they are compared in this paragraph.

$$H_{crit} = 1.22 \cdot 10^{-6} \cdot \frac{i_{slope}{}^{-2.56} \cdot D_{50}{}^{2.36}}{30 \cdot \rho_s \cdot (1 - n_0)k_0} \quad (3.14)$$

The power for the D_{50} is very similar in both equations. The k_0 in (3.14) has a power of -1, in (3.13) the D_{10} has a power of -2.027. However the D_{10} is quadratic related to the k_0, which makes the two parameters match very well. The power of the slope angle shows a bigger difference between (3.13) and (3.14), but it is still not a very drastic difference. The largest difference is in the power of the particle

34

density. In (3.14) Van Rhee gives a power of -1 to the ρ_s, but in (3.13) the ρ_s has a power of -2.613. This difference might be caused by the same phenomena as discussed in paragraph 3.4.2.3. The sedimentation effect of dense particles might be wrongly implemented as a result of the empirical relations. Figure 3-19 shows the calculated critical cut height per slope angle for both equations. This is only a comparison of one type of soil. In Appendix B a more extensive comparison with multiple soil types is presented. Both equations result in the same trend for the critical cut height for every type of soil tested. It is observed that for the smallest tested slope angles of 18 to 20 degrees, the difference is on average not higher than 10%. For higher slope angles up to 30 degrees, the differences are larger. The largest differences are about 30-40% for slope angles of 30°. The absolute difference however stays very constant for all tested slope angles. It is difficult to say something about the correctness of the two methods at this point, because the results cannot be compared to realistic experiments. In order to find out which equation gives a better approximation, the results must be compared to lab tests on the correct scale.
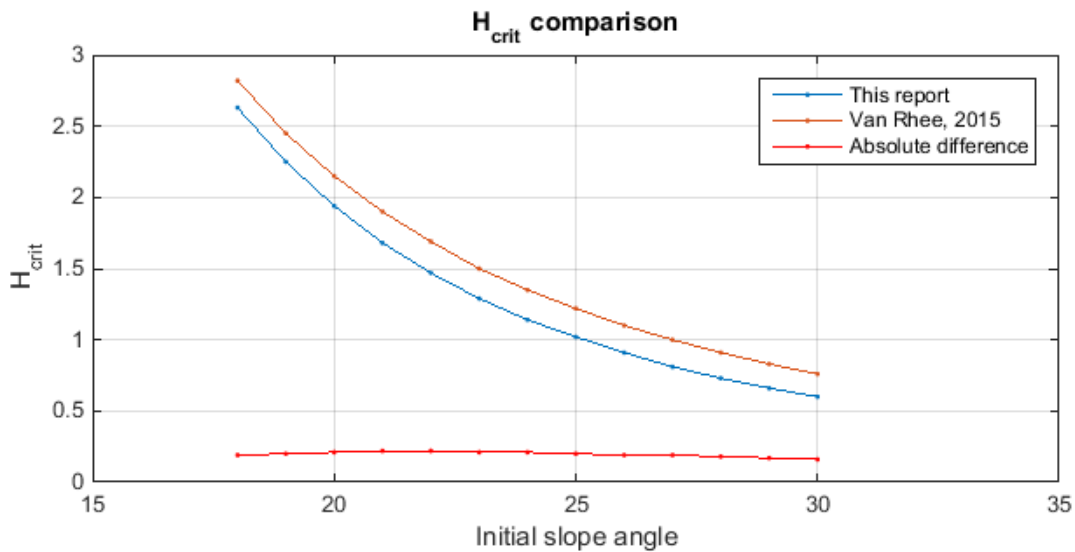
Figure 3-19: Comparison of critical cut height equations for reference soil

3.6 Summary

The process of breaching is very important during dredging of a slope. If the behaviour of the slope is not well predicted, a very unfavourable failure of the slope can cause losses or damage to the equipment or the shore. The difference between the initiation of a stable or an unstable breach can be very small, but the consequences can be large. It is important to quantify the consequences of every size of a cut. An unstable breach can cause large damage to the shore if an unwanted unstable breach is created. If a slope has started breaching, it is very difficult to stop the process. This makes it very important to predict whether a slope will breach unstable or stable.

The breaching model predicts the breaching process of a 2D section of a slope after a cut has been made at the toe of the slope. The slope consists of homogeneous soil and is described by a number of soil parameters. Table 3-5 gives a summary of the trends in the breaching stability of the main soil parameters.

- An increase in the permeability will cause a decrease in the breaching stability. The same trend is caused by the D_{10}, because they are positively correlated by the Hazen equation.
- An increase in the D_{50} causes an increase in the breaching stability. This is mainly a result of a larger outflow angle at a higher D_{50}.
- An increased particle density causes a decreased breaching stability. This is a result of a higher wall velocity at a higher particle density. However, this phenomena might be overshadowed by the fact that denser particles sediment faster, which increases the breaching stability. This phenomena is not represented in the empirical relations used for the model.
- The geometry of the slope also has a large influence on the breaching behaviour. The steeper the slope or the higher the initial breaching wall, the faster the breaching becomes unstable.

Table 3-5: Influence of geotechnical parameters on the stability of the breach

		Stability of breach
Permeability	Increase	Decrease
	Decrease	Increase
D_{50}	Increase	Increase
	Decrease	Decrease
D_{10}	Increase	Decrease
	Decrease	Increase
ρ_s	Increase	Decrease
	Decrease	Increase
Slope angle	Increase	Decrease
	Decrease	Increase
Initial wall height	Increase	Decrease
	Decrease	Increase

It is observed that the D_{10} value has the largest influence and that the particle density has the smallest influence on the breaching behaviour. In order to quantify the influence of the parameters on the breaching stability, an empirical relation is developed based on the model, given in (3.13). The empirical relation can be used to calculate the critical cut height of the specific slope. A comparison is made with a similar relation developed by van Rhee (2015) given in (3.14).

The model presented in this chapter is only a 2D model which shows a section of a breaching wall. In order to say something about the dredging production, a 3D model needs to be created. In the next chapter a 3D model is presented. The advantages and disadvantages of the 3D model are explained.

4   Production model

In order to make a model which incorporates a dredging sequence with multiple cuts, a production model is constructed for this research. This is a simplified version of the breaching model, extended in 3D. More about the differences between the models is explained in paragraph 4.4. In contrast to the breaching model, the production model can model the breaching result of a sequence of cuts. Depending on the dredging movements, the production rate and the dependency on the behaviour of the slope can be modelled. The difference between the breaching model and the production model will be explained in detail.

4.1   Scenario

The initial situation is simplified as a slope with a constant angle (β) and a given maximum height (H). The top of the slope is horizontal and the geometry does not differ in the third dimension. It is assumed the soil in the slope is packed dense enough that it will cause dilatancy when it is sheared, this will initiate breaching. This model assumes a breaching wall which retrogrades beyond the top of the slope. The soil flowing down from the breach ends up at the toe of the slope. The top of the outflow volume is estimated as a line with a constant angle (α).

In contrast to the breaching model, the dredging scenario will influence the behaviour of the slope, so the dredging scenario must be given as input parameters. The cutter will always start with a forward cutting motion until the required cutting depth is reached. The second step is a cutting swing in which the initial soil is cut. During this swing a breaching wall is initiated over the full width of the slope. After the cutting swing, as many clean-up swings as necessary are done until the next forward step is initiated. The volume of soil which is cut is removed from the model. The physics behind the model will be explained in the next paragraph.

4.2   Method and physics

The production model is based on a simplified version of the breaching model. The differences and comparison between the breaching model and the production model will be explained in paragraph 4.4. In this paragraph the method and physics of the production model will be explained in detail.

4.2.1   Basic process

The breaching behaviour is modelled as a stepwise process, but every step is independent of the previous step. Every time step the volume V_{breach} is calculated and transferred into the outflow volume ($V_{outflow}$). The outflow volume is recalculated every time step, but $V_{outflow}$ is independent of the previously calculated $V_{outflow}$. Figure 4-1 gives a schematic display of the final situation after breaching has ended. The initial slope has an angle β and the toe of the slope is cut until a vertical wall with a height of h_{wall} is created. The volume V_{cut} is removed from the model. After this moment the breaching wall starts retrograding with the wall velocity (v_{wall}), which is calculated similarly to the breaching model. The line from point p to point q in Figure 4-1 has the same angle as the top of the initial slope. The initial soil in the slope has a porosity of n_0 and the outflow soil has a porosity of n_1, which is higher than n_0. The angle of the outflow volume is calculated as given in (4.1):

$$\tan\alpha = 0.0049 \cdot D_{50}^{0.92} \cdot s^{-0.39} \tag{4.1}$$
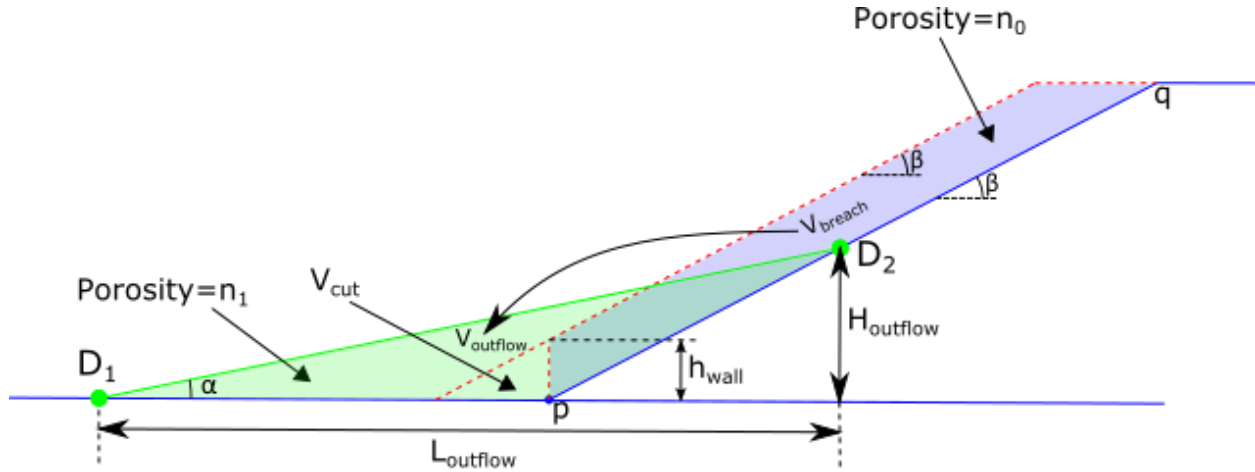
Figure 4-1: Production model process

In equation (4.1), s is the production based on the initial wall height (h_{wall}), which can be calculated as given in (4.2):

$$s = h_{wall} \cdot v_{wall} \cdot (1 - n_0) \cdot \rho_s \tag{4.2}$$

The volume V_{breach} is removed from its original position. Due to the porosity increase from n_0 to n_1, the breached volume increases. The volume increases into $V_{outflow}$ as given in (4.3):

$$V_{outflow} = V_{breach} \cdot \left(\frac{1 - n_0}{1 - n_1} \right) \tag{4.3}$$

The volume $V_{outflow}$ is positioned under an angle α on the newly created slope as illustrated in Figure 4-1. Point p is one of the vertices of the outflow volume, the other two vertices are determined based on $L_{outflow}$ and $H_{outflow}$. These are respectively the length and height of the outflow volume. The height $H_{outflow}$ is calculated as given in (4.4) and the length $L_{outflow}$ is calculated as given in (4.5).

$$H_{outflow} = \frac{\sqrt{2} \cdot \sqrt{V_{outflow}}}{\sqrt{\cot \alpha - \cot \beta}} \tag{4.4}$$

$$L_{outflow} = \frac{H_{outflow}}{\tan \alpha} \tag{4.5}$$

The whole process for a single step is now finished and can start over after the wall has retrograded for a specific time step. This process is repeated until the wall height is reduced to zero.

4.2.2 Advanced volume placement

In the case of Figure 4-1 the step is finished, because there are no overlaps created. This means mass conservation is assured. In some situations it is possible that an overlap between the outflow volume and the initial soil is caused by the model, this disproves mass conservation and must be solved. The stated scenario is illustrated in Figure 4-2. This scenario occurs often during the initial moments of breaching when the wall has retrograded only a small distance. To solve the issue a volume replacement is executed, which is illustrated schematically in Figure 4-2. The grey area on the right is modelled over the existing soil, its volume can be calculated with equation (4.6):

$$V_{over} = \frac{L_{over}^2 \cdot (\tan \varphi - \tan \alpha)}{2} \tag{4.6}$$

Equation (4.6) is derived by goniometrical analysis of Figure 4-2. V_{over} is part of the total outflow volume and has to be placed on top of $V_{outflow}$ in order to make the complete figure correct. The vertices given as green dots in Figure 4-2 are shifted in order to create a new fitting area which has no overlap with the initial dense soil.
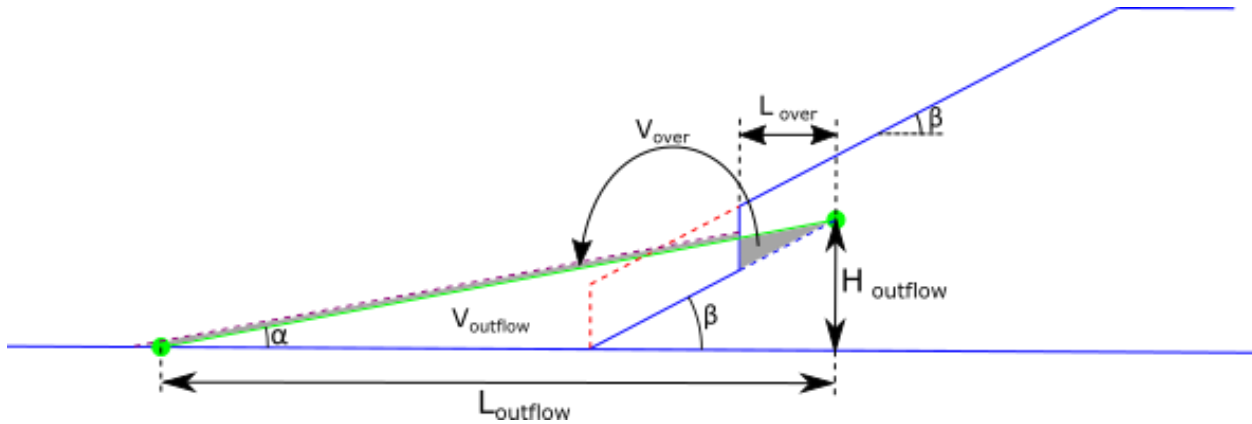
Figure 4-2: Overlap correction

The overlap correction is the last action executed during the particular step. An example of some successive steps is given in Figure 4-3. The green lines modelling the top of the loose packing are all parallel. In this figure an extra phenomenon resulting from the overlap correction is visible. The pink dashed line gives the virtual border between the dense and the loose packed soil, which will be accurate in the case where there is no further cutting after the first cut. It is similar to the scenarios modelled by the breaching model. However, in this model it is assumed more cutting will take place. This will result in the removal of the loose packed soil which keeps the virtual loose-dense border in place. If a second cut is conducted, the dense packed soil in Figure 4-3 will become unstable again, because the slope surface has an angle higher than the angle of repose. It is estimated that the soil given in the grey area will fail, this soil will add to the outflow volume and to the soil which can be dredged. The reason for this assumption is to create a stable situation after cutting of all the loose soil. More about the comparison between the production model and the breaching model will be explained in paragraph 4.4.
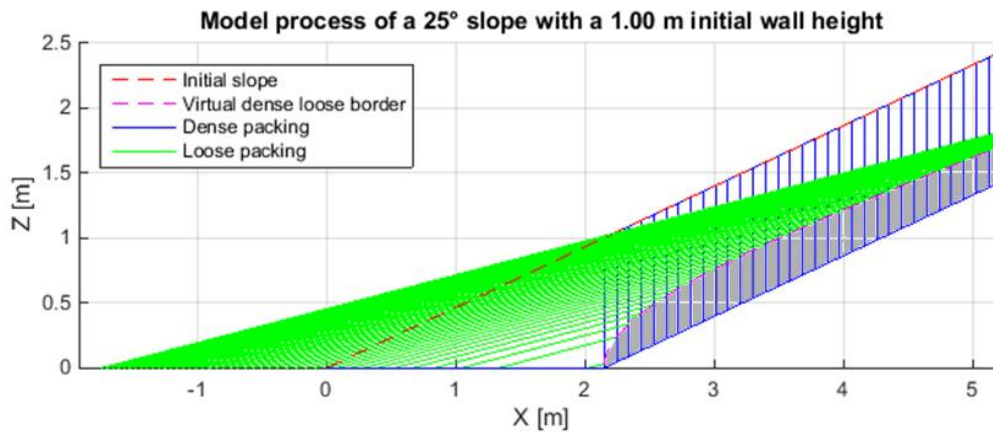
Figure 4-3 Outflow build-up modelling

4.2.3 Conservation of mass

The conservation of mass between the breached soil and the outflow soil is essential for the correctness of the model. The cumulative volume in time of the breached soil and the outflow soil is given in Figure 4-4. The difference between the lines is exactly the volume expansion due to dilatancy as given in equation (4.3). This figure proves conservation of mass.
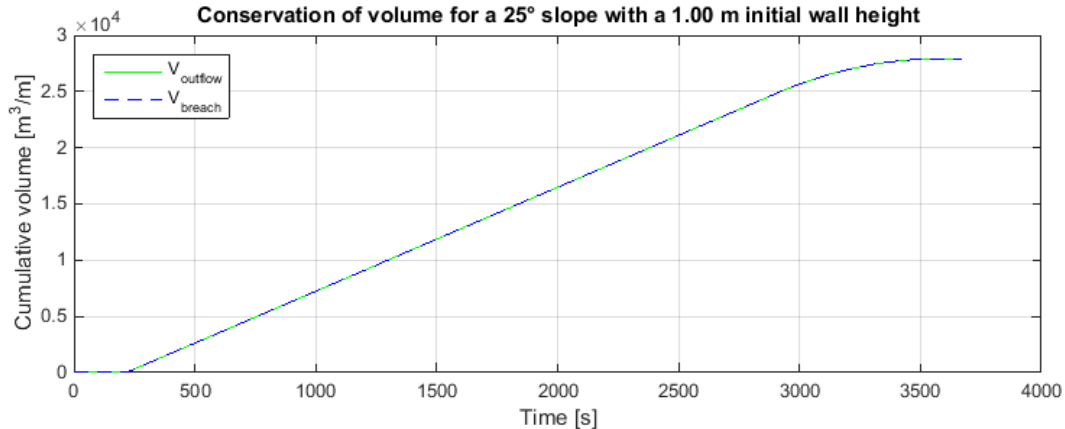
Figure 4-4: Conservation of mass

4.2.4 Dredging process

The previously explained part of the model only consisted of one initial cut, but in reality a sequence of cuts is executed. In this paragraph the cutting part of the model will be explained. There are two possibilities for making a cut in the slope. It is possible to make a clean-up swing in which only the loosely accumulated material at the toe of the slope is dredged and it is possible to make a cut swing in which the dense material of the initial slope is cut. In the second case, a new breaching wall is initiated which will start retrograding.

During a clean-up swing, the cutter does not cut into the densely packed soil. Only material accumulated in front of the slope due to breaching is cut. A schematic illustration of a clean-up swing before the soil is cut is given in Figure 4-5a. The total volume of the dump $V_{outflow}$ is split into three volumes. The volume which is already accumulated behind the cutter is called $V_{outflow,1}$. This volume is considered spillage volume and cannot be dredged, because the cutter does not move backwards to collect spillage material. The volume $V_{outflow,1}$ is modelled in such a way that it stays in place, which is illustrated in Figure 4-5a. This volume does not change over time. During every cut it is possible that soil has moved passed the reach of the dredging wheel and all of these volumes are modelled. The second volume is called V_{cut}, illustrated as the volume between the red dashed lines in Figure 4-5a. This is the volume which is cut, it is removed from the model and it is counted as production. A correction factor will be applied to correct for the round shape of the dredging wheel in contrast to the angular shape of the volume V_{cut}. The third volume is $V_{outflow,2}$, this volume is not cut during this swing, but it is still available for cutting in successive swings. $V_{outflow,2}$ slides down to the toe of the slope after the dredging wheel is passed. No breaching will take place in this soil, because it is already very loosely packed. It forms a new outflow volume $V_{outflow}$ at the toe of the slope with the same angle α, this is illustrated in Figure 4-5b. The new outflow volume will be enlarged in time if breaching is still active.

a) Before cut

b) After cut
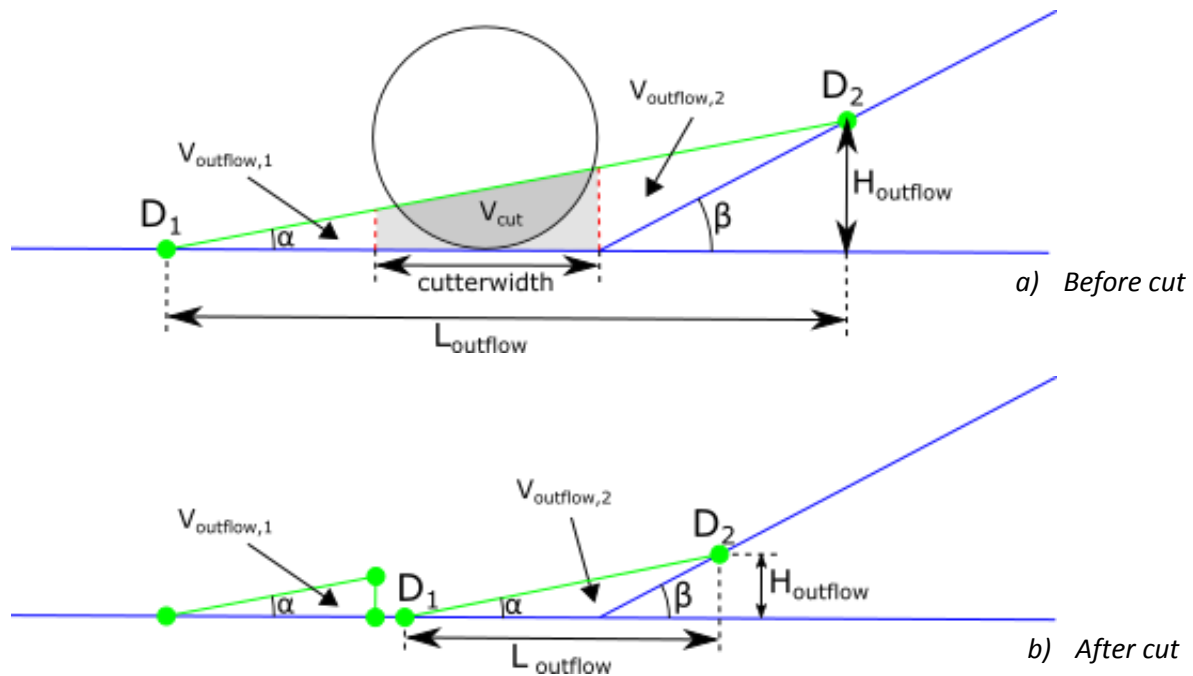
Figure 4-5: Modelling of a clean-up swing

The second type of swing is a cut swing. This is a type of swing which is executed following a forward step. It cuts through the initial slope and creates a new breaching wall. It is schematically illustrated in Figure 4-6a. In this case V_{cut} is the volume which is removed from the model. Similar to a clean-up swing $V_{outflow,1}$ the spillage stays in position after the cut, see Figure 4-6b. In this case both loosely packed soil and densely packed soil from the initial slope is cut. After the cut is executed, a new breaching wall is initiated, which will create a new outflow volume at the toe.

a) Before cut

b) After cut
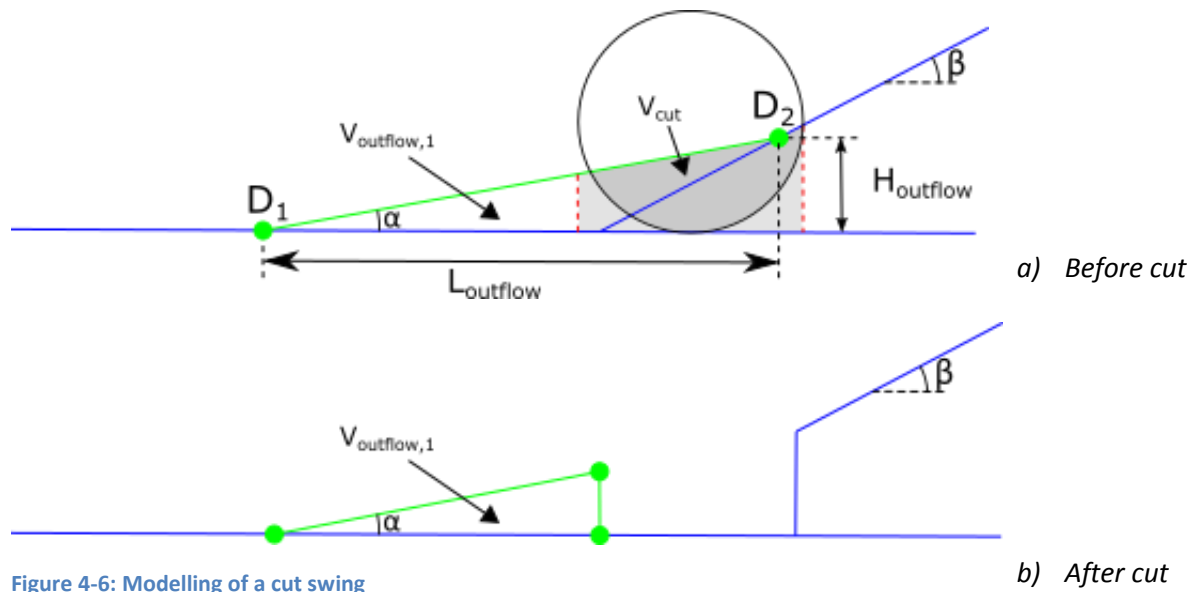
Figure 4-6: Modelling of a cut swing

During normal retrograding of one or multiple breaching walls, point D_1 moves to the left and point D_2 moves up the slope while keeping α constant. It is possible that point D_1 is modelled in such a way that it intersects with a $V_{outflow,1}$ volume which is the result of earlier spillage, this scenario is illustrated in Figure 4-7. The red volume in Figure 4-7 called V_{extra}, is creating an overlap which disproves conservation of mass. This overlapping volume is calculated continuously through the time. When a cut is made in this section, the volume V_{extra} is spread out over the active top of the $V_{outflow,2}$ area with a length of L_{top}. The actual top of the cut volume is L_{cut}. The extra volume V_{extra} is taken in to account during a cut as follows:

$$V_{cut,total} = V_{cut} + V_{extra} \cdot \frac{L_{cut}}{L_{top}} \tag{4.7}$$

After a long sequence of clean-up swings and cut swings, it is possible that many spillage volumes are created in the model. The V_{extra} correction must be separately executed for every overlapping volume present during a cut.
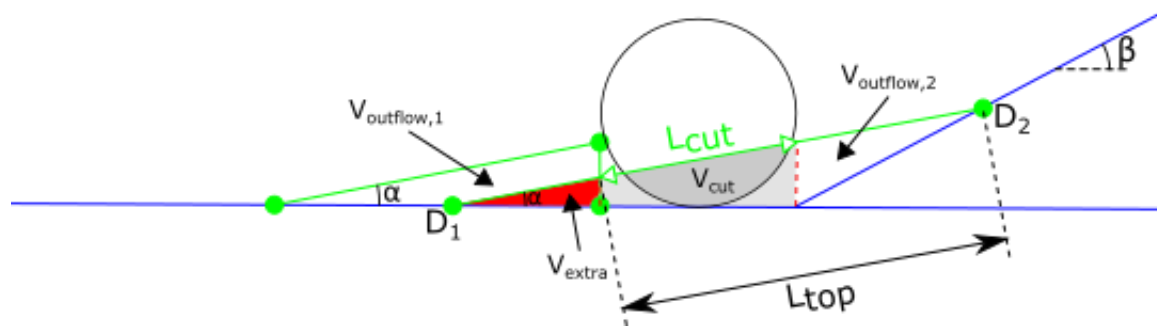
Figure 4-7: Spillage overlap correction

4.3 Model validation experiment

The same lab test discussed in paragraph 3.3 is used in comparison to the production model. The difference in this case is that the outflow angle is constant, which is more in agreement with the lab test. However the breaching model gives a more realistic rendition of a large scale breach.

The wall velocity from the breaching soil in the lab test is measured and put in the production model. The production is very small due to the small layer of soil of only 8 cm. This causes a high outflow angle almost equal to the angle of repose. Only one cut is made, so the top of the dense soil after breaching is modelled as the pink dashed line in Figure 4-3 discussed earlier. The grey area in Figure 4-3 stays stable in the simulations in Figure 4-8, because only one cut is made. In a case of multiple cuts this area must however be taken in to account as unstable. The shape of the initial soil and the outflow soil can be compared with the predictions of the production model. Figure 4-8a gives the initial situation of the lab test and the same situation modelled. Figure 4-8b gives the situation while breaching is active and Figure 4-8c gives the end situation of the lab test. All situations are compared with the model prediction which are respectively given to the right of the lab test situations.
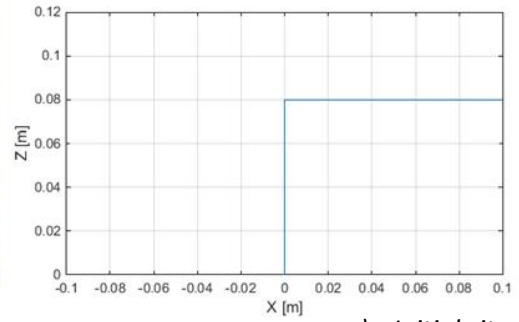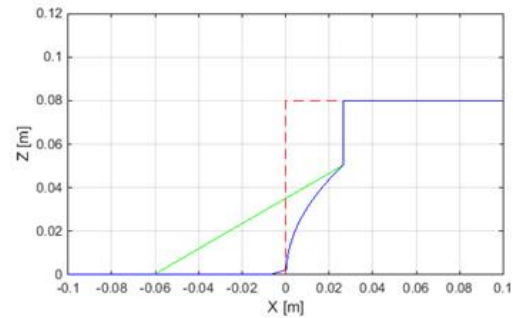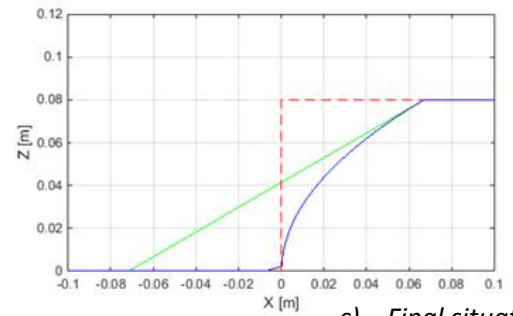
Figure 4-8: Breaching lab test comparison

As can be seen in Figure 4-8, the border between the densely packed soil and the loosely packed soil has a high similarity between the lab test and the model. The same curve is visible in the lab tests as is predicted in the model. This gives a good confidence that the process is modelled in an accurate way. The shape of the outflow volume can show some differences, because the angle is kept constant in the model and in reality this angle can differ in time. In Figure 4-8b the lab test has an outflow length of 5,5 cm and the model predicts an outflow length of 6 cm. In the final situation the lab test has an outflow length of 5,5 cm and the model predicts an outflow length of 7 cm. this shows that the outflow in the lab test terminates earlier and the soil sediments under a steeper angle at the end of the test. The difference is small in the early stages of breaching and increases in time. This will also happen in real cases if the breaching wall decreases higher up a slope. However, the dredging production will not be influenced a lot by this, because a dredger only cuts the outflow soil and not the soil sedimented higher up the slope. More about this phenomena is explained in the next paragraph.

4.4 Production model versus breaching model

The production model is a simplified model, which can predict the production of a breaching process. The reason to create a simplified model is the increasing uncertainty of a sequence of cuts in the breaching model. If a second cut would be introduced in the breaching model, a very complicated situation would arise, which cannot be predicted by only using a theoretical approach. The production model simplifies the process in order to create a repeated situation for every cut. This way a sequence of cuts in 3D can be modelled and can say something about the production. The difference in calculation time is also an important factor. The calculation time for the breaching model is a factor 10 higher than the production model. If the breaching model would be extended to the third dimension, this would result in very long calculation times. The production model is more simplified, so it needs much less calculation time.

Table 4-1: Differences between models

Production model	Breaching model
All steps are independent of each other	Every step depends on the previous step
Constant outflow angle (α)	Variable outflow angle (α)
Constant breaching wall height	Variable breaching wall height
Low calculation time	High calculation time
Simulation in 3D	Simulation in 2D
Able to simulate a sequence of cuts	Only simulates a single cut scenario
Only valid for a limited number of soil types	Valid for all possible soil types

The differences between the models are ordered in Table 4-1. The main difference between the modelling of the production model and the breaching model is that in the breaching model a step is dependent on the previous step and in the production model a step is independent of the previous step. As a result of this, in contrast with the breaching model, the production model has a constant outflow angle and a constant breaching wall height. In the previous chapters, both models are compared with the same lab test. The breaching model comparison is given in Figure 3-4 and the production model comparison is given in Figure 4-8. The lab test simulations of both models are given in Figure 4-9. As explained before, the breaching model is simulated at a scale which is a factor 10 higher. The outflow distance is slightly larger in the breaching model, due to the curved shape of the top of the outflow volume. The lab test is too small to create a density flow, so the outflow angle stays constant. However the curved outflow angle modelled by the breaching model is more realistic for a large scale scenario. The breaching model terminates before the top of the layer is reached, this is a result of the chosen step size. The difference becomes too small to calculate in a single step.
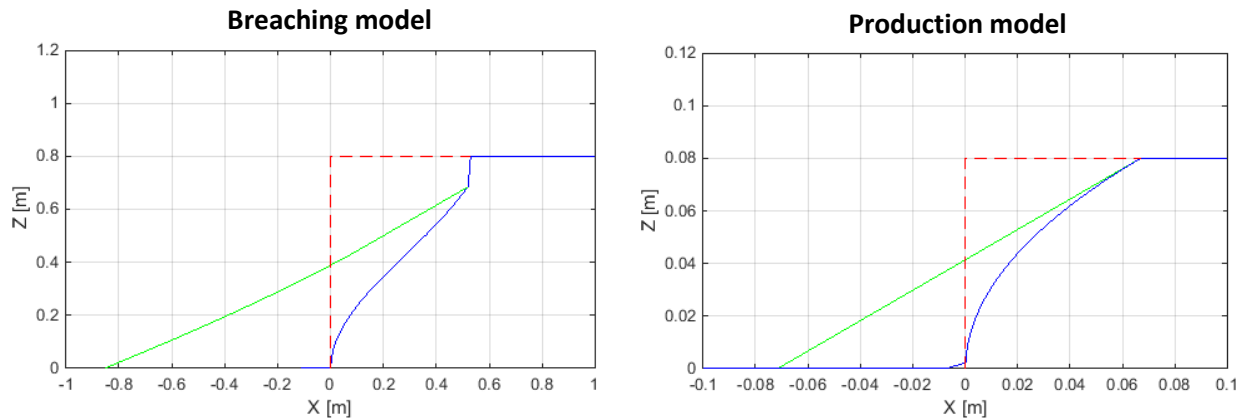
Figure 4-9: Comparison of models

Figure 4-10 gives a graph with the end result of both models for the same scenario. A slope of 25° and a height of 5 meter is used. The soil parameters of the reference soil given in Table 3-1 are used for the soil in both models and a cut height of 1.0 m is initiated. The top of the loose soil in both models is very similar. Just like the lab tests, the breaching model predicts a slightly larger outflow distance. The top of the dense soil shows more deviation between the models, but the average differences are not very large for this particular situation. A more extensive comparison is presented in Appendix E.

Figure 4-11 quantifies the differences between the models. The cuttable soil is plotted versus the time for both models. Cuttable soil is the soil the cutter can potentially accumulate if it would make a swing through the slice at the given time, illustrated in Figure 4-5a. This is the most important parameter to compare the models on, because the prediction of the soil production by the dredger is the goal of the model. The red line gives the absolute difference in cuttable soil between the models. The maximum error appears to be after 2900 seconds and is 8% of the expected result calculated by the breaching model, this is an accepted deviation for this type of soil. The example with a slope of 25° and the soil similar to the reference soil is used further in this chapter.

Because of the simplification of the production model, the exact production numbers cannot be proven for every type of soil. However it is possible to predict phenomena which might occur during the dredging of the concerned slope of soil. Some of the phenomena resulting from dredging choices are explained in paragraph 4.6.
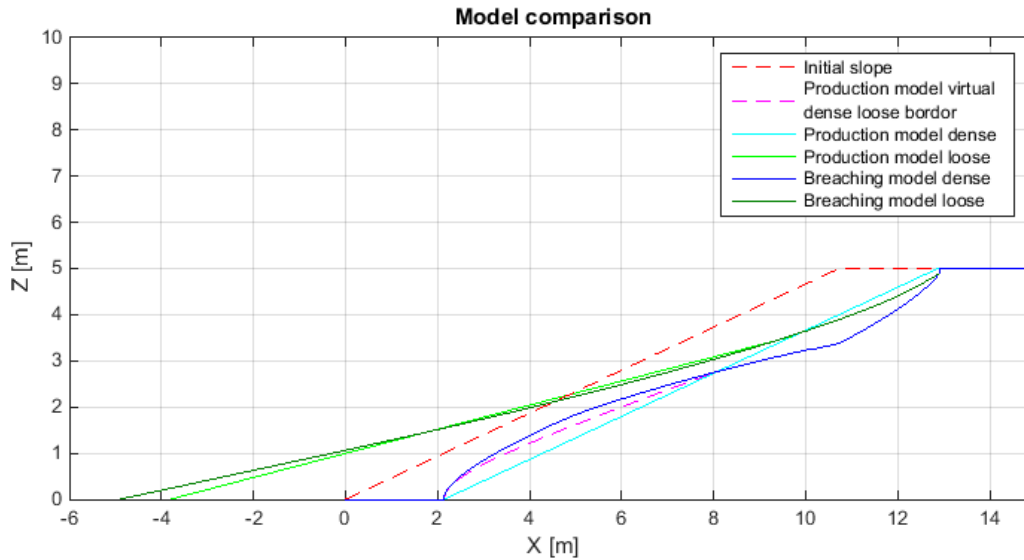
Figure 4-10: Production model vs breaching model comparison
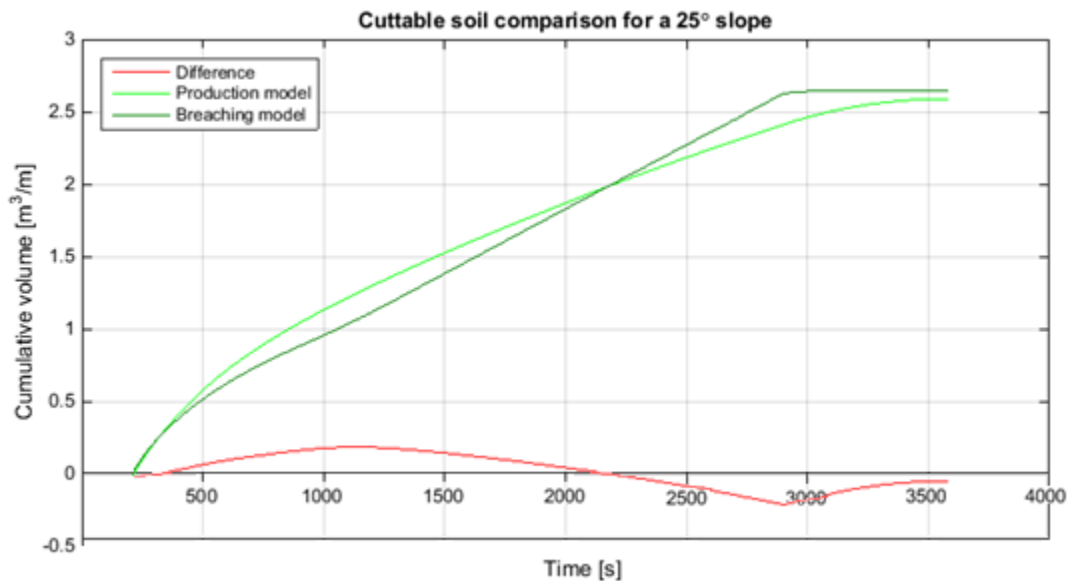
Figure 4-11: Absolute differences between the models

4.5 3D model

The previously described 2D variant of the production model is the base model for the three dimensional model. Dredging is a 3D process, because the cutting wheel does not only move forward. It swings sideways while cutting the soil. This sideway motion is essential for calculating the production rate of the process and can impossibly be calculated from a 2D model. The 3D model is described as a line model, which means that the 2D sections are repeated in the third dimension. A swing width is given which determines the extension in the third dimension. Over this length perpendicular lines are plotted that describe the behaviour of the soil on that line. The 3D model can be used to determine the

production of breached soil and the production of cut sand depending on the cutting sequence chosen. The exact procedure is further described in this chapter.
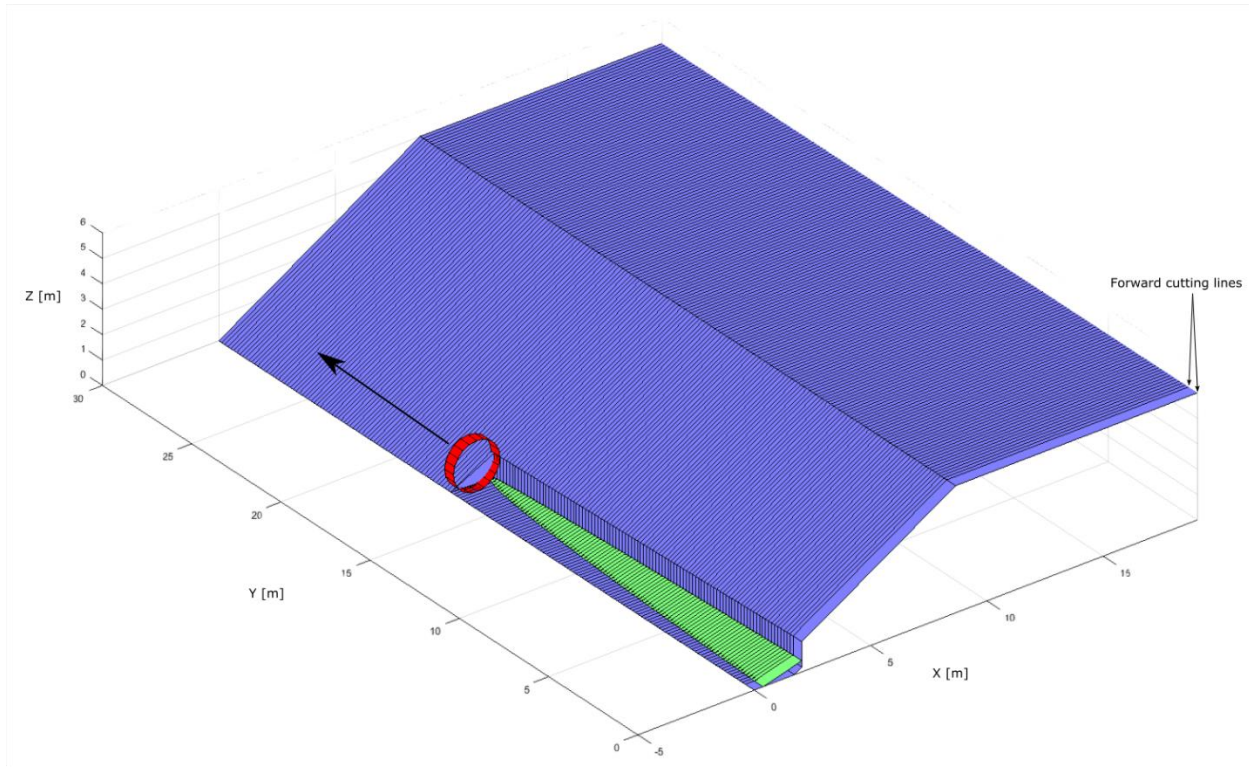
Figure 4-12 gives a possible initial situation of the 3D model. The swing width extents in the y-direction and the height of the slope extents in the z-direction. It is assumed this initial slope is stable over the entire length. The dredging wheel is the red wheel moving through the slope. The forward cut is modelled using the forward cutting lines, these two lines are differently modelled from the other lines that cover the swinging part of the slope. The forward cutting lines are located on the outmost right side of the slope with a distance between them equal to the wheel width. To the left the field is filled up with normal lines, these lines have a step size equal to the swing speed. This ensures that every second, a new position of all the lines is created.

4.5.1   Explanation of the model

There are two types of swings that can possibly be made by the dredging wheel. The first swing is always a cutting swing preceded by a forward step. In the production model the forward step is always executed on the right side of the dredged area at the forward cutting lines. The wheel is now moved sideways through the initial slope in which the wheel creates a new cut. The cutting ends when the wheel is on the other side of the dredged area. After a possible delay, the wheel swings back to the other side of the dredged area without cutting into the initial slope. When the wheel is back at the starting line, it can make some clean-up swings. As many clean-up swings as necessary can be executed before another forward step is made. The process can start over again until enough material is collected.

The model creates a 3D animation of the slope in which the movement of the dredging wheel is plotted. The final output is a graph in which the production per second is plotted against the time and a graph for the cumulative production.

Every line needs to be filled up with geometrical information, but due to the lateral movement of the dredging wheel, the starting time of an event is different for every line. The model starts with determining the starting times of events happening at a certain line. An event can be the start of a cut or the passing of a clean-up swing through a line. The time these events happen and the time between the events is different for every line. A 2D simulation for every line is made with the specific starting times for the events. The 3D model consists of all the 2D simulations lined up with the given distance between the lines. The two lines on the right side of the dredging area are calculated differently from the other lines. These are the forward step lines, they describe the position where a forward step is executed. The distance between these lines is defined as the wheel width, which is an input parameter. Instead of an instant cut situation, they must be calculated with a forward cutting velocity. The forward step lines are calculated separately from the other lines.

4.6 Results

The model can simulate every possible dredging sequence on the given slope. Figure 4-13 shows the production rate per second for a single cut made on the 25° slope. The grey area is the time needed to make the forward step into the slope. During the forward motion, the production is very low. The blue line gives the production rate during the cutting swing. It is constant, because the cutter goes through an undisturbed slope. The green line gives the production rate for the clean-up swings. The production rate goes up and down, because at the start of a swing the cutter moves through an area which is just cut in the previous swing. This results in a lower production rate. The production rate is the highest at the end of a swing. The black line gives the spillage created by soil which flows out behind the cutter. In this example the spillage is very small compared to the production. The models assumes a constant swing speed, but in reality the swing speed can be adjusted to keep the production constant.
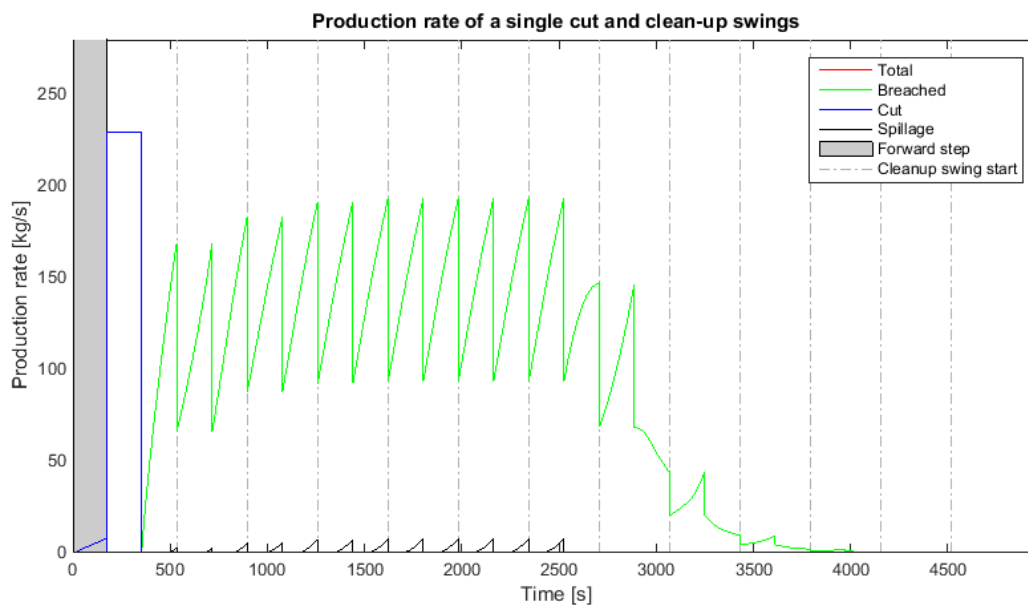
Figure 4-13: Single cut production rate

The cumulative production for the same slope and dredging sequence is given in Figure 4-14. It is visible that after around 3000 seconds, the production starts to decrease and a new cut might need to be made. A new cut should be made when the production becomes too low. A second cut situation is given in Figure 4-15. The second cut is made after 3000 seconds, which keeps the production at a high level. The spillage stays at low rates after the second cut. The time to initiate a second cut is important, because it has an influence on the spillage and production.
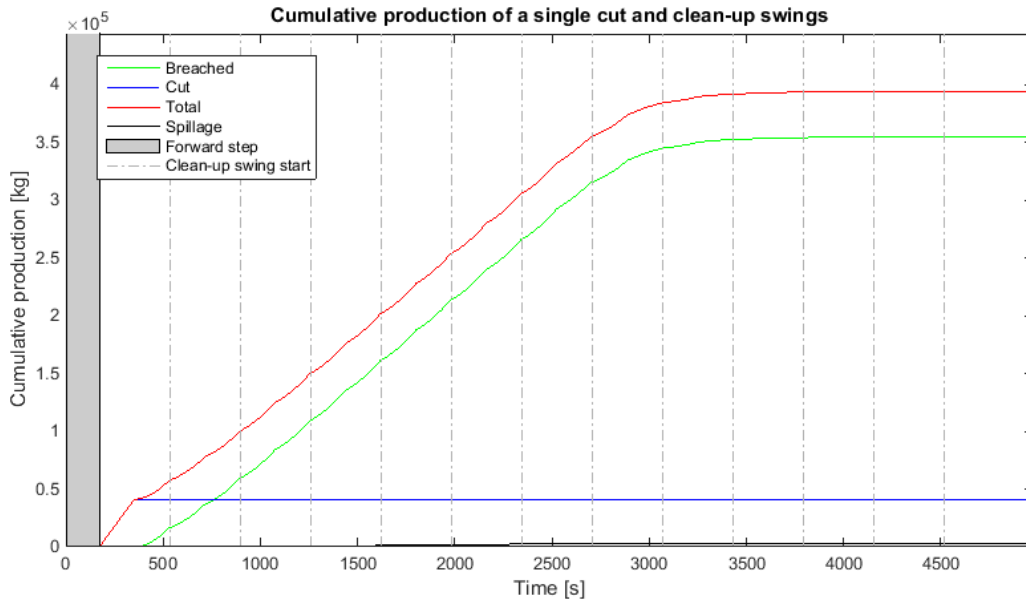
Figure 4-14: Single cut cumulative production
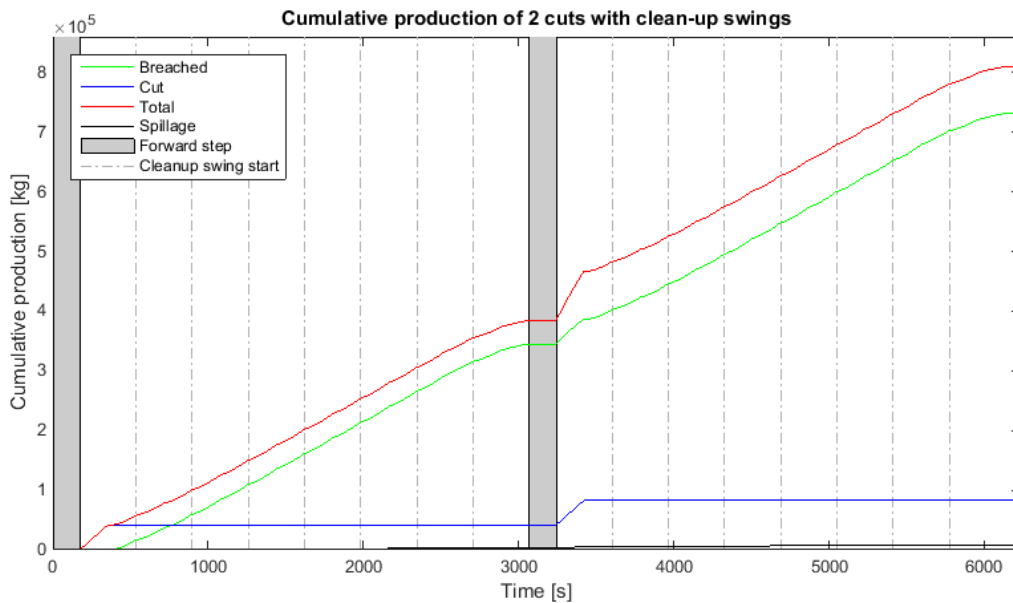
Figure 4-15: Second cut cumulative production

Figure 4-16 gives an example of a second cut which is made too early. The spillage is much higher than in the previous case. The production just after the second cut will be high, but in the end the total production will be lower. The moment to make a new cut should be carefully chosen if the spillage must be minimalised.
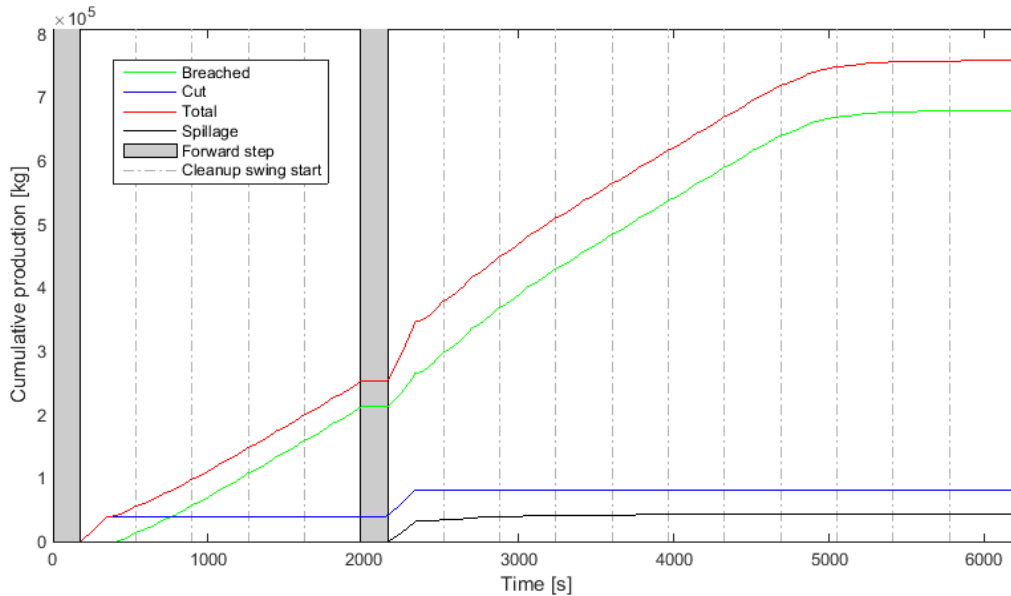
Figure 4-16: Second cut too early

4.7 Summary

The production model is developed for this research in order calculate the dredging production of a slope. The production model is based on a simplified version of the breaching model. The production model is extended in 3D and can incorporate a sequence of cuts, whereas the breaching model can only handle a single cut. The simplified version of the breaching model needs a factor 10 less calculation time than the breaching model itself, so it is much more useful for large dredging simulations.

Except for the calculation time, there are more reasons to use a simplified version of the breaching model for the 3D production model. The full breaching model as explained in chapter 3 cannot be expanded to a 3D model at this moment. If a sequence of cuts is executed, a very complicated combination of dense and loose soil exists, which has an influence on the breaching behaviour. The initial situation for every cut would be different and the uncertainty would be too large to create a reliable model. In order to extend the breaching model directly into the third dimension, more research must be done into the influence of loose and dense soil on breaching. The simplified model creates a repeating situation for every cut, which makes it suitable for a sequence of cuts and extension in 3D.

The disadvantage of the production model is that it is only valid for certain soil types, for instance the reference soil used in chapter 3. The model is based on many 2D sections lined up to create a 3D model. A consequence of this is that there cannot be any volume transport in the third dimension.

The model can calculate the production of a dredging sequence consisting of cut swings and clean-up swings. The cumulative production in time of a certain dredging sequence can be calculated. The total production can be optimised by adjusting the dredging sequence.

5 Parameter estimation

As explained in the previous chapter, there is a list of input data necessary to calculate the breaching behaviour. In this chapter the input data will be described and several field and lab tests will be suggested to obtain the necessary data. Some parameters are trivial and easy to obtain and some are more difficult and might need an extra test on top of the standard tests executed during a field investigation.

5.1 Geotechnical data

The input data can be distinguished in different types. The first type is the geotechnical data, which are given in Table 5-1.

Table 5-1: Required geotechnical parameters

Geotechnical Input parameters	Explanation
k_0 [m/s]	Initial permeability
n_0 [-]	Initial porosity
n_1 [-]	Loose soil porosity
ρ_s [kg/m^3]	Particle density
ρ_w [kg/m^3]	Water density
φ [°]	Angle of repose
D_{50}	Median particle size

5.1.1 Permeability

The first parameter is the initial permeability. This parameter is relatively easy to obtain in-situ. There are a few methods to measure the permeability. The auger-hole method is a rapid, simple and reliable method. It is originated by Diserens (1934) and was improved by Hooghoudt (1936) and later by Kirkham (1945, 1948), Van Bavel (1948), Ernst (1950), Johnson (1952) and Kirkham (1955). The method is performed in a borehole with a depth under the water table. When the groundwater in the borehole is in equilibrium with the surrounding groundwater, a part of the water in the hole is pumped out. The surrounding groundwater will seep back into the hole until equilibrium is restored. The rate at which the water flows back into the hole is a measurement for the in-situ permeability around the hole.

5.1.2 Porosity increase and dilative behaviour

The porosity change from initial porosity to critical porosity might be the hardest parameter to obtain. This parameter depends on the in-situ conditions, which makes lab testing difficult. It is possible to acquire the porosity of the soil from CPT data, by doing a state parameter analysis. The state parameter can be directly determined from CPT data and is defined as the measure of the deviation between the void ratio at the in situ state and the void ratio at the critical state (van Duinen et al., 2014). The state parameter can be recalculated to the difference between the in-situ porosity and the critical porosity. This difference is essential for determining the breaching behaviour of the soil.

A CPT is however an uncommon field investigation device outside of the Netherlands. It is more common to use an SPT combined with a drilling to obtain soil samples. An SPT gives a direct indication of the relative density of the soil. Correlations are available to calculate the relative density [%] from the blow count obtained from an SPT test. According to (roughly chosen) criteria generally applied in Dutch engineering practise a relative density above 67% indicates a potentially dilative soil (Van Duinen et al., 2014). The relative density in combination with the particle density can give an estimate of the in-situ porosity. It is also possible to take an undisturbed sample from a borehole and determine the porosity in the lab. It is however difficult to obtain a fully undisturbed sample.

5.1.3   Density

The density of the soil particles must be measured. This can be done with a small lab test and does not require in-situ conditions. The particle density can be measured using a disturbed sample and a pycnometer. The sample must be dried and weighed and placed into the pycnometer. The pycnometer is filled with a fluid of known density in which the sample is not soluble. The volume of the powder is determined by the difference of the volume of the pycnometer and the volume of fluid added. The particle density can be calculated.

5.1.4   Angle of repose

In theory the angle of repose of soil above water and under water are the same, so there is only one angle (φ) which must be measured. This angle is important for determining the wall velocity and the geometry of the breaching process. The angle of repose is the maximum angle at which a slope of dry soil can dip. It can be determined by using a lab test or an in-situ test. The blow count of an SPT gives a direct indication of the friction angle of the soil. The friction angle is similar to the angle of repose in a loose soil. The angle of repose can also be determined by a lab test. A dry sample is needed, a pile is made by dropping the soil on a horizontal plate. The angle of repose is the outflow angle of the soil with the horizontal plate.

5.1.5   Particle size

The particle size is a trivial parameter, which does not depend on the in-situ conditions. It is very easy to take a sample, which can be a disturbed sample, and do a sieve analysis on it. The sample does not need to be contained at in-situ conditions and the sample does not go lost after the test has been executed. A particle size distribution is created by the sieve analysis. The D_{50} and the D_{10} values are the most important for the model. The D_{50} is used for the empirical relation which describes the outflow angle of the breached soil. The D_{50} value is also very important just for understanding the type of soil which is dredged. The D_{10} value is used in the Hazen equation as a measure of the permeability.

Another parameter which is often used in a field investigation is the D_{15} percentile of the particle size distribution. This parameter gives a value for the amount of fines in the material in the Den Adel equation given in (5.1). It is possible to relate this value to the permeability as follows:

$$k_0 = \frac{g}{160 \cdot v} \cdot D_{15}{}^2 \cdot \frac{n_0{}^3}{(1 - n_0)^2} \tag{5.1}$$

In this equation:

v [m²/s] = kinematic viscosity
g [m/s²] = gravity acceleration

n_0 [-] = initial porosity

D_{15} [m] = 15th percentile of particle size distribution

This is an example of what can be done with the data from the particle size distribution. It is however more reliable to measure the permeability in the field than to use an empirical relation which is again based on parameters measured in the field.

The particle size distribution is already a common test, which often belongs to the standard tests during a field investigation. No big changes need to be made to obtain the value D_{50}.

5.2   Geometrical data

The second type of input data is the geometrical data, which are given in Table 5-2.

Table 5-2: Required geometrical parameters

Geometrical Input parameters	Explanation
H_{cut} [m]	Wall height
H [m]	Slope height
β[°]	Slope angle

The geometrical data describe the shape of the initial slope and the height of the cut made by the cutter. The wall height is determined by the depth of the cut, which is dependent on the type and size of the equipment. The slope is easily modelled as a slope with angle β and height H. the slope is considered to have an infinitely long width.

6 Conclusion and recommendations

6.1 Conclusion

6.1.1 Breaching model

The breaching model is developed with the aim to predict the breaching behaviour of a slope based on the geometry of the initial slope and the geotechnical parameters of the soil. The breaching behaviour can be predicted based on the initial permeability (k_0), the angle of repose (φ), the median particle size (D_{50}), the porosity change ($n_1 - n_0$) and the particle density (ρ_s). The parameters have the following influence on the stability of the breach:

- An increase in the permeability will cause a decrease in the breaching stability. The same trend is caused by the D_{10}, because they are positively correlated by the Hazen equation.
- An increase in the D_{50} causes an increase in the breaching stability. This is mainly a result of a larger outflow angle at a higher D_{50}.
- An increased particle density causes a decreased breaching stability. This is a result of a higher wall velocity at a higher particle density.
- The geometry of the slope has a large influence on the breaching behaviour. The steeper the slope or the higher the initial breaching wall, the faster the breaching becomes unstable.

In order to validate the implementation of the parameters in the model, an empirical relation for the critical cut height is developed which can be compared to a similar equation by Van Rhee (2015). The equation quantifies the influence of every single parameter. Only the particle density does not result in a similar influence on the breaching process in the two equations.

The fact that denser particles sediment quicker and increase the stability of the breach is not represented in the empirical relations for the model. This process probably overshadows the process in which the wall velocity increases due to a higher particle density. If the wall velocity increases, the dense particles will still sediment quicker, which increases the stability of the breach. This is probably the reason for the deviations in the implementation of the particle density in the model.

6.1.1.1 Limits of the model

The breaching model is based on several theoretical equations combined with conservation of mass. The model must be suitable to be used for cases on a large scale, however in this research the model can only be validated by comparing it with small scale lab tests. There is an uncertainty in the effects of scale enlargement.

A feature which is not taken into account is the erosion at the toe of the breaching wall due to a density flow. It might be possible that a dent is created at the toe of the breaching wall due to erosion. This phenomena is neglected in the breaching model in a way that soil which has been sedimented cannot be picked up and replaced again.

6.1.2 Production model

The production model is based on a simplified version of the breaching model and can demonstrate different phenomena which might occur during a dredging operation. A few phenomena which can be illustrated are:

- Spillage of soil due to a too low swing velocity or a too wide swing width.
- Spillage of soil due to a delay in the turnaround time of the cutter.
- Differences in production which are caused by different choices made in the dredging sequence.

The ratio between the production from cutting and the production by breaching can be calculated, but the exact production amounts calculated by the model cannot be considered reliable enough for every type of soil put into the model.

6.1.3 Parameter estimation

The soil parameters necessary for the models presented in this report are usually obtained from a standard field investigation. Therefore no extra field- or lab tests need to be executed in order to predict the breaching behaviour of a slope. In order to find out if the slope will breach after cutting, a state parameter analysis must be conducted. This can be done by using CPT data. A second option is to use SPT data in combination with samples taken from the SPT drilling. If breaching is expected, more tests need to be conducted to predict the breaching behaviour.

- Sieving to obtain the particle size distribution in order to obtain the D_{50} and the D_{10}.
- Pycnometer test in order to obtain the particle density.
- Angle of repose lab test or correlation with SPT results.
- Optional auger hole test in order to calculate the permeability. This test can be used to confirm the permeability calculated from the D_{10} value.

6.2 Recommendations

- The breaching model is constructed according to theory, but the model itself has not been validated on a large enough scale. Scale enlargement in breaching is still an unknown feature. It is predicted that for large scale breaches, the wall velocity will be higher than small scale breaches consisting of the same soil. It is however not known in what extent the wall velocity increases. Lab tests with large scale breaching walls need to be conducted in order to understand the influence of scale enlargement on breaching.

- The breaching model only predicts the breaching behaviour of a slope in two dimensions. However, dredging is a 3D process and can only be accurately predicted in a 3D model. The breaching model must be extended in 3D. The time available for this research was too limited to do this, but a successive research can focus on the 3D extension of the breaching model.

- The models presented in this report assume that breaching happens when an instability is created in the slope. It means that the under pressure in the soil due to dilatancy is high enough to maintain a vertical breaching wall. If the under pressure is too low, the breaching might transform to wedge failure or liquefaction. The transition between breaching, liquefaction and wedge failure needs more research in order to make an accurate prediction about the failure of a slope.

- More research needs to be done into the effect of a sequence of cuts on the breaching behaviour. At this moment the breaching model cannot be expanded with multiple cuts, because it is unknown what the resulting breach will look like. A better estimation can be derived if the influence of a sequence of cuts on the slope is better researched.

References

Been, K., & Jefferies, M. G. (1985). A state parameter for sands. *Géotechnique*, *35*(2), 99-112.

Bezuijen, A., & Mastbergen, D. R. (1988). On the construction of sand fill dams. Part 2: soil mechanical aspects. *Mod. of Soil-Water Interactions, Delft*.

Breusers, H. N. C. (1974). Suction of sand. Bulletin of the International Association of Engineering Geology-Bulletin de l'Association Internationale de Géologie de l'Ingénieur, 10(1), 65-66.

Brownlie, W. R. (1981). Compilation of alluvial channel data: laboratory and field (p. 37). California Institute of Technology, WM Keck Laboratory of Hydraulics and Water Resources.

De Groot, M. B., Mastbergen, D. R., Van der Ruyt, M., & Van den Ham, G. A. (2009). Bresvloeiing in zand. *Geotechniek*, *13*(3), 34.

Diserens, E. (1934). Beitrag zur bestimmung der durchlässigkeit des bodens in natürlicher bodenlagerung. Schweiz, Landw. Monatstr. 12.

Ernst, L. F. (1950). A new formula for the calculation of the permeability factor with the auger hole method. T.N.O. Groningen 1950. Translated from the Dutch by H. Bouwer. Cornell Univ. Ithaca. N.Y. 1955.

Hazen, A. (1892). Some physical properties of sands and gravels: with special reference to their use in filtration. publisher not identified.

Hooghoudt, S. B. (1936) Bepaling van den doorlaatfactor van den grond met behulp van pompproeven, (z.g. boorgatenmethode). Verslag Landbouwk. Onderzoek 42, Pp. 449-541.

Johnson, H. P., Frevert R. K., & Evans D. D. (1952). Simplified procedure for the measurement and computation of soil permeability below the water table. Agric. Eng. Pp. 283-286.

Kirkham, D. (1945). Proposed methods for field measurements of permeability of soil below the watertable. Proc. Soil. Sc. Soc. Am., pp. 58-68.

Kirkham, D. & van Bavel, C. H. M. (1948). Theory of seepage into auger holes. Proc. Soil. Sc. Soc. Am., pp. 75-82.

Kirkham, D. (1955). Measurement of the hydraulic conductivity of soil in place. Symposium on permeability of soil. Am. Soc. For testing materials. Spec. Techn. Publ. No. 163.

Mastbergen, D. R. (2009). Oeverstabiliteit bij verdieping waterbodems: Rekenmodel HMBreach. Delft Cluster.

Mastbergen, D. R., & Bezuijen, A. (1988). Zand-watermengselstromingen-het storten van zand onder water, 5: verslag experimentele vervolgstudie middelgrof zand. Deltares (WL).

Mastbergen, D. R., & Van den Berg, J. H. (2003). Breaching in fine sands and the generation of sustained turbidity currents in submarine canyons. *Sedimentology*, *50*(4), 625-637.

Mastbergen, D. R., Winterwerp, J. C., & Bezuijen, A. (1988). On the construction of sand fill dams. Part 1: hydraulic aspects. *Modelling Soil-Water structure interaction, Kolkman, et al.(eds.)*, 353-362.

Richardson, J. F., & Zaki, W. N. (1954). The sedimentation of a suspension of uniform spheres under conditions of viscous flow. Chemical Engineering Science, 3(2), 65-73.

Silvis, F., & Groot, M. D. (1995). Flow slides in the Netherlands: experience and engineering practice. *Canadian geotechnical journal*, *32*(6), 1086-1092.

Van Bavel, C. H. M. & Kirkham D. (1948). Field measurements of soil permeability using auger holes. Proc. Soil. Sc. Soc. Am., pp 90-96.

Van den Berg, J. H., Van Gelder, A., & Mastbergen, D. R. (2002). The importance of breaching as a mechanism of subaqueous slope failure in fine sand. *Sedimentology*, *49*(1), 81-95.

Van der Schrieck, G. L. M. (2012). Lecture notes dredging technology. *Delft University of Technology*.

Van Duinen, A., Bezuijen, A., Van den Ham, G., & Hopman, V. (2014). Field measurements to investigate submerged slope failures. In *Submarine mass movements and their consequences* (pp. 13-21). Springer International Publishing.

Van Rhee C. (2010). Sediment entrainment at high flow velocity. *Journal Of Hydraulic Engineering*, *136*(9), 572-582.

Van Rhee, C. (2015). Slope failure by unstable breaching. *Proceedings Of The ICE - Maritime Engineering*, *168*(2), 84-92.

Van Rhee, C., & Bezuijen, A. (1998). The breaching of sand investigated in large-scale model tests. *Coastal Engineering Proceedings*, *1*(26).

Van Rijn, L. C. (1984). Sediment pick-up functions. *Journal of Hydraulic Engineering*, *110*(10), 1494-1502.

Verruijt, A., & Van Baars, S. (2007). *Soil mechanics* (pp. 19-25). Delft, the Netherlands: VSSD.

Vlasblom, W. J. (2003). College WB3413 Dredging Processes.

Winterwerp, J. C., Bakker, W. T., Mastbergen, D. R., & van Rossum, H. (1992). Hyper concentrated sand-water mixture flows over erodible bed. *Journal of Hydraulic Engineering*, *118*(11), 1508-1525.

Appendix A

Advanced volume placement

In paragraph 3.2 it is explained that the volume $V_{outflow,n}$ is placed with the outflow angle α_n on top of the previously placed volumes $V_{outflow,n}$. The angle α_n can be larger or smaller than α_{n-1}. It is not certain if the volume $V_{outflow,n}$ must be placed against the wall (as illustrated in Figure A-1), at the bottom of the outflow or somewhere in the middle. In this paragraph it will be explained how the volume placement is designed assuming full mass conservation.

After a sequence of steps a situation as illustrated in Figure A-1 will happen. This is a schematic illustration, because in reality the outflow angles will be lower. The green line is the top of the outflow volume, this volume has an increasing slope angle. The new volume placed on top of this line must be placed in such a way that the increasing slope angle is maintained. An example to show how the volume $V_{outflow}$ can be placed is given in Figure A-1. In this figure the angle α_c is the outflow angle of the concerned $V_{outflow}$. The position is chosen in such a way that the angle α_c is larger than α_a and smaller than α_b. The volume can now be placed as a triangle over point p with $L_{outflow}$ the base and $H_{outflow}$ the height of the triangle. The height $H_{outflow}$ can be calculated from the angles α_a, α_b and α_c and the volume $V_{outflow}$ as given in equation (A.1). $L_{outflow}$ can be calculated as given in equation (A.2). These equations are derived geometrically.
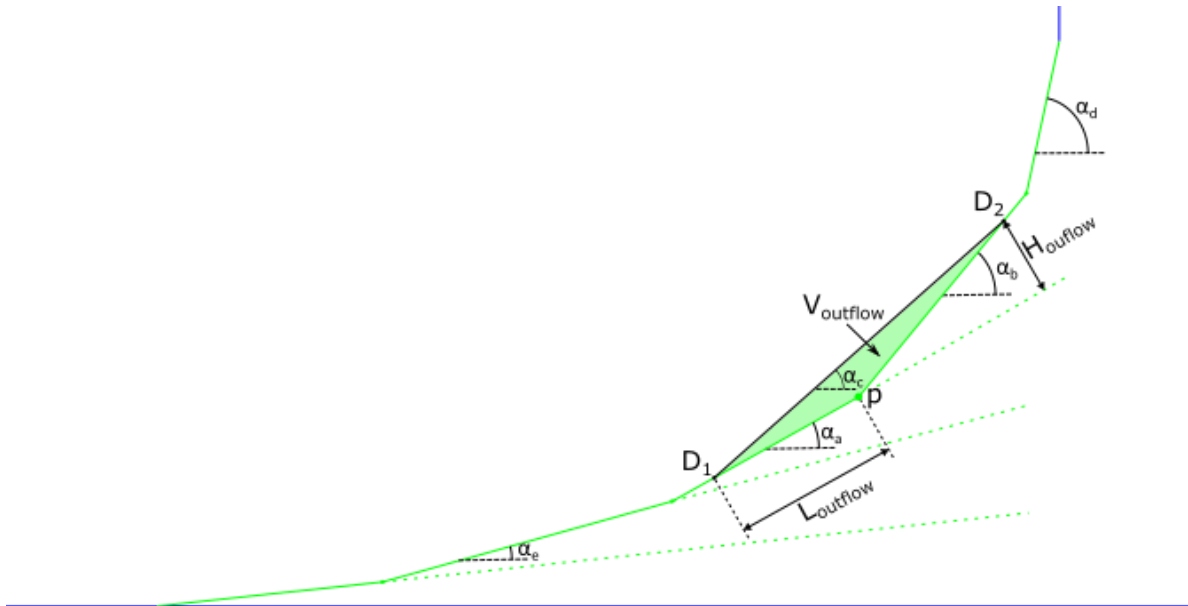
Figure A-1: Outflow volume placement

$$H_{outflow} = \frac{\sqrt{2} \cdot \sqrt{V_{outflow}}}{\sqrt{\cot(\alpha_c - \alpha_a) - \cot(\alpha_b - \alpha_a)}} \tag{A.1}$$

$$L_{outflow} = \frac{H_{outflow}}{\tan(\alpha_c - \alpha_a)} - \frac{H_{outflow}}{\tan(\alpha_b - \alpha_a)} \tag{A.2}$$
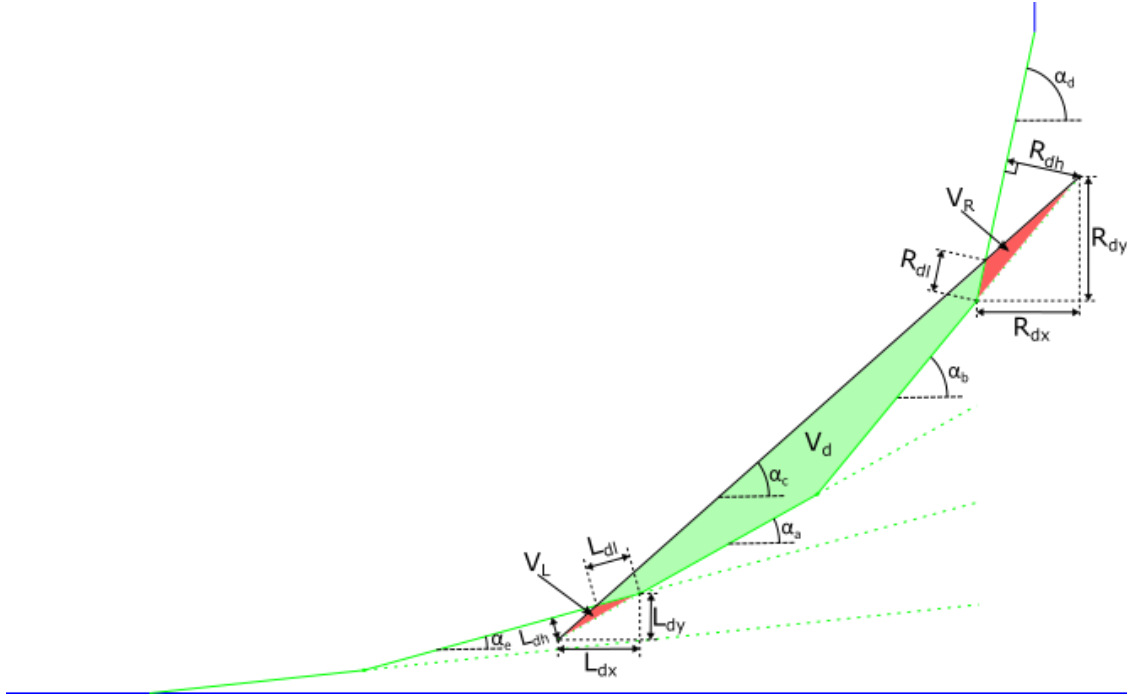
Figure A-2: Outflow volume correction

By positioning the new volume $V_{outflow}$ with the vertices p, D_1 and D_2, the location of the total outflow volume can be obtained. The initial positioning does only take the lines connecting from point p into account. In the case of Figure A-1, the distances $L_{outflow}$ and $H_{outflow}$ are small enough so that $V_{outflow}$ has no overlap with the top of the outflow volume. If $V_{outflow}$ is larger, there might be an overlap as illustrated in Figure A-2. The overlap might become very large when the angles α_a, α_b, α_d and α_e are almost similar, so the overlap volume must be calculated and taken into account. The overlap on the left is called V_L and the overlap on the right is called V_R. The distances L_{dx}, L_{dy}, R_{dx} and R_{dy} are known, with the equations (A.3) to (A.8) the volumes V_L and V_R can be calculated. These equations are completely based on the geometry of the model.

$$L_{dh} = \sin(\alpha_a - \alpha_e) \cdot \frac{L_{dx}}{\cos \alpha_a} \tag{A.3}$$

$$L_{dl} = \frac{L_{dx}}{\cos \alpha_a} \cdot \cos(\alpha_a - \alpha_e) - \frac{L_{dh}}{\tan(\alpha_c - \alpha_e)} \tag{A.4}$$

$$R_{dh} = \sin(\alpha_d - \alpha_b) \cdot \frac{R_{dx}}{\cos \alpha_b} \tag{A.5}$$

$$R_{dl} = \frac{R_{dx}}{\cos \alpha_b} \cdot \cos(\alpha_d - \alpha_b) - \frac{R_{dh}}{\tan(\alpha_d - \alpha_c)} \tag{A.6}$$

$$V_L = \frac{L_{dl} \cdot L_{dh}}{2} \tag{A.7}$$

$$V_R = \frac{R_{dl} \cdot R_{dh}}{2} \tag{A.8}$$

The volumes V_L and V_R must be put together to create the total volume which is modelled in the wrong place:

$$V_{plus} = V_L + V_R \tag{A.9}$$

V_L and V_R must be removed and V_{plus} is the volume which must be added on top of the existing volume $V_{outflow}$. This will create a situation in which the mass conservation is guaranteed and no overlap of volumes will happen. The vertices D_1 and D_2 which were initially modelled below the surface of the outflow area must be shifted to the top of the outflow area in such a way that V_{plus} has the right volume. The points D_1 and D_2 are shifted to respectively D_1' and D_2'. The shift of the overlap volume is illustrated in Figure A-3. The volume V_{plus} is an irregular shape, the dimensions of this volume are calculated by using some trigonometry as given in equations (A.10) to (A.12):

$$c_1 = \frac{1}{\tan \alpha_c - \tan \alpha_e} + \frac{1}{\tan \alpha_d - \tan \alpha_c} \tag{A.10}$$

$$c_2 = dV_d \tag{A.11}$$

$$h_{plus} = \frac{-c_2 + \sqrt{4 \cdot c_1 \cdot V_{plus} + c_2^2}}{2 \cdot c_1} \tag{A.12}$$

h_{plus} is the vertical height of the volume V_{plus}, which will be used to calculate the coordinates of the vertices D_1' and D_2' of V_{plus}. The x- and y-coordinates of D_1 and D_2 are shifted to the coordinates of D_1' and D_2'. The coordinates D_1' and D_2' are calculated as given in (A.13) to (A.24). Mass conservation is now guaranteed and the breached volume during this step is modelled with the right angle on top of the previous outflow volume. For the new step the top of the outflow volume is reformulated with the top of $V_{outflow}$ (including V_{plus}) taken into account. During the next step, the exact same procedure is carried out again.

$$L_{h,x} = L_{dx} - L_{dl} \cdot \cos \alpha_e \tag{A.13}$$

$$L_{h,y} = L_{h,x} \cdot \tan \alpha_c \tag{A.14}$$

$$R_{h,x} = R_{dx} - R_{dl} \cdot \cos \alpha_d \tag{A.15}$$

$$R_{h,y} = R_{h,x} \cdot \tan \alpha_c \tag{A.16}$$

$$L_{plus,x} = \frac{h_{plus}}{\tan \alpha_c - \tan \alpha_e} \tag{A.17}$$

$$L_{plus,y} = L_{plus,x} \cdot \tan \alpha_e \tag{A.18}$$

$$R_{plus,x} = \frac{h_{plus}}{\tan \alpha_d - \tan \alpha_c} \tag{A.19}$$

$$R_{plus,y} = R_{plus,x} \cdot \tan \alpha_d \tag{A.20}$$

The coordinates of the adjusted vertices can be determined by using the equations (A.21) to (A.24):

$$D_{1,x}' = D_{1,x} + L_{h,x} - L_{plus,x} \tag{A.21}$$

$$D'_{1,y} = D_{1,y} + L_{h,y} - L_{plus,y} \qquad\qquad\text{(A.22)}$$

$$D'_{2,x} = D_{2,x} - R_{h,x} + R_{plus,x} \qquad\qquad\text{(A.23)}$$

$$D'_{2,y} = D_{2,y} - R_{h,y} + R_{plus,y} \qquad\qquad\text{(A.24)}$$
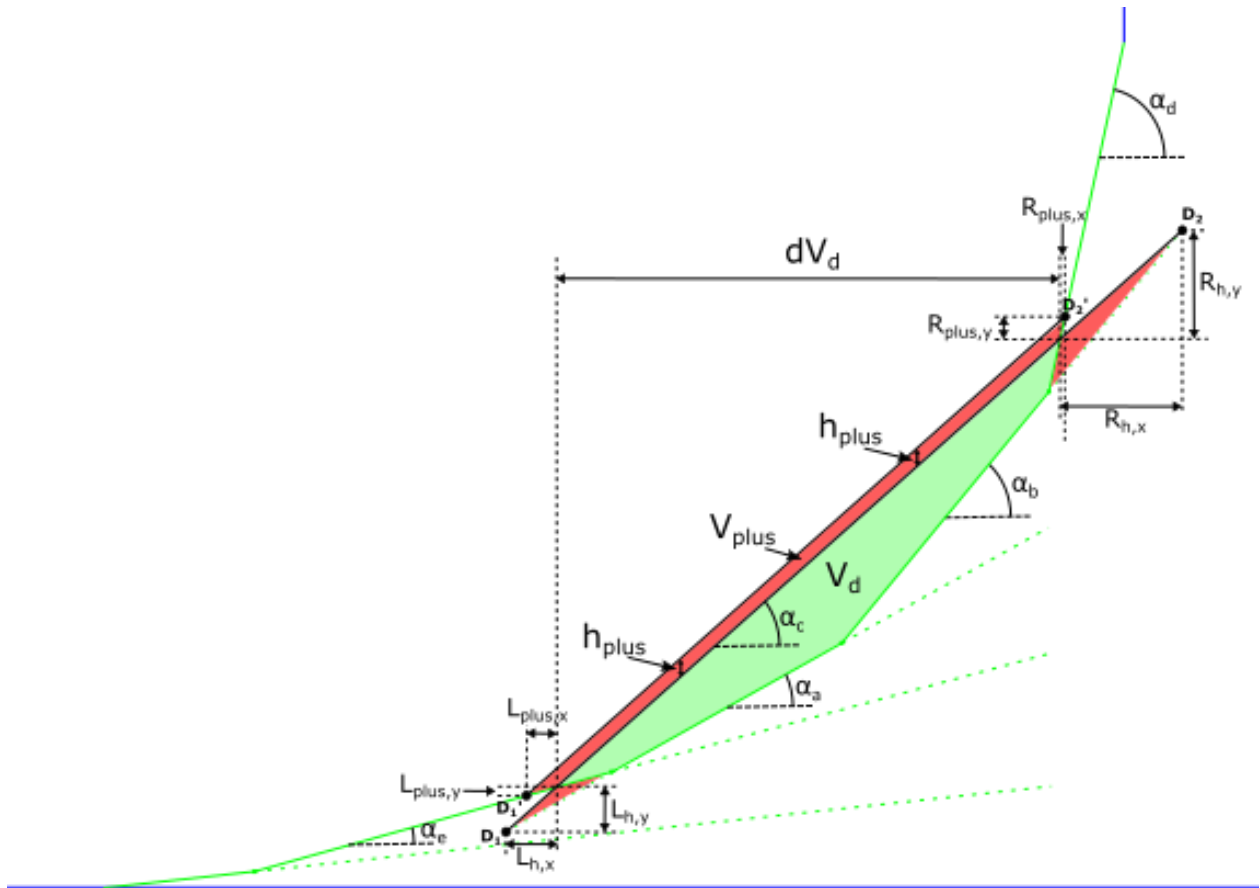
Figure A-3 Outflow volume replacement

Appendix B

The equation for the critical cut height derived in this research is compared to the critical cut height derived by van Rhee (2015). The equations are compared by using the soils given in Table 3-3. The results for the critical cut height for equation (B.1) are given in Table B-1.

$$H_{crit} = 8.193 \cdot 10^{11} \cdot \rho_s^{-2.613} \cdot D_{50}^{2.358} \cdot D_{10}^{-2.027} \cdot \beta^{-2.889} \tag{B.1}$$

The critical cut height for the same slope consisting of the same soil parameter sets is calculated with equation (B.2). The results are given in Table B-2.

$$H_{crit} = 1.22 \cdot 10^{-6} \cdot \frac{i_{slope}^{-2.56} \cdot D_{50}^{2.36}}{30 \cdot \rho_s \cdot (1 - n_0)k_0} \tag{B.2}$$

The trends for the equation by Van Rhee and the equation made in this research are similar, but Van Rhee gives on average higher values. The ratios between the equations are given in Table B-3. This table gives the critical cut height calculated by (B.2) divided by the corresponding critical cut height calculated by (B.1), ($H_{crit, B.2}$ / $H_{crit, B.1}$). It can be observed that the two equations have an average difference with a range of 10% to 40%. The differences are the largest for high slope angles and are the smallest for the lowest measured slope angles. However the absolute differences stay very similar for every slope angle.

Table B-1: Critical cut height for equation developed in this research (B.1)

	Reference soil	Soil 1	Soil 2	Soil 3	Soil 4	Soil 5	Soil 6	Soil 7
Slope angle	H_{crit}	H_{crit}	H_{crit}	H_{crit}	H_{crit}	H_{crit}	H_{crit}	H_{crit}
18	2.63	4.70	2.63	1.67	1.01	5.17	3.06	2.27
19	2.25	4.02	2.25	1.43	0.86	4.43	2.62	1.95
20	1.94	3.47	1.94	1.23	0.74	3.82	2.26	1.68
21	1.68	3.01	1.68	1.07	0.65	3.31	1.96	1.46
22	1.47	2.63	1.47	0.94	0.57	2.90	1.71	1.27
23	1.29	2.32	1.29	0.82	0.50	2.55	1.51	1.12
24	1.14	2.05	1.14	0.73	0.44	2.25	1.33	0.99
25	1.02	1.82	1.02	0.65	0.39	2.00	1.18	0.88
26	0.91	1.63	0.91	0.58	0.35	1.79	1.06	0.79
27	0.81	1.46	0.81	0.52	0.31	1.60	0.95	0.70
28	0.73	1.31	0.73	0.47	0.28	1.44	0.85	0.63
29	0.66	1.19	0.66	0.42	0.25	1.30	0.77	0.57
30	0.60	1.08	0.60	0.38	0.23	1.18	0.70	0.52

Table B-2: Critical cut height for Van Rhee equation (B.2)

	Reference soil	Soil 1	Soil 2	Soil 3	Soil 4	Soil 5	Soil 6	Soil 7
Slope angle	H_{crit}	H_{crit}	H_{crit}	H_{crit}	H_{crit}	H_{crit}	H_{crit}	H_{crit}
18	2.82	5.01	2.82	1.80	1.08	5.56	2.99	2.67
19	2.45	4.36	2.45	1.57	0.94	4.84	2.60	2.32
20	2.15	3.83	2.15	1.38	0.83	4.24	2.28	2.04
21	1.90	3.38	1.90	1.22	0.73	3.74	2.01	1.80
22	1.69	3.00	1.69	1.08	0.65	3.32	1.79	1.60
23	1.50	2.67	1.50	0.96	0.58	2.97	1.59	1.42
24	1.35	2.40	1.35	0.86	0.52	2.66	1.43	1.28
25	1.22	2.16	1.22	0.78	0.47	2.40	1.29	1.15
26	1.10	1.95	1.10	0.70	0.42	2.17	1.17	1.04
27	1.00	1.77	1.00	0.64	0.38	1.97	1.06	0.94
28	0.91	1.62	0.91	0.58	0.35	1.79	0.96	0.86
29	0.83	1.48	0.83	0.53	0.32	1.64	0.88	0.79
30	0.76	1.35	0.76	0.49	0.29	1.50	0.81	0.72

Table B-3: Critical cut height ratios

	Reference soil	Soil 1	Soil 2	Soil 3	Soil 4	Soil 5	Soil 6	Soil 7
Slope angle	H_{crit}	H_{crit}	H_{crit}	H_{crit}	H_{crit}	H_{crit}	H_{crit}	H_{crit}
18	1.07	1.06	1.07	1.08	1.07	1.07	0.98	1.17
19	1.09	1.08	1.09	1.10	1.09	1.09	0.99	1.19
20	1.11	1.10	1.11	1.12	1.11	1.11	1.01	1.21
21	1.13	1.12	1.13	1.14	1.13	1.13	1.03	1.23
22	1.15	1.14	1.15	1.15	1.15	1.15	1.04	1.25
23	1.16	1.15	1.16	1.17	1.16	1.16	1.06	1.27
24	1.18	1.17	1.18	1.19	1.18	1.18	1.07	1.29
25	1.20	1.19	1.20	1.20	1.19	1.20	1.09	1.31
26	1.21	1.20	1.21	1.22	1.21	1.21	1.10	1.32
27	1.23	1.22	1.23	1.23	1.23	1.23	1.12	1.34
28	1.24	1.23	1.24	1.25	1.24	1.24	1.13	1.36
29	1.26	1.25	1.26	1.26	1.25	1.26	1.14	1.37
30	1.27	1.26	1.27	1.28	1.27	1.27	1.16	1.39

Appendix C

Many simulations are performed using the breaching model in order to investigate the influence of certain parameters on the breaching process. Additional results are presented in this appendix. First of all, the graphs for the reference soil are presented. The cuttable soil is the soil which can possibly be cut if a cut swing would cut through the concerned section. It is calculated for a range of initial cut heights. For the same cases the wall height of the breaching wall though time is calculated and presented in a graph. Both graphs show the difference between stable and unstable breaching very clearly.

For all soil scenarios used in this report the graphs for the cuttable soil and the wall height are presented in this appendix. The soil parameters concerned are presented in the graph.

Reference soil results
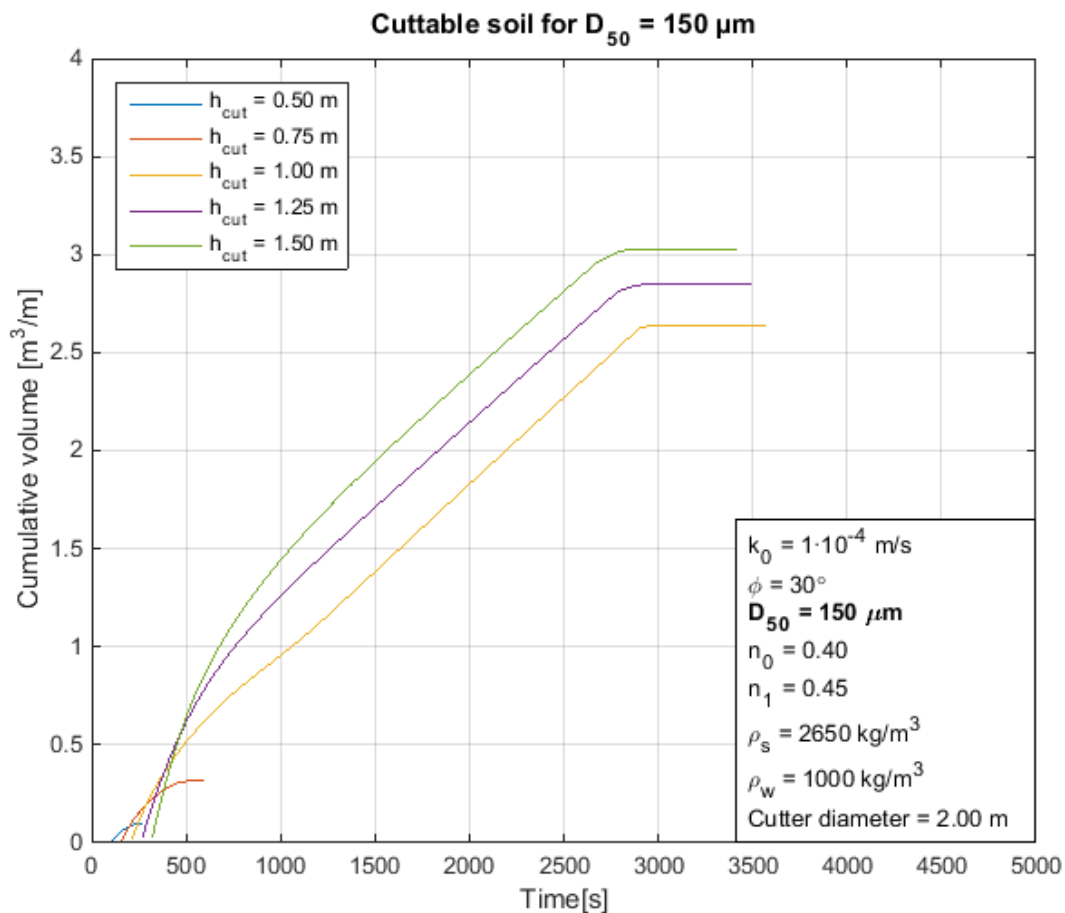
Figure C-1: Cuttable soil for the reference soil
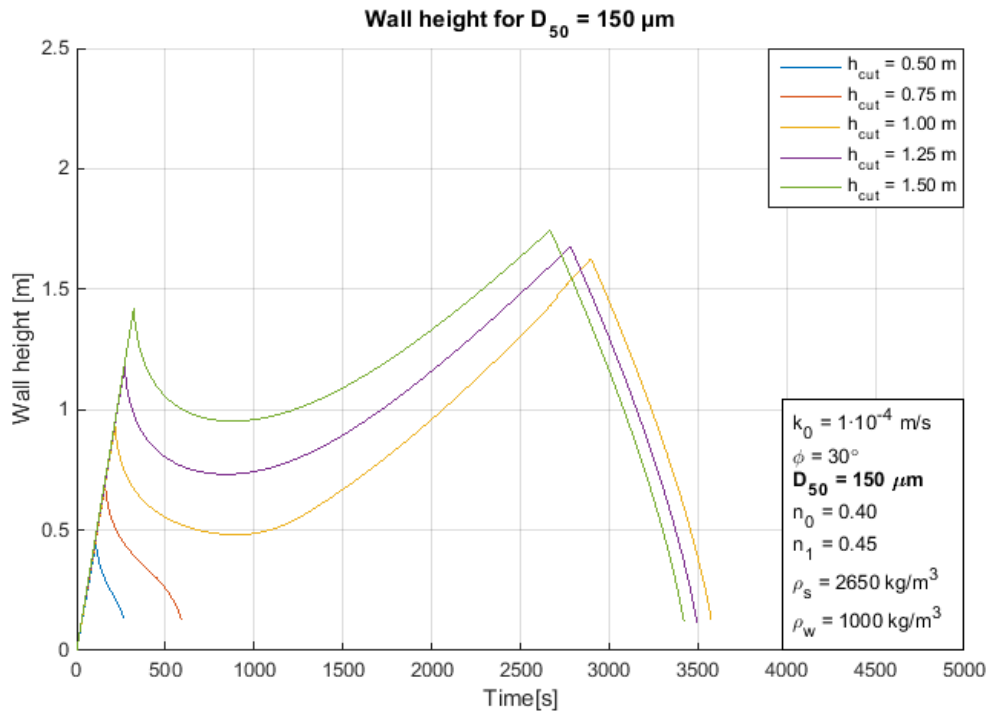
Figure C-2: Wall height for the reference soil

D₅₀ results
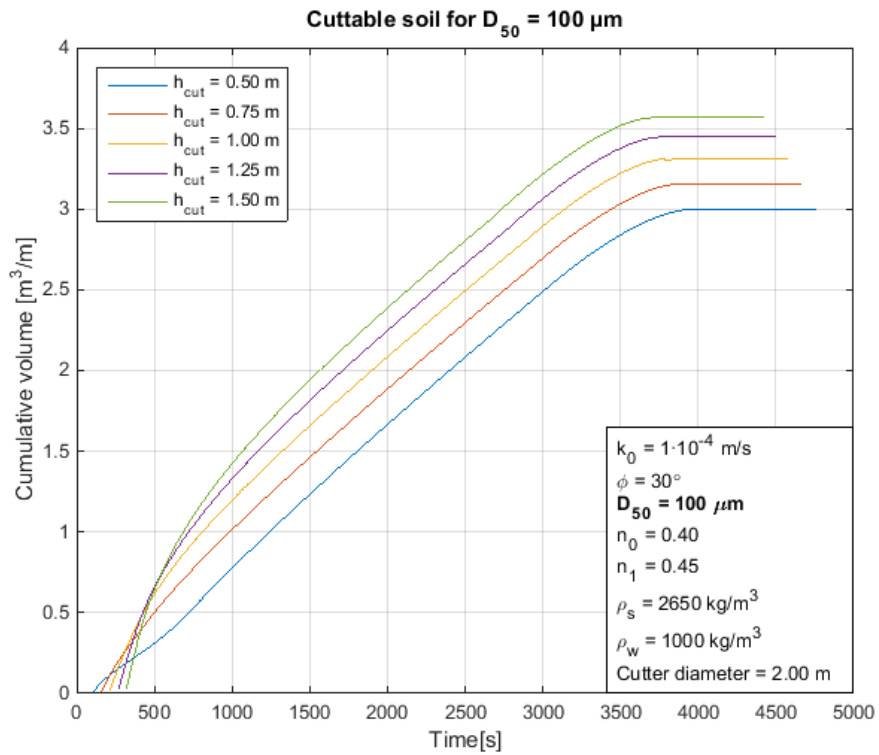
Figure C-3: Cuttable soil small D₅₀
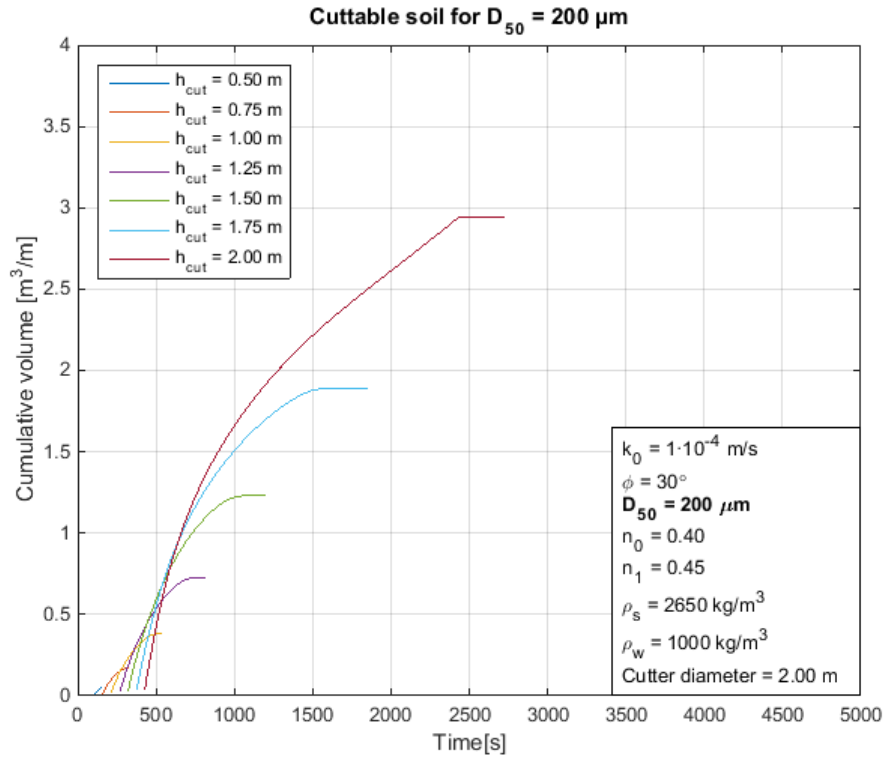
Figure C-4: Cuttable soil large D$_{50}$
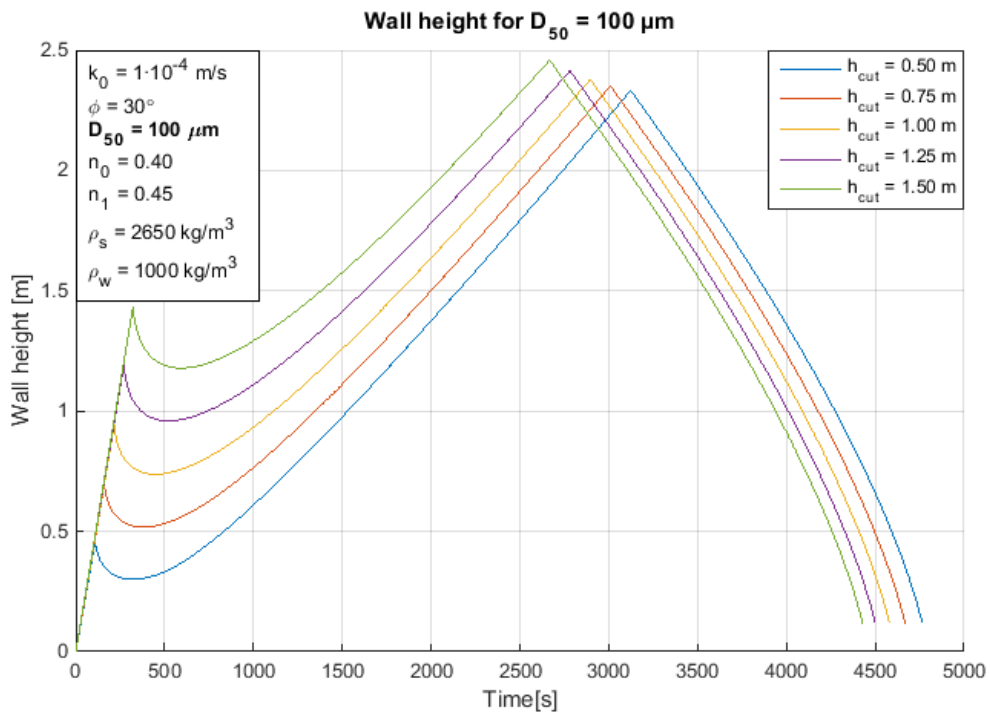
Figure C-5: Wall height small D$_{50}$
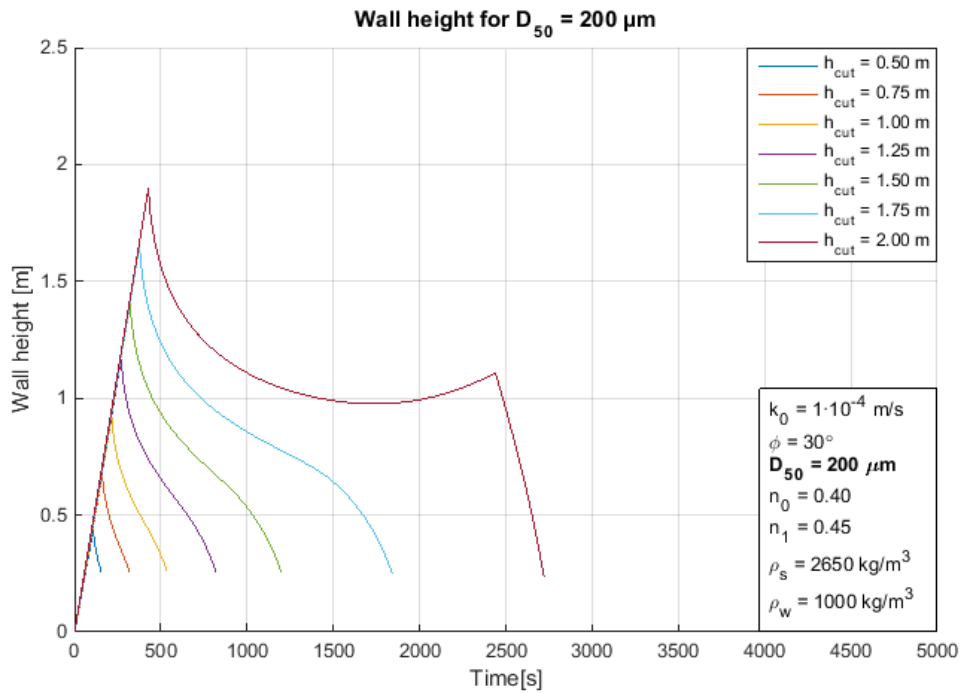
Figure C-6: Wall height large D_{50}

Permeability
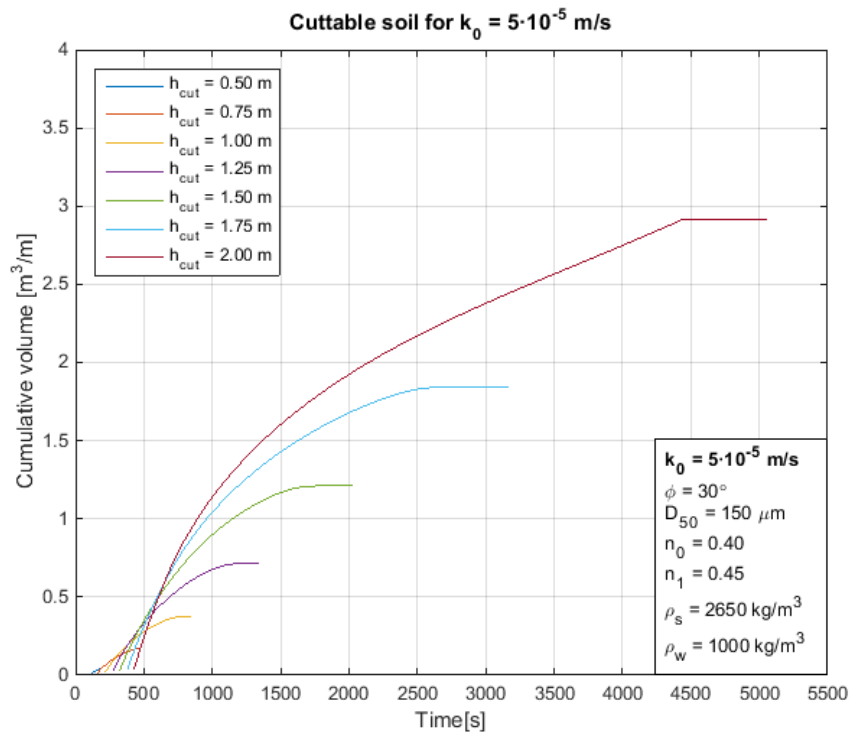
Figure C-7: Cuttable soil small permeability
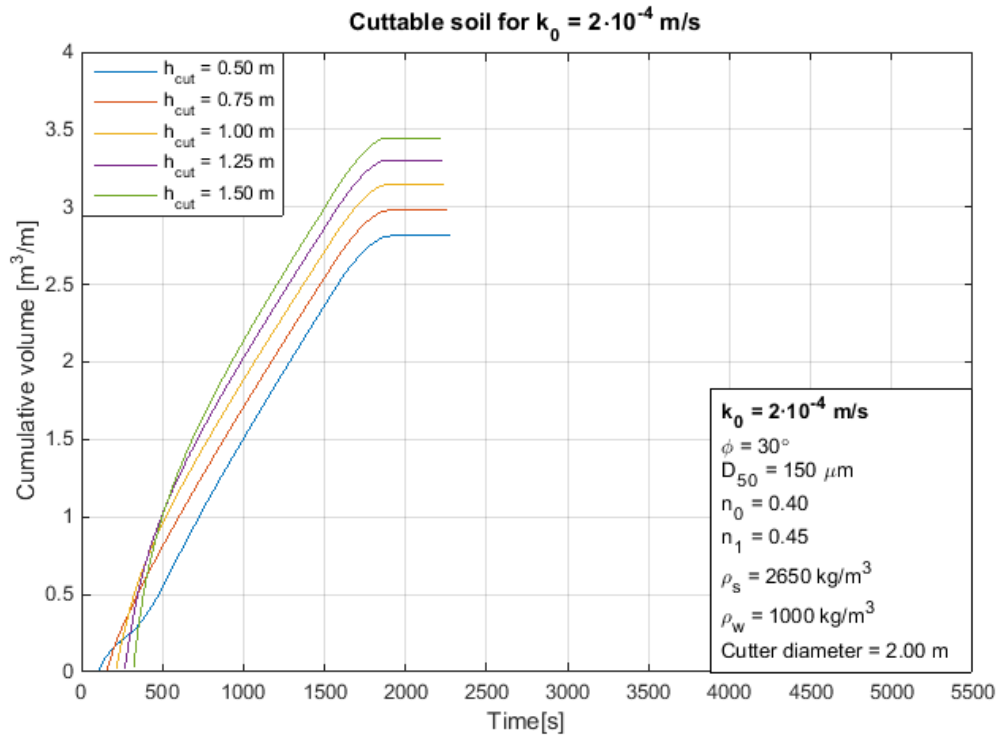
Figure C-8: Cuttable soil large permeability
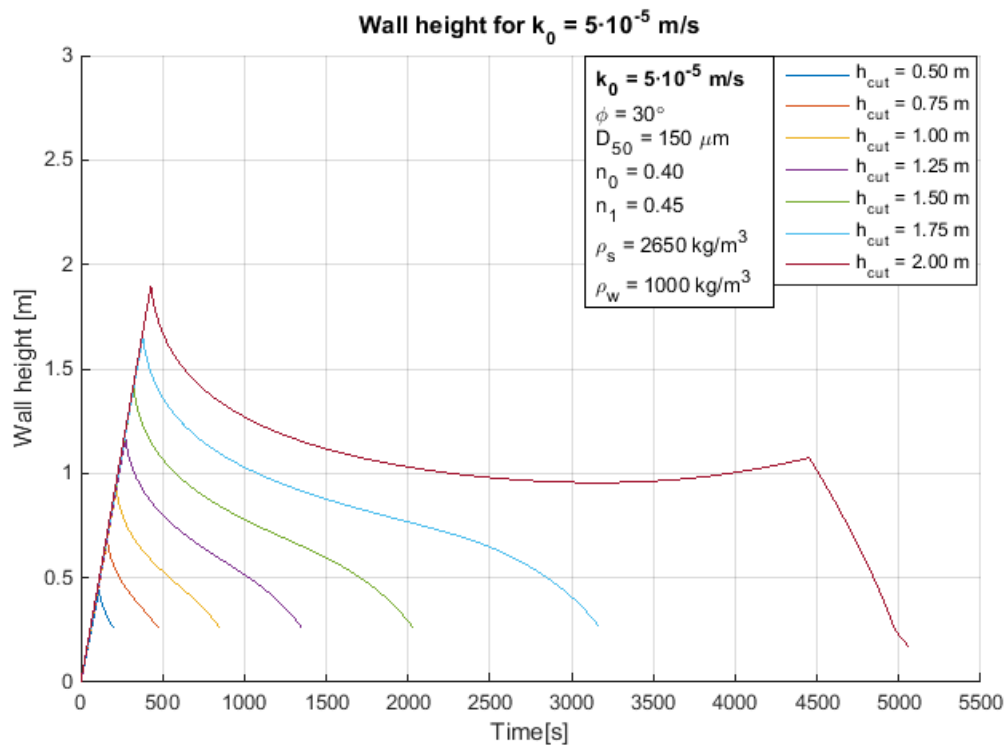
Figure C-9: Wall height small permeability
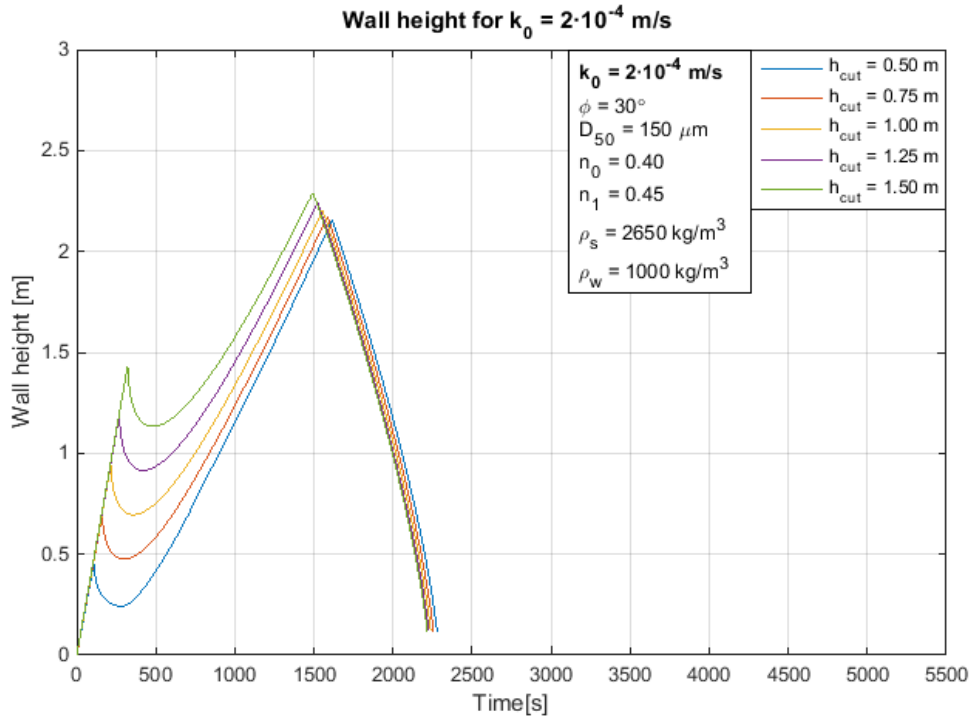
Figure C-10: Wall height large permeability

Particle density results
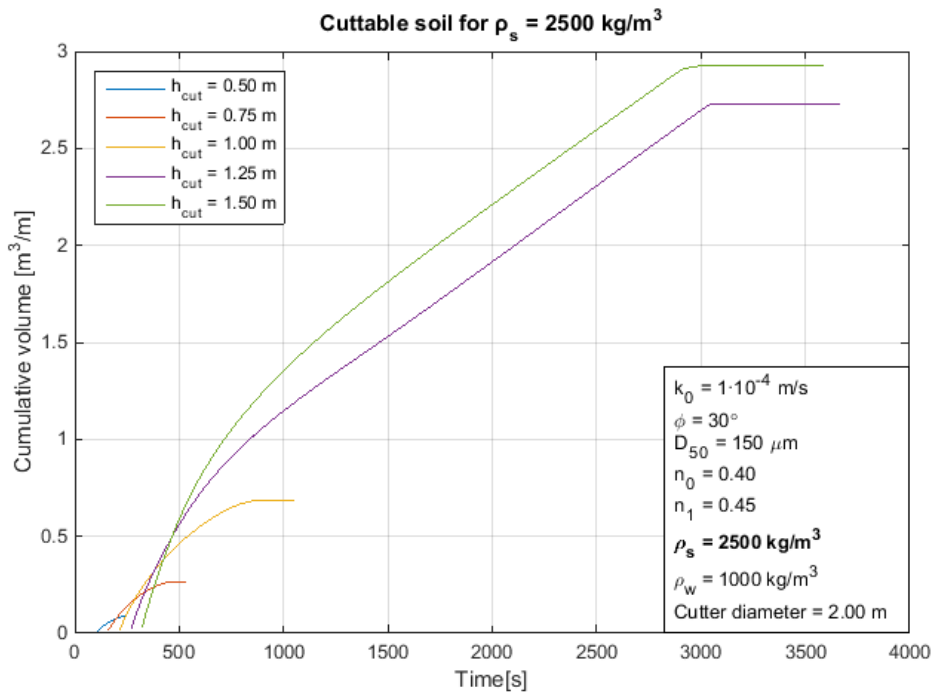
Figure C-11 Cuttable soil small particle density
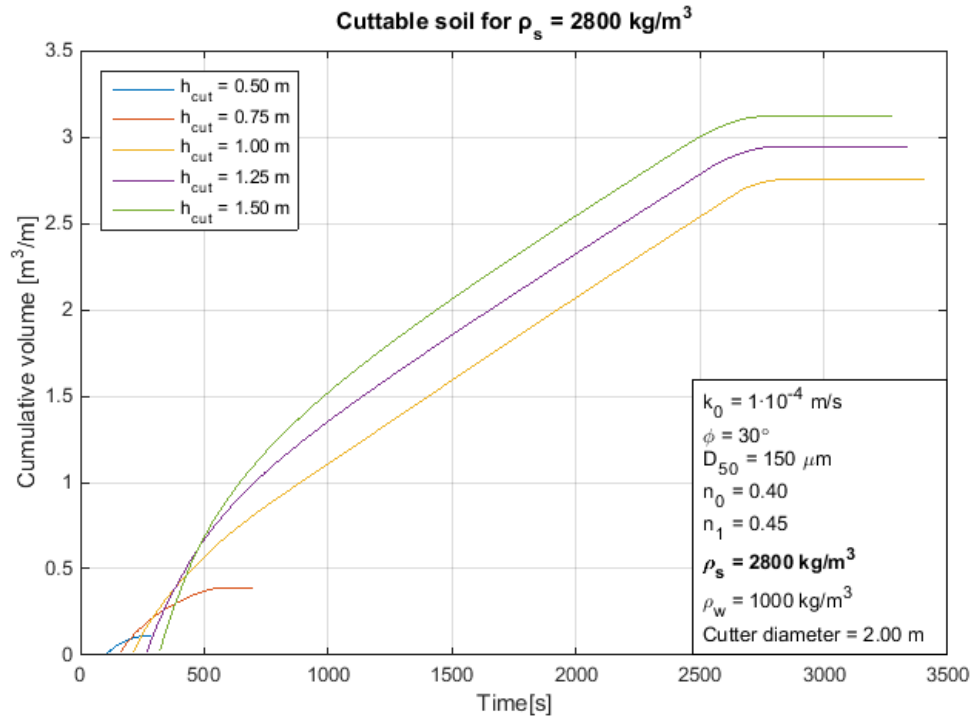
Figure C-12: Cuttable soil large particle density
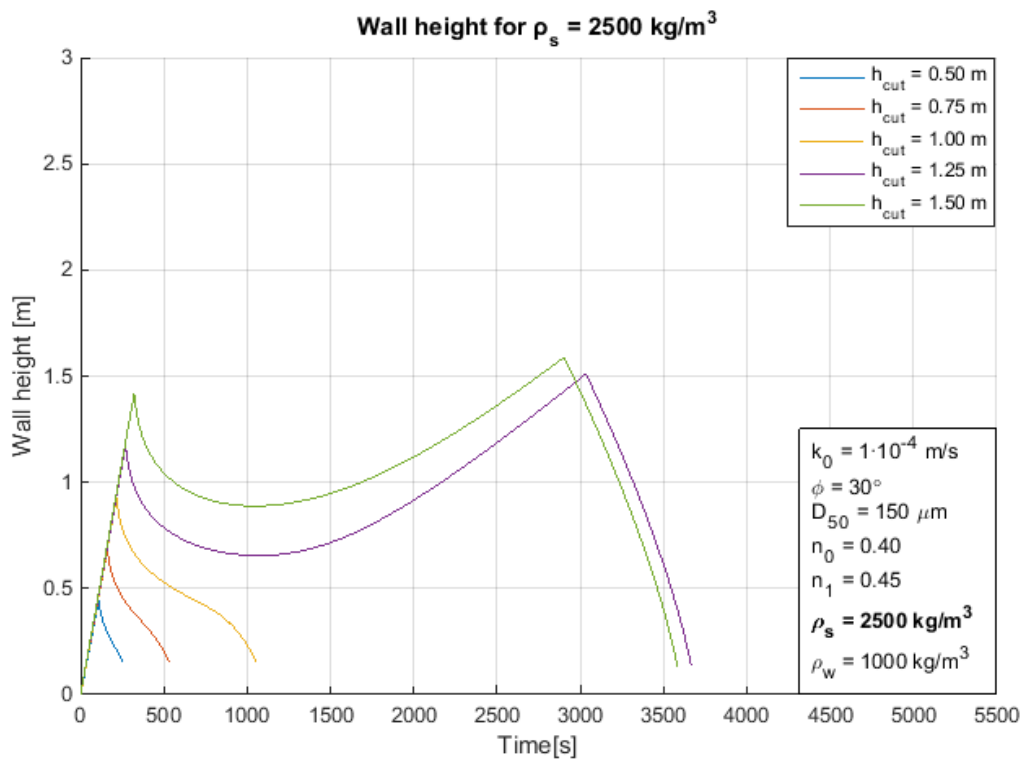
Figure C-13: Wall height small particle density
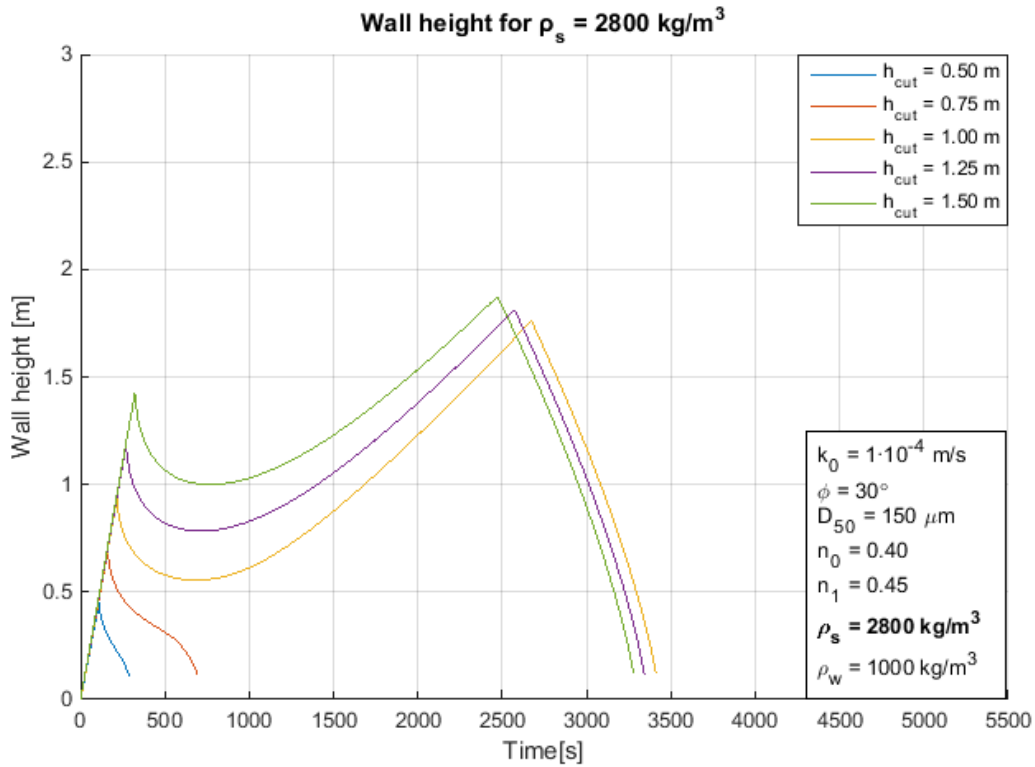
Figure C-14: Wall height large particle density

Particle size distributions results
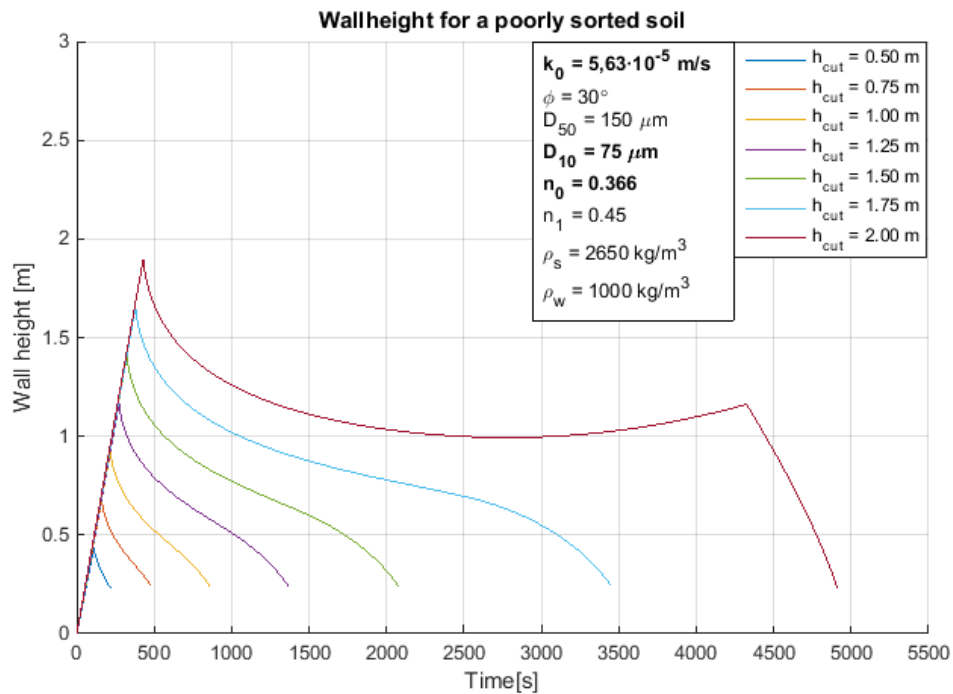
Figure C-15: Wall height poorly sorted soil
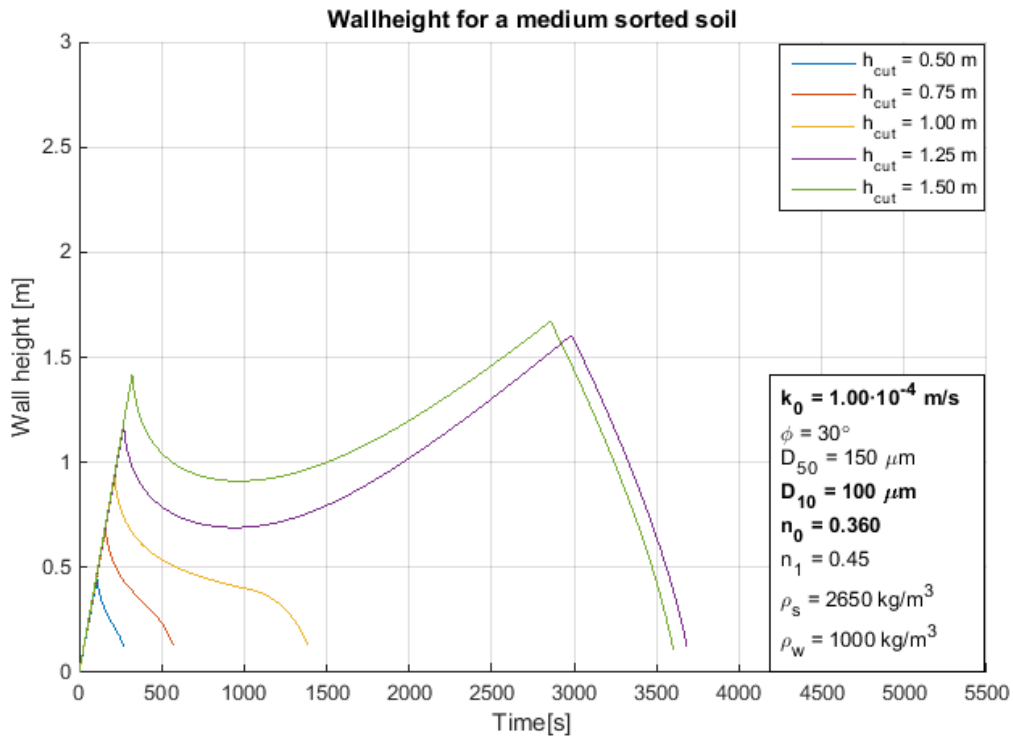
Figure C-16: Wall height medium sorted soil
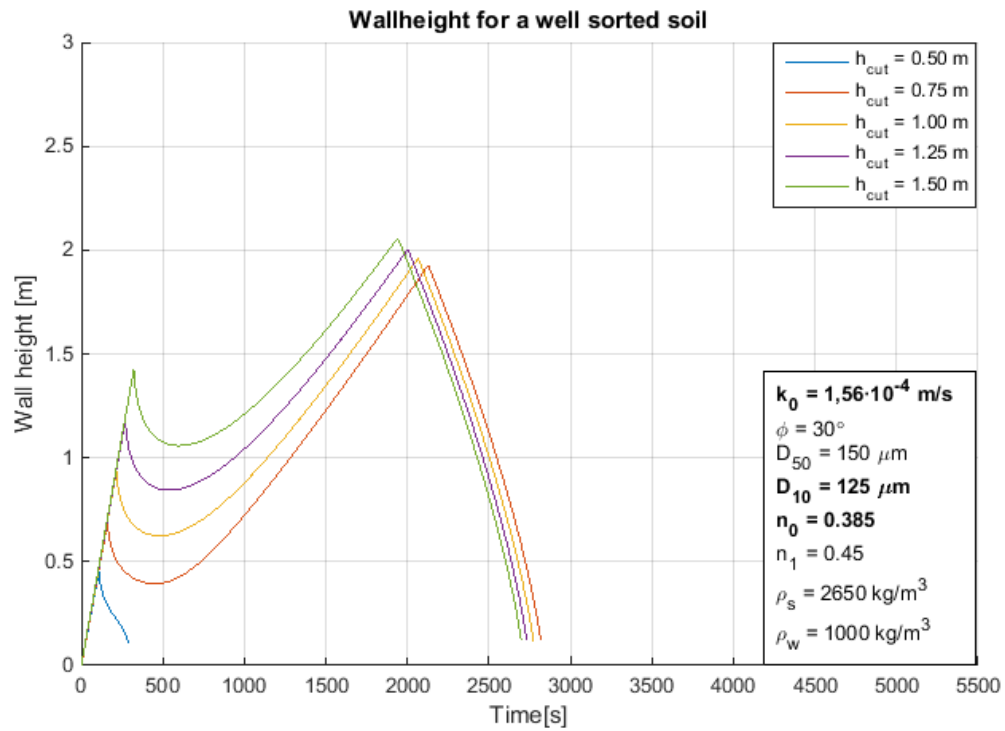
Figure C-17: Wall height well sorted soil

Appendix D

In order to calculate a critical cut height, a test needs to be executed to decide if a slope breaches stable or unstable. During a step of the breaching model the breaching wall moves backwards and the top and bottom of the wall move up. The difference in height of the top of the wall during a step is always the same if a constant slope angle is maintained. The height difference at the bottom is variable throughout the time. If the height change at the bottom of the wall is larger than the height change at the top, the total height of the breaching wall decreases and the breach is stable. If the height change at the bottom of the wall is smaller than the height change at the top, the total height of the breaching wall increases and the breach is unstable. This process is illustrated in the figures below.

Figure D-1 shows the process for a slope of 20° and 5 meter height. The bright red line is the difference at the top, which is constant until the top of the slope is reached after 3150 s. The other lines give the height difference of the bottom of the breaching wall. In this slope only the case where a cut is made with a height of 2.00 m becomes unstable, because after 2100 s the height difference at the bottom is smaller than the height difference at the top. When the breaching wall reaches the top of the slope, the breach turns stable again. Figure D-2 gives the same situation for a slope of 25°. It is visible that the breach turns already unstable at a cut height of 1.00 m. Figure D-3 shows the case for a slope angle of 30°, the breach turns unstable from a cut height of 0.75 m.

In order to find the critical breach height, the line for the bottom height difference should just not cross the bright red line in the graph. This is the line with an initial wall height corresponding to the critical cut height (H_{crit}).
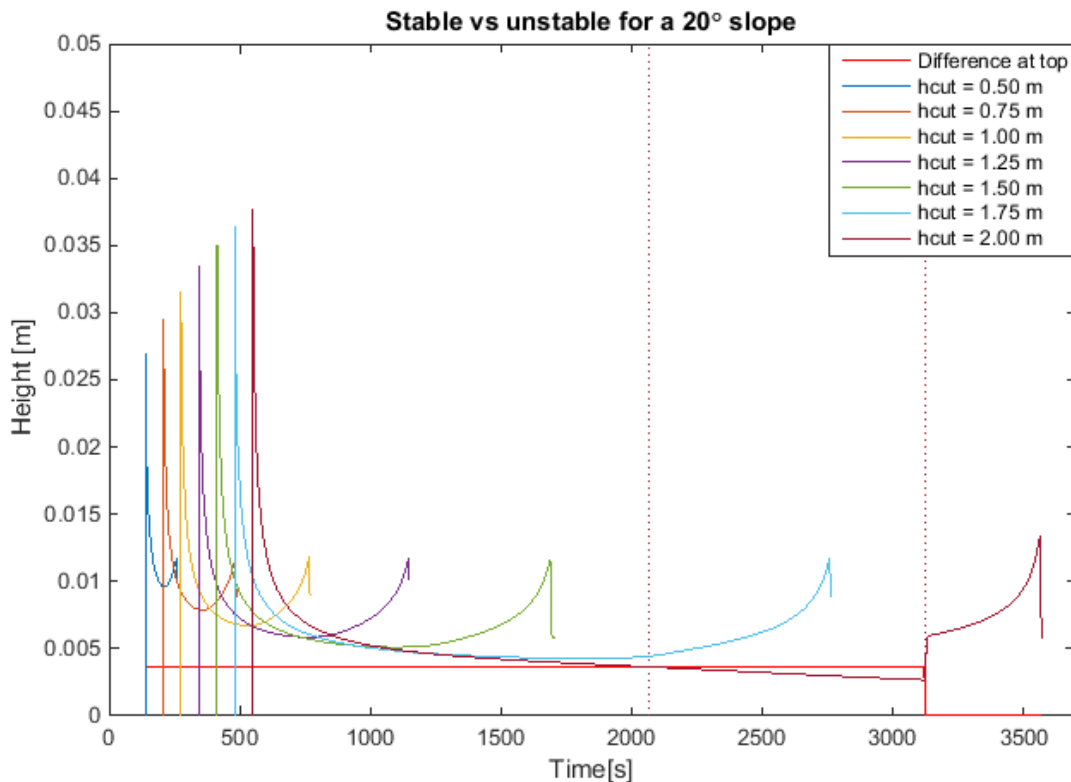
Figure D-1: 20° slope
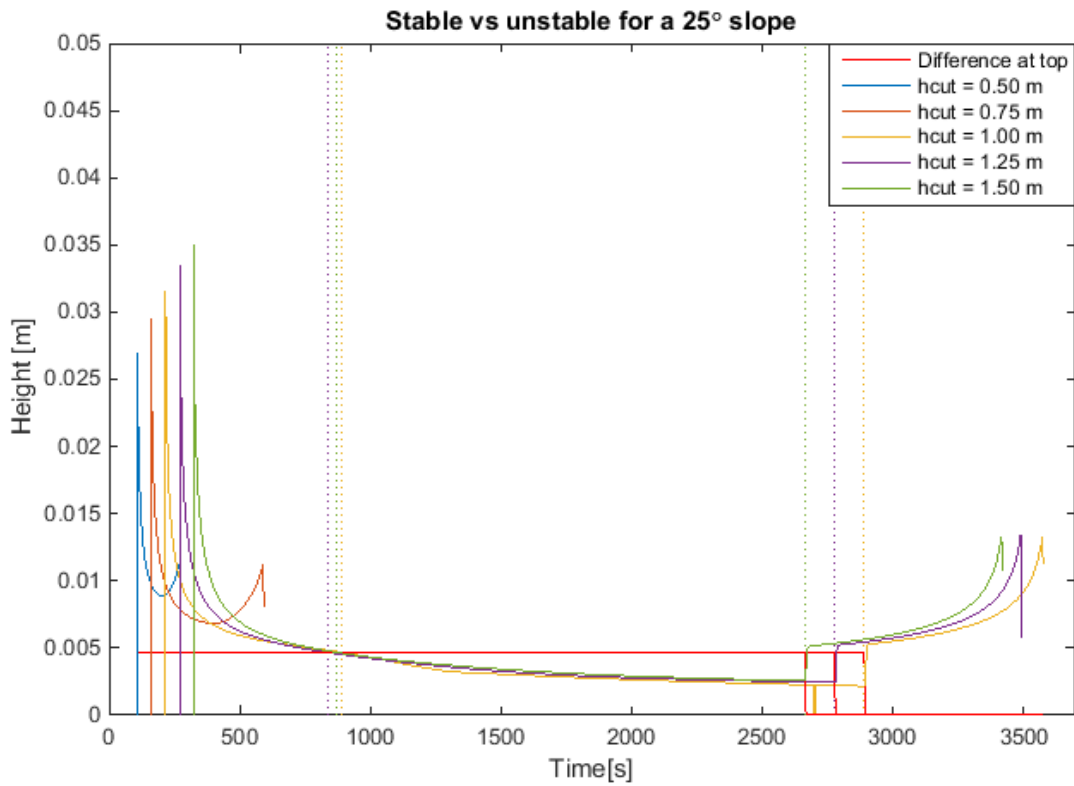
Figure D-2: 25° slope
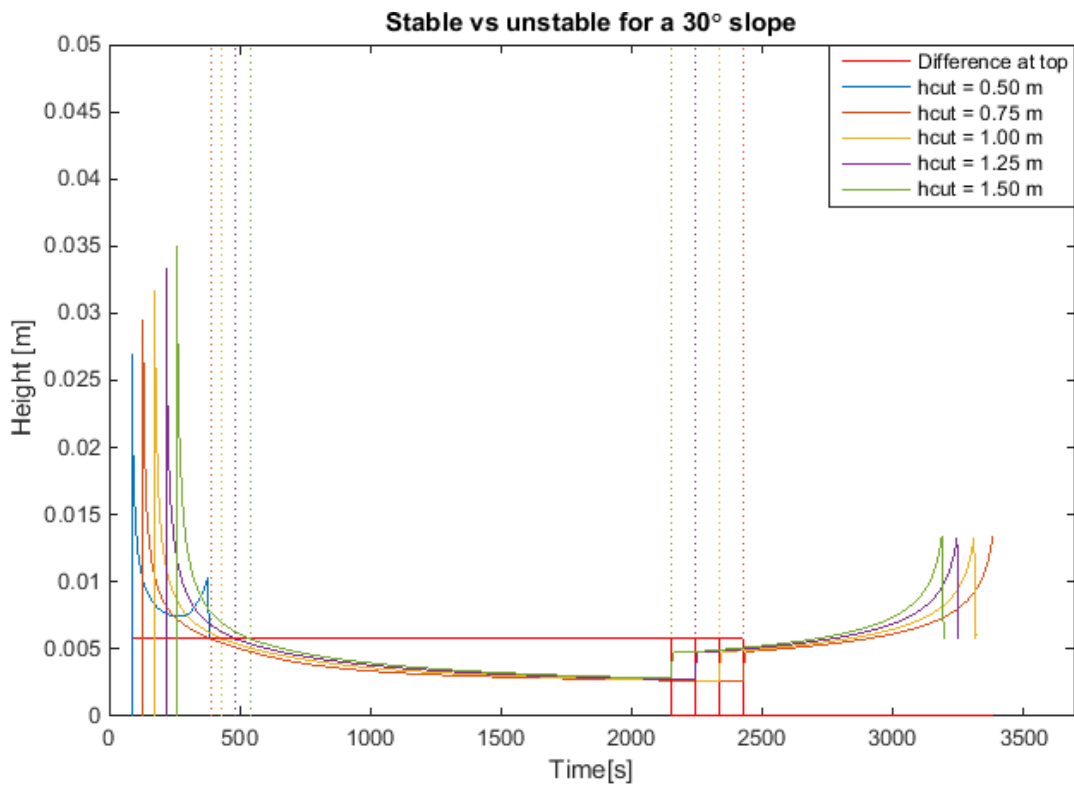
Figure D-3: 30° slope

Appendix E

The breaching model and the production model are compared at a time interval of 500 seconds. This appendix shows the prediction of both models for a slope with an angle of 25° consisting of the reference soil with the parameters given in Table 3-1.
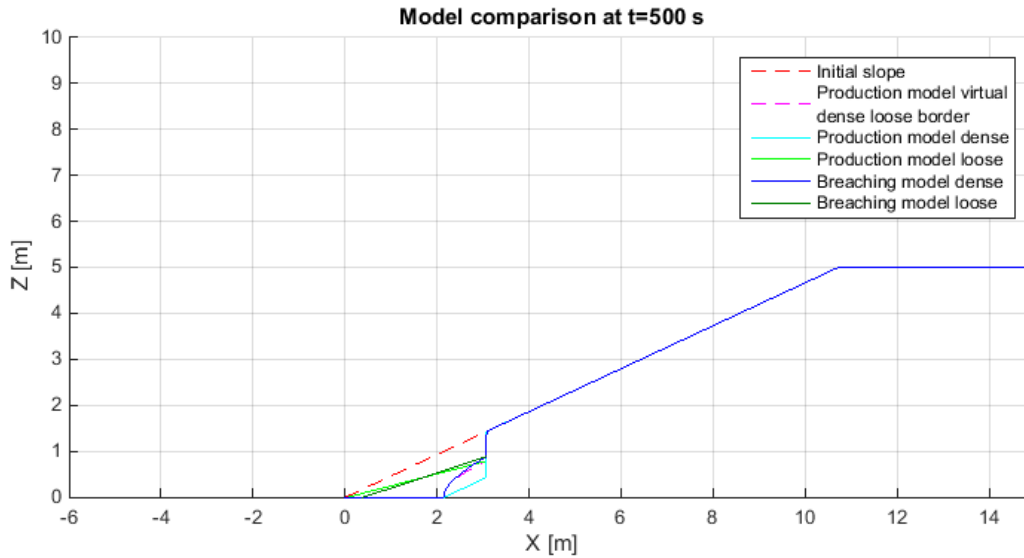
Figure E-1: t=500 s
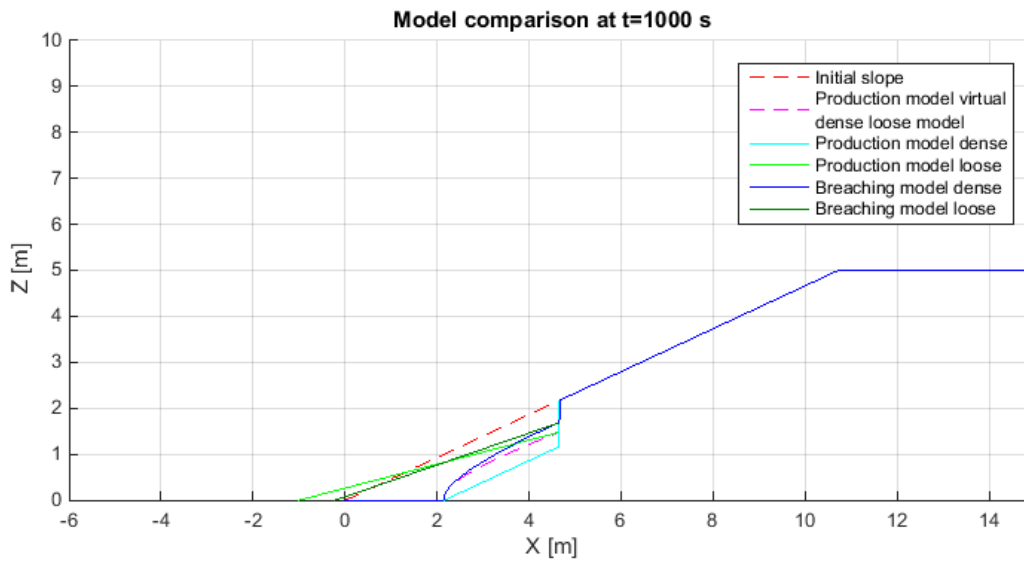
Figure E-2: t=1000 s
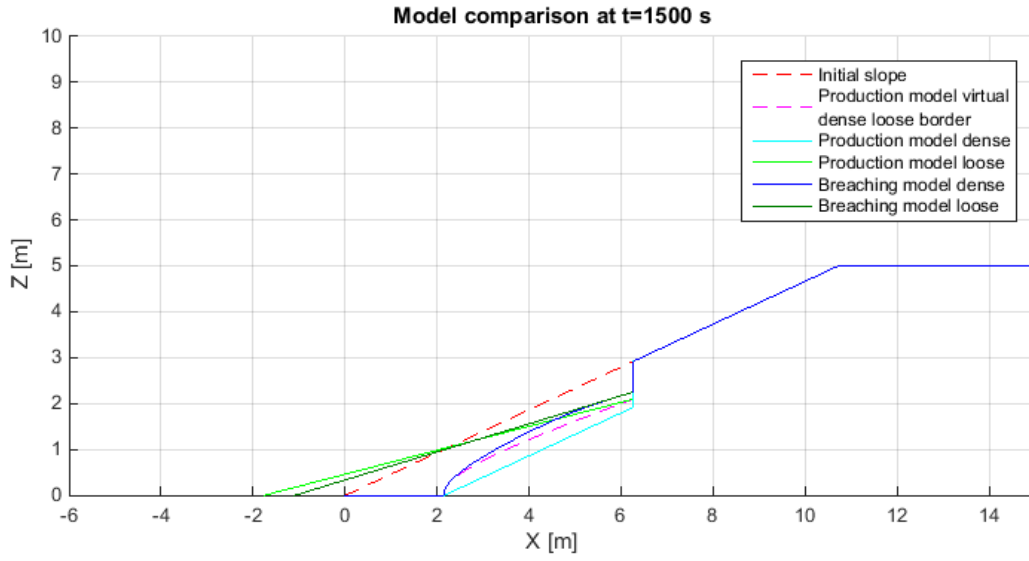
Figure E-3: t=1500 s
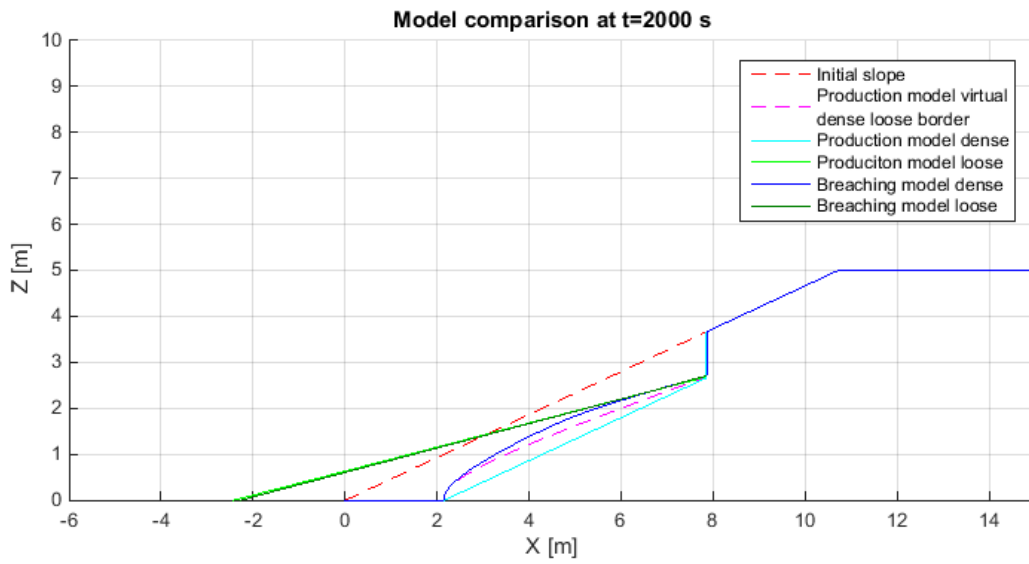
Figure E-4: t=2000 s
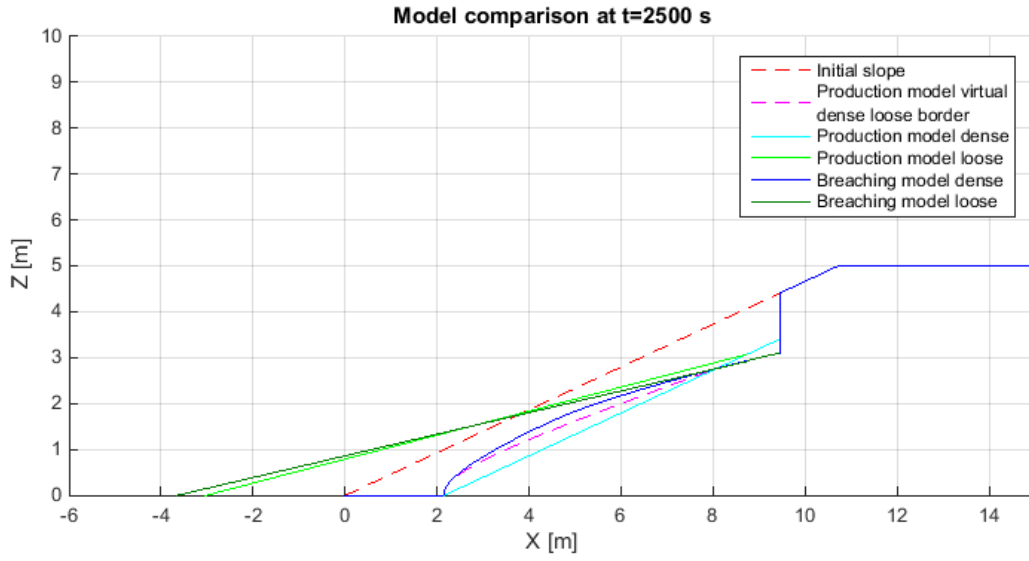
Figure E-5: t=2500 s

Figure E-6: t=3000 s